2010-01-04

Distributed Digital Radios for Land Mobile Radio Applications

Abhijit C. Navalekar
Worcester Polytechnic Institute

DISTRIBUTED DIGITAL RADIOS FOR LAND MOBILE RADIO APPLICATIONS

By

Abhijit C. Navalekar

A Dissertation
Submitted to the Faculty of the
Worcester Polytechnic Institute
In partial fulfillment of the requirements for the
Degree of Doctor of Philosophy
in
Electrical and Computer Engineering
December 2009

Approved By:

_____
Dr. William Michalson, Thesis Advisor

_____
Dr. James Matthews, Committee Member

_____
Dr. Jeffrey Smith, Committee Member

_____
Dr. Fred Looft, Head Of Department

Abstract

The number of wireless devices has increased exponentially over the past decade. Wireless networks today exist in a variety form factors, from Metropolitan Area Networks (MAN) like 802.16 (WiMAX) to Personal Area Networks (PANS) like 802.15 (ZigBee) and are used in a wide range of applications like cellular networks and RFIDs. In addition to these next generation networks, attempts are also being made to integrate the legacy networks like Land Mobile Radio (LMR), which are used in public safety and law enforcement applications, into the internet backbone. Traditionally, the use of LMR networks has been restricted to that of transmitting voice signals. However over the past few decades, digital radio based LMR networks like TETRA and APCOs P-25 have incorporated data transmission along with voice over LMR channels. The Digital Distributed Radios (DDR) provide low-cost IP-based connectivity using convention analog LMRs. The next generation LMR networks based on DDR technologies allow radios with different standards to interoperate and co-exist in the same network.

The main objective of this dissertation is to develop the next generation of DDR technology. The DDR II modem developed provides an integrated voice/data service platform, higher data rates and better throughput performance as compared to DDR I modems. In order to improve the physical layer performance of DDR modems an analytical framework is first developed to model the Bit Error Rate (BER) performance of Orthogonal Frequency Division Multiplexing over Frequency Modulation (OFDM/FM) systems. The use of OFDM provides a spectrally efficient method of transmitting data over LMR channels. However, the high Peak-to-Average (PAR) of OFDM signals results in either a low Signal-to-Noise (SNR) at FM receiver or a high non-linear distortion in FM transmitter. This dissertation presents an analytical framework to highlight the impact of high PAR of OFDM on OFDM/FM systems. A novel technique for reduction of PAR of OFDM called Linear Scaling Technique (LST) is developed. The use of LST mitigates the signal distortion occurring in OFDM/FM systems.

Another important factor which affects the performance of LMR networks is Push-to-Talk (PTT) delays. A PTT delay refers to the delay between the instant when a PTT switch on a conventional

LMR radio is keyed/unkeyed and a response is observed at the radio output. This dissertation presents typical PTT values, their distributions and their impact on throughput performance of LMR networks. An analytical model is developed to highlight the asymmetric throughput problem occurring in heterogeneous LMR networks consisting of radios with different PTT delay profile. This information will be useful in performance and capacity planning of LMR networks in future.

Acknowledgment

First and foremost, I would like to express my deepest gratitude to my advisor, Prof. William R. Michalson for his support and guidance without which this work would not be possible. He has been a constant source of motivation and knowledge during the course of my studies at WPI. I would also like to thank Prof. James W. Matthews and Dr. Jeffrey Smith for being a part of my PhD dissertation committee.

I would like to thank my current and former lab colleagues Jitish Kolanjery, Andrew Dupont, Turin Pollard and Vishwanath Iyer for their support and company. A special thanks to my dear friends Hemish, Kunal and Mahim for their encouragement, guidance and support.

As always, I am deeply indebted to my mother, father and sister for their unwavering love, support and confidence in me. Finally, I would like to thank my wife for her unconditional love, understanding and support.

Dedicated To

My Mother and Father

TABLE OF CONTENTS

LIST OF FIGURES

LIST OF TABLES

1. Introduction

1.1. Current trends in Wireless Networks

The use of wireless devices has increased exponentially over the past decade. With the advent of next generation wireless data networks like WiMax (802.16) and ZigBee Pro (802.15), a whole new range of applications like sensor networks and IPTV have emerged. In addition to these data technologies, next generation cellular networks like WCDMA and LTE are targeting higher data rates in addition to voice connectivity. Figure 1-1 highlights the current trend in wireless industry. Wireless networks started off by catering to only one type of traffic viz. voice or data, but over recent years efforts have been made to provide an integrated service platform capable of supporting both data and voice services [1],[2]. This has resulted in an influx of data/voice hybrid applications like Voice over IP (VOIP) implementation in WiFi networks or Multimedia Messaging Services (MMS) over cellular networks. Another consequence of ubiquitous connectivity resulting from wireless access is that IP based communication is evolving as a de-facto standard for addressable communications [3],[4].

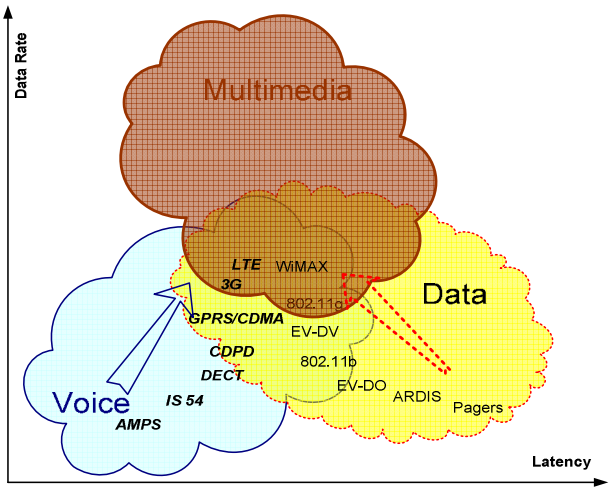

Figure 1-1: Convergence in wireless networking

In spite of these advances in the next generation wireless standards, widespread implementation and availability of broadband connectivity is still many years away. Furthermore, broadband networks typically suffer from reliability, quality of service (QoS) and coverage issues

which are important considerations for success of Public Safety applications like Law Enforcement and Emergency Medical Services (EMS). Due to these limitations of broadband technologies, a large number of users and critical services are still largely dependent on narrowband analog connectivity. One such example of a legacy network is a Land Mobile Radio (LMR) network. Mobile communications for emergency response and disaster recovery are prime applications of LMR networks. The dominant form of communication in these applications is voice calls between law enforcement, fire and other Public Safety organizations, although a few data only applications such as taxicabs and truck fleets also use LMR channels [5]. Most of the Public Safety organizations have a dedicated infrastructure and operate in dedicated VHF/UHF bands. As seen in Table 1-1, LMR networks typically operate in lower VHF/UHF bands which have better propagation and coverage characteristics than higher UHF/SHF bands (1.8/2.4/5 GHz) that are used by most broadband networks. Due to difficulties in interoperability with existing infrastructure, coverage and cost of a network overhaul, current Public Safety organizations haven't been able to leverage broadband technologies as envisioned by initiatives like SAFECOM and hence depend on their LMR infrastructure for communications [6],[7]. This provides an impetus for developing the next generation of LMR networks. The next section traces the evolution of LMR networks.

Land mobile radios have been traditionally used to transmit analog voice data. Most of the early systems used amplitude modulation (AM) or frequency modulation (FM) to transmit voice signals. Use of FM for analog radios started in early 1940's. Most of these FM/AM systems were capable of transmitting voice data alone. They were later succeeded by systems like facsimile and radio teletype which were capable of transmitting data. This was made possible by using select audio tones to transmit textual data. Thus these systems, although capable of transmitting data by means of encoding them into analog signals, were still analog systems. One of the earliest versions of digital radios was a packet radio. Packet radio is a particular mode of amateur radio communications and has been around since mid-1960. It took any data stream sent from a computer and passed it through a packet modem to create X.25 format packets which were sent via radio to another similarly equipped amateur radio station. The data rates supported varied according to the frequency used and the type of radio. For data rates of 1200/2400 bps, commonly available narrowband FM voice radios were used in the UHF/VHF bands. For HF packets, 300 bps data was passsed using single side band (SSB) modulation. For higher packet rates (> 9600 bps), special radios or modified FM radios were required. In addition to amateur packet radio networks, private mobile data networks, such as

Advanced Radio Data Integrated Services (ARDIS) and RAM Mobitex also evolved during the early 1990s [8],[9]. ARDIS was a public wireless data service started by Motorola and IBM in 1991 which used a FM radio to provide data rates of 9.6 kbps using single LMR channel in UHF LMR bands. It used a propriety technology to transmit digital data and was based on cellular type architecture. ARDIS radio supported a number of packet radio protocols like X.25 and IBM's SNA. RAM Mobitex was a packet switched, narrowband data only transmission technology. It supported data rates of 8 Kbps over UHF channels.

Table 1-1: LMR frequency Allocations

Frequency Band	Frequency (MHz)	Applications
VHF	30-32, 33-34, 35-36, 42-46.6, 47-49.5,50.8-156.24, 157.1875-161.575, 161.625-162.0125, 173.2-173.4	Dispatch Frequency, Law Enforcement, Multi-Use Radio Service (MURS).
UHF	450-460, 470-512, 608-614, 806-849, 851-894, 940-941, 1427-1430	ARDIS, RAM, P25.

1.2. State-of-Art in LMR Networks

Present day LMR technology has come a long way from its early day voice only inception. Recent advances in technology have brought the world of high-quality digital communications to LMR applications, offering data and imagery as well as priority voice to users. LMR networks today support a variety of topologies like simulcast, multicast and trunking. A growing emphasis is being placed on efficient utilization and management of channel resources [5],[7]. A number of proprietary solutions like Tyco's OpenSky and EDAC systems exist for LMR networks which support efficient multiuser communications. The section below provides a preview of the promising LMR networks of the future.

1.2.1. APCO Project 25

APCO Project 25 or simply P 25 is a digital FDMA trunked radio system with a backward compatibility mode to traditional analog FM radios [5],[10]. The fundamental objective of Project 25 was to develop a standard digital LMR system which is capable of both digitized voice and data communications including a full set of voice, packet, and circuit data services. It supports data rate of

9.6 Kbps using digital modulation. P 25 is implemented in two phases which differ in modulation scheme, bandwidth required and the radio access methods. For Phase I the allocated bandwidth per channel is 12.5 kHz rather than a 25 kHz as required by legacy LMR networks. For Phase II the bandwidth allocation is further reduced to 6.25 kHz. Most of the P 25 compatible digital radios have a backward compatibility mode for the legacy analog FM radios. However it is important to note that the even though the radio is compatible, rest of the network infrastructure may not be. For example, repeaters which support P 25 signaling cannot support conventional FM transmission. The modulation scheme implemented for Project P 25 is a form of Quadrature Phase Shift Keying (QPSK). For Phase I, a constant envelope frequency modulated waveform called C4FM is used while Phase II uses an amplitude modulated waveform called compatible QPSK (CQPSK). The digitized voice is encoded using an Improved Multi-band Excitation (IMBE) vocoder. A P 25 network can support both conventional and multicast LMR setups as well as trunking. A major drawback in installing P 25 networks is the cost associated with the network overhaul which includes a P 25 base station controller and the mobile radios. Conservative estimates can run into several hundred thousand dollars to convert even a small network to P 25 as opposed to a the several thousand dollars associated with upgrading conventional FM radios and base stations. The Table 1-2 summarizes the various features of P 25.

Table 1-2: Project P 25 features

Modes	Modulation	Bandwidth	Data rate	Radio Access Protocol
Conventional	Analog	25/12.5 kHz	Voice Only	Legacy
Digital (Phase I)	C4FM	12.5 kHz	9.6 kbps	FDMA
(Phase II)	CQPSK	6.25 kHz	9.6 kbps	FDMA/TDMA

1.2.2. Terrestrial Trunked Radio (TETRA)

TETRA is a multifunction European mobile radio standard that provides a comprehensive suite of mobile radio standards supporting both Infrastructure Mode Operations (IMO) and Direct Mode Operation (DMO) LMR topologies [5],[11]. In addition to voice communication TETRA also facilitates circuit mode data, short data messages, and packet mode data transfers. The standard was written such that DMO can be used to provide mobile-to-mobile communications when one or more mobile stations are outside the coverage of network, or it can be used as a more secure communication channel within network coverage creating a hybrid DMO-infrastructure topology. It

supports both 25 kHz and 12.5 kHz channels bandwidths and uses a π/4 DQPSK modulation scheme to transmit digital data. TETRA provides a raw data rate of 7.2 kbps on a communication channel. The effective data rate achievable varies depending upon the nature of data and protocol used. The radio access mechanism used is a four slot TDMA. Thus if necessary, up to four channels can be banded, increasing the burst data rate to as high as 28.8 kbps.

Table 1-3: TETRA Features

Modes	Modulation	Bandwidth	Data rate	Radio Access Protocol
Conventional	Analog	25 kHz	Voice Only	Legacy
Digital	π/4 DQPSK	12.5 kHz	7.2 kbps	TDMA

1.2.3. Distributed Digital Radios (DDR)

The use of Distributed Digital Radios (DDR) in LMR applications was first proposed in [12]. The first generation DDR prototype (DDR I) supports data rates of 4/ 8/ 12 Kbps and a full TCP/IP and UDP/IP ISO network protocol. It interfaces with an existing analog FM radios without any need for external modification to the radio. The data rates achieved using the DDR are comparable to those achieved using packet-based radio technologies like GSM (2G), P25 or TETRA. The DDR technology is a bridge technology, providing moderate data rate IP connectivity over VHF/UHF LMR bands. The Physical Layer (PHY) of the DDR uses Orthogonal Frequency Division Multiplexing (OFDM) to transmit data over FM channels. The radio access method is implemented by the Medium Access Layer (MAC) of a DDR and is based on the Carrier Sense Multiple Access (CSMA) protocol.

1.3. Challenges in Next Generation LMR Networks

The next generation LMR networks are targeting higher data rates and integrated voice/data services consistent with the convergence trends for next generation wireless networks described in Section 1.1. One of the major issues that plague the LMR networks are the incompatibilities between proprietary signaling and control technologies [5],[6],[7]. This issue of interoperability is of great relevance to Public Safety applications. Presently, a large number of Public Safety LMR systems consist of antiquated equipment not fully supported by vendors, and the resulting maintenance costs are forcing many public organizations to replace these independent systems. The cost of replacing aging equipment is at times prohibitively expensive resulting in selective upgrades that give rise to networks in which users use incompatible technologies [13]. Some proprietary technologies like

VIDA (Voice Interoperability Data Access) provided by MACOM, allow base stations to support users with multiple standards in a given cell area [14]. At critical times, however, most of the LMR networks are effectively mobile adhoc networks (i.e. without connectivity to a base station) [15]. A simple example of such a situation would be police and fire department personnel converging in the area of an incident. The situation is further exacerbated due to lack of control/trunking channels required to form talk groups. Another aspect of interoperability which is often neglected is the performance compatibility between different radios. For example, disparate Push-To-Talk (PTT) delay profiles can severely impact the effective throughput observed by a radio network [16].

Another important factor for next generation LMR networks is resource utilization [5],[7]. In some LMR bands, capacity limits are being reached. Furthermore, to address the ever growing demand for additional spectrums from competing broadband technologies, a number of land mobile radio channels are being considered for reallocation. As a result of this mounting pressure to relinquish their spectral allocations, the LMR community has made plans to migrate from 25 KHz channels to 12.5 KHz/6.25 KHz. There is also a growing emphasis on bandwidth efficiency and frequency management schemes so as to maximize the data rate achievable and to serve maximum number of users over a wide area network.

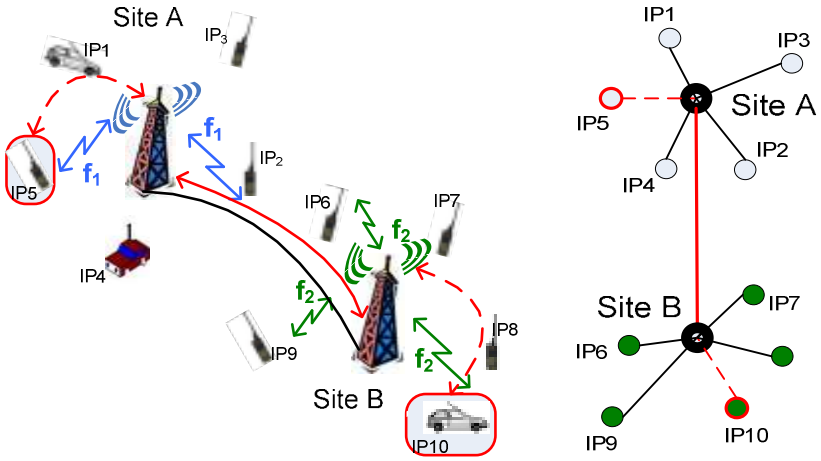

Figure 1-2: (a) DDR based radio network (b) Network Connectivity

1.4. Research Objectives

The main objective of this research is to work on the next generation of DDR technology to enhance the features provided by DDR I. The DDR technology discussed in [12] offers promising solutions to the two main problems confronting the LMR networks as discussed next. A DDR based

LMR network can be viewed as Wireless Local Area Network (WLAN) which can support both infrastructure mode (base station/repeater) and direct mode operation (adhoc), as shown in Figure 1-2. Each mobile radio has a unique IP address and can talk to one other person (point-to-point link), a talk group (multicast link) or broadcast to all users [17]. Since the system has an IP based architecture, forming talk groups or dynamically adding new users and providing mobility between cell sites becomes trivial. LMR networks supporting adhoc and base station modes can be established by using a simple router/switch and with the aid of well defined routing protocols like Routing Information Protocol (RIP) and Interior Gateway Routing Protocol (IGRP) [18]. This means that interoperability between disparate networks can be accomplished merely by using IP based addressing which is supported by most next generation LMR technologies. As compared to P25 and TETRA, DDRs also provide superior scalability due to use of IPv4 addressing. A DDR uses OFDM/FM transmission to achieve high data rates over narrowband FM channels. The use of OFDM provides a spectrally efficient way of data communications [19],[20]. The current generation of DDR (DDR I) supports single channel data rates of up to 12 kbps using M-ary modulation which is as fast or faster than the available P-25/TETRA technologies [21],[22].

Although DDR I has significant advantages, it also has some limitations. First and foremost is the fact that DDR I is tailored to facilitate data traffic as will be described in Chapter 2. This means that the DDR I technology fails to provide an integrated data/voice service. In addition, to support hybrid applications like VOIP which requires a data rate of 14.4 Kbps, there is a need to increase the data rate and throughput performance of DDR I radios [23], [24].

The main objective of this research is to develop the next generation of Distributed Digital Radio (DDR II). To reach this main objective, several sub-objectives have to be established for this dissertation. These sub-objectives are as follows:

- Redesign the DDR I system to support data and voice traffic. This includes changes to the hardware and software architecture. Existing DDR I protocols have to be extended to accommodate integrated voice/data transmissions.
- In order to support higher data rates through the narrow band FM channel, detailed analysis of OFDM/FM systems needs to be performed. Theoretical analysis of multicarrier signals over FM is lacking in literature.
- One of the major drawbacks of OFDM signal is the Peak-To-Average Ratio (PAR) characteristic. High PAR values in OFDM signals require larger dynamic range at the input of

FM modulators. Effects of PAR in OFDM/FM systems have to be analyzed. It is important to develop a PAR reduction algorithm which suits the latency and architectural requirements of LMR applications.

- Most next generation LMR technologies use TDMA/FDMA to provide multiple access amongst individual nodes. Such systems have strict synchronization and control requirements as compared to DDR technology which is based on Carrier Sense Multiple Access (CSMA). A CSMA protocol is well suited for mobile adhoc networks as it de-centralizes the channel access mechanism. In case of DDR I, it was observed that the achievable network throughput was limited due to PTT delays. The characterization of PTT delays and their impact on performance of LMR networks has been neglected in literature.

Thus, the main purpose of this dissertation is development of second generation of DDR technology (DDR II) which provides an integrated service platform, a higher data rate and throughput performance than its predecessor and contemporary LMR standards as highlighted in Table 1-4.

Table 1-4: Comparison between current LMR standards

Technology	Data Rate (kbps)	Traffic Type	Modulation	Addressing	Radio Access Method	TCP/IP Protocol	Compatibility with legacy networks
P 25[1]	9.6	Voice/ Data	C4FM/CQPSK	2 Bytes	FDMA	Supported	No
TETRA[1](I)	7.2	Voice/ Data	$\pi/4$ DQPSK	6 Bytes	TDMA	Supported	No
DDR I [2]	12	Data	M-ary QAM/ OFDM	4 Bytes	CSMA	Inherent	Yes
DDR II [2,3]	14	Voice/ Data	M-ary QAM/ OFDM	4 Bytes	CSMA/ CA	Inherent	Yes

[1] Single Channel, Audioband width= 3Khz [2] Single Channel, Audioband width = 2 KHz [3] Max audioband width = 3 KHz (≈ 21 Kbps)

1.5. Thesis Contributions

To the best of author's knowledge, DDR modem is the only true IP based addressable LMR communication system based on OFDM signals which uses a conventional voice-grade analog FM radio. The work presented in this dissertation is an extension of the author's master thesis titled "Design of a High Data Rate Audioband OFDM modem" [24]. In his master thesis, the author had described the system requirements and design of the first generation of DDR hardware and firmware. In this dissertation, enhancements made to the first generation of DDR firmware and hardware which resulted in a higher data and improved throughput rate for the second generation have been discussed. The primary contributions of the author in the areas of system design, digital communications, signal processing and network theory are summarized below:

- Hardware and software upgrades for the DDR II modem. DDR I was capable of transmitting data alone. Both the software and the hardware were tailored towards supporting data communications. For DDR II, a proprietary hardware board was built to support voice and data traffic. The software framework and modem protocols were extended to facilitate switching between voice and data [17], [21], [22], [25], [26].
- Analytical framework for performance evaluation of OFDM/FM systems. Frequency Modulation is a non-linear modulation scheme as the output of the FM transmitter is not linearly dependent upon the input signal. Theoretical analysis of the FM modulator/demodulator was conducted to calculate the signal-to-noise (SNR) ratio at the output of a FM discriminator.
- Analytical framework to evaluate impact of high PAR of OFDM signal on FM transmissions. A theoretical background of PAR in OFDM signals is presented. The characterization of PAR values and theoretical bounds on PAR, depending upon different M-ary QAM modulation schemes and number of sub-carriers, is presented.
- A Linear Scaling Technique (LST) to improve OFDM/FM performance. A new technique is proposed to mitigate the signal distortion occurring in OFDM/FM systems due to high PAR values. An experimental testbed is built to validate the working of LST. The results obtained using theoretical analysis, simulations and experiments are presented and compared [27],[28].
- Modeling of Push-to-talk (PTT) delays in LMR radio handsets. PTT delays affect the throughput performance of a LMR network. A typical PTT delay observed in LMR handsets ranges from tens to several hundreds of milliseconds. Since the use of LMR networks was traditionally

restricted to voice traffic in which a user provided a de-facto channel access mechanism, the PTT delays were mostly overlooked [16].

- Theoretical model to calculate the collision probability between DDR nodes in a LMR network. Most of the collision analysis found in literature accounts for collision probability based on contention interval which depends on the backoff algorithm implemented. In these cases the collision window is assumed to be limited to few microseconds corresponding to the propagation delays. A PTT delay protracts the collision window to several hundred milliseconds and hence needs to be included in collision analysis [29].
- Highlighted the unintentional denial of service problem (UDOS) in DDR based LMR networks. A PTT delay can be separated into two categories viz Receive-To-Transmit Interval (RTSI) and Transmit-To -Receive Interval (TRSI). RTSI delays can result in an unintentional denial of service (DOS) for a transmitting node in a DDR based LMR network [30].
- Highlighted the Asymmetric Throughput problem in DDR based heterogeneous LMR networks. In a LMR network with nodes having different PTT delay profiles the UDOS can result in asymmetric throughput amongst nodes. This has implications in performance and capacity planning of LMR networks [31].

1.6. Thesis Organization

The dissertation is organized as follows:

- Chapter 2 introduces the system architecture for Distributed Digital Radios (DDR II). It provides an overview of hardware and software upgrades made to the first generation. It also provides an insight into some advantages of using DDR technology.
- Chapter 3 provides an overview on FM technology. This chapter also provides a mathematical model of the FM transmitter and FM receiver. Analytical expressions for signals at the output of FM receiver are also derived.
- Chapter 4 provides an insight into the PAR problem in OFDM signals. Detailed derivation for PAR values observed in case of the OFDM baseband signal used in DDR radios is provided. The large values of PAR result in a non-linear distortion of OFDM signals during to FM transmissions. The resulting deterioration in performance is also provided.
- Chapter 5 introduces the Linear Scaling Technique (LST) for OFDM/FM transmissions. A theoretical model is developed to model the performance of LST in OFDM/FM systems. The

results of simulation are also documents along with the results from the experimental testbed developed.

- Chapter 6 talks about the MAC layer performance. We present the PTT delay values observed for some commonly used LMR terminals along with their distributions. An analytical model for determining the probability of collisions which leads to a denial of service is developed in this chapter. Results using model developed and simulations highlight the asymmetric throughput problem.
- Chapter 7, the research achievements of this work are highlighted and outlined along with recommendations for future work.

References

[1] A. Odima, L Oborkhale and M.Kah, "The trends in broadband wireless network technologies", The Pacific Journal of Science and Technology, May 2007.

[2] K. Pahlavan and A. Levesque, " Wireless Information Networks", 2nd Edition, Wiley Publications 2005.

[3] M. Veeraraghavan, N. Cocker and T. Moors, "Support of voice services in IEEE 802.11 wireless LANs", IEEE INFOCOM, 2001.

[4] _____ , "2G and 3G cellular networks: Their impact on today's enterprise mobility solutions and future mobility strategies" , Motorola White Paper 08.

[5] R. Desourdis *et al.* , "Emerging Public Safety wireless communication systems", Artech House 2002.

[6] _____ , " Statement of Requirements for Public Safety Wireless Comunications and Interoperability", Office of Interoperability and Compatibility, DHS, Vol II , August 2008.

[7] L. Miller, "Wireless Technologies and the SAFECOM SoR for Public Safety Communications", National Institute of Standards, 2005.

[8] M. Taylor,W. Waung and M. Banan, " Internetwork Mobility: The CDPD Approach" , Prentice-Hall, 1996.

[9] M. Khan, " Wireless data over RAM's Mobitex network" , Proc. SPIE Vol. 2601, Dec 1995.

[10] _____ , " APCOs P 25 Radio System", Daniel Electronics, TG 001-200, Jan 2007.

[11] _____ , " TETRA for Public Safety" , Exir Telecom, White Paper, 08.

[12] J. Matthews and W. Michalson, "Distributed Digital Radios (DDR) and WLAN Interoperability", IEEE Conference on Technologies for Homeland Security, May 07.

[13] S. Valcourt *et al*, "System Engineering of of Datacasting for Public Safety Vehicles", IEEE Conference on Technologies for Homeland Security, May 07.

[14] _____ , "VIDA: Network Solutions", Tyco Electronics, White Paper, 2008.

[15] S. Sharp, " Adpating Adhoc Network Concepts in Land Mobile Radio Systems" , Master's Thesis, University of Alberta, 2002.

[16] A.C. Navalekar, W.R. Michalson, J. Kolanjery and J. Matthews , "Effects of Push-To-Talk delays on CSMA based capacity limited LMR networks", IEEE ISWPC, Santorini, Greece 2008.

[17] A.C. Navalekar, W.Michalson and J. Matthews, "Apparatus and Methods for addressable communication using voice-grade radios", Utility Patent, Publication No: WO/2007/002772, April, 2007.

[18] K. Dooley , "Designing Large-Scale LANs" , O'Reilly Publications, 2001.

[19] E.Casas and C.Leung, "OFDM for Digital Communication over mobile radio FM Channels-Part I", IEEE Transactions on Communication, May 1991.

[20] M. Ridder-de Groote, et al. " Analysis of new methods for broadcasting digital data to mobile terminals over an FM channel", IEEE Transactions on Broadcasting, March 1994.

[21] A.C. Navalekar and W. Michalson, "High Data rate Audioband OFDM/FM Modem", Provisional Patent, Serial No. 60/717812, Sep 05.

[22] A.C. Navalekar and W. Michalson, "Design of a OFDM based VHF/UHF Modem", Provisional Patent, Serial No. 60/694878, June 05.

[23] _____ , "Including VOIP over WLAN in a seamless Next- Generation Wireless Enviornment", Texas Insturments, White Paper.

[24] A.C. Navalekar, " Design of High Data Rate Audioband OFDM Modem", Master's Thesis, Worcester Polytechnic Institute, 2006.

[25] A.C. Navalekar, H.K. Parikh, W.R. Michalson and J.W. Matthews, "OFDM based Highdata rate Audioband Modem" , ATA Annual Conf. Denver, CO 2005.

[26] A.C. Navalekar, W.R Michalson and J.W. Matthews, "OFDM based Integrated Transceiver System (OBITS) Modem" , ATA Annual Conf. San Diego, CA 2006.

[27] A.C. Navalekar and W.R. Michalson, " A new approach to improve the BER perfoamnce of a high PAPR OFDM signal over FM based Land Mobile Radios", IEEE WTS, Pomona, CA 2008.

[28] A.C. Navalekar and W.R. Michalson, " A Linear Scaling Technique (LST) for improving BER perfoamnce of a high PAR OFDM signal over LMR networks", *submitted* (*first revision)*, IEEE Trans. on Broadcasting, 2009.

[29] A.C. Navalekar, W.R. Michalson , J.S. Kolanjery and J.W. Matthews, " Effects of PTT delays on Throughput of CSMA/CA based Distributed Digital Radios for LMR networks", IEEE ICPP, Portland, OR, 2008.

[30] A.C. Navalekar and W.R. Michalson, " Effects of Unintentional Denial of Service (DOS) due to PTT delays on performance of CSMA/CA based adhoc LMR networks", ICST Adhocnets, Nigara Falls, CN, 2009.

[31] A.C. Navalekar and W.R. Michalson, " Asymmetric throughput problem due to PTT delays in CSMA/CA based heterogeneous LMR networks", IEEE Milcom, Boston, MA, 2009.

2. Distributed Digital Radios (DDR)

2.1. Introduction

A DDR is a six-way analog radio providing voice over radio frequency (Voice/ RF), voice over Ethernet and data over RF (Data/ RF) connectivity [1]. A DDR handset consists of a baseband modem and a full network protocol stack Ethernet card in addition to typical speaker and microphone circuitry. Figure 2-1, shows a first and second generation of DDR system connected to a commercially available Motorola XTS 5000 series LMR. The baseband electronics of a DDR is contained in a prototype handset along with the interfacing circuitry, and retrofits into a conventional analog FM radio without the need for any modifications to the later [2],[3]. This is true for both fixed (base stations) and mobile or portable radio sets [4]. Each DDR handset supports IP based addressing schemes which enables a DDR based network to be connected with a wired or any of the next generation broadband (4G) technology like WiMAX and LTE [5].

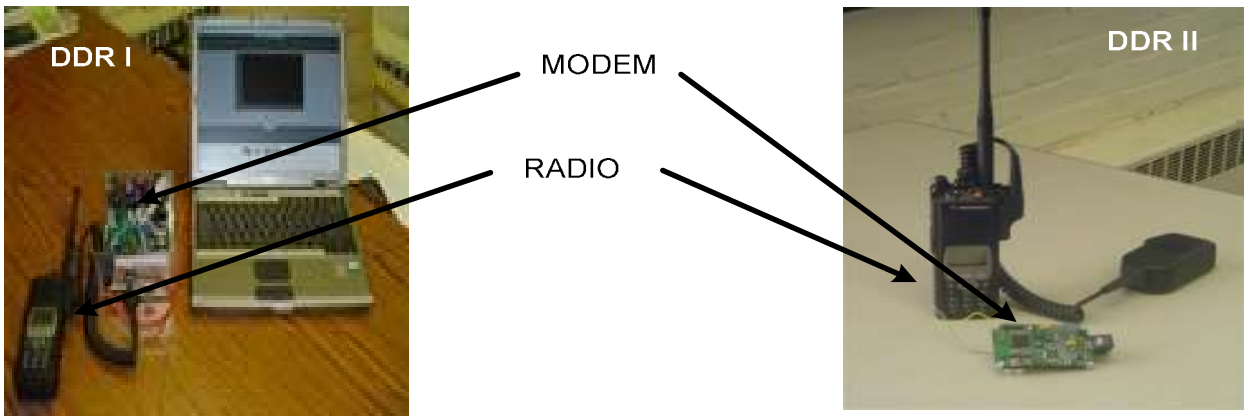

Figure 2-1: DDR I and DDR II prototypes

The DDR handsets have applications in all LMR networks and are of a tremendous value to Public Safety (Law Enforcement/Emergency Medical Services) and military applications. Since the DDRs can be easily deployed in preexisting infrastructure environments, and with equal ease in infrastructure-less environments, they are ideal candidates for deployment by rural Public Safety and military operating in hostile grounds. They also provide novel solutions to the problems of interoperability, multiuser and store and forward utility described in Chapter 1. Sections 2.1.1 and

2.1.2 illustrate the advantages of DDR technology in interoperability and store and forward applications. Sections 2.2 and 2.3 briefly describe the DDR I and DDR II systems. In Section 2.4, key differences between DDR I and DDR II are highlighted.

2.1.1. Interoperability using DDRs

As described in Section 1.3, one of the persistent issues with LMR has been the prevalence of incompatible radio sets and standards [6], [7], [8]. Different radio systems from different manufacturers often contain some proprietary element that makes it difficult, or in some cases impossible, to communicate with other manufacturer's radios in the same network. The impediment may be in a form of different control tones/protocols, different frequency bands of operation or in the very nature of the waveform generated. A real world example of incompatibility due to different frequency bands is situation with the police and fire departments in Boston. The Boston police department uses UHF while the Boston Fire department uses VHF channels.. An example of different waveforms are departments that use APCO P 25 radios which cannot communicate with conventional analog FM radios. Thus, in the event of an emergency, the response teams belonging to different departments may not be able to communicate with each other, resulting in difficulties coordinating people and resources. One way to solve the interoperability issue will be to discard the existing infrastructure and revamp the entire Public Safety infrastructure with a single technology. Another solution will be to equip base stations with an RF conversion and interoperability module (such as an ACU-1000 from JPS Communications). Each of the aforementioned solutions can be prohibitively expensive.

The DDRs provide an elegant solution to address these problems of interoperability due to its IP based addressability [9],[10]. To further elaborate on the interoperability paradigm using DDRs, consider the network shown in Figure 2-2. Assume that all radios are DDRs. Figure 2-2b shows the mesh connectivity for such a network. It can be seen that two independent networks (using different frequencies or different waveform) can be connected to each other via an Ethernet router. It illustrates interoperability between two local public service agencies, the agency discussed above; say the police department and the local fire department. Both agencies have radio networks that have been converted to WLANs with DDRs, but the police and fire operate in different frequency bands. There are two ways to achieve interoperability. The first is over-the-air; for example, the police department has a fire transceiver connected. This transceiver is part of the fire network over-the-air, while

simultaneously being a part of the police network over the Ethernet. It is not necessary for every police officer or vehicle to carry a fire radio, and in the network architecture it is not necessary for any fire personnel to carry a police radio. If broadband is available at each station, the Internet can provide an alternative approach to interoperability [11]. Connecting both ways creates a level of redundancy and reliability. If the fire department has a P25 digital network, or a conventional analog radio network, over-the-air interoperability can still be achieved the same way without the requirement of expensive network overhauls.

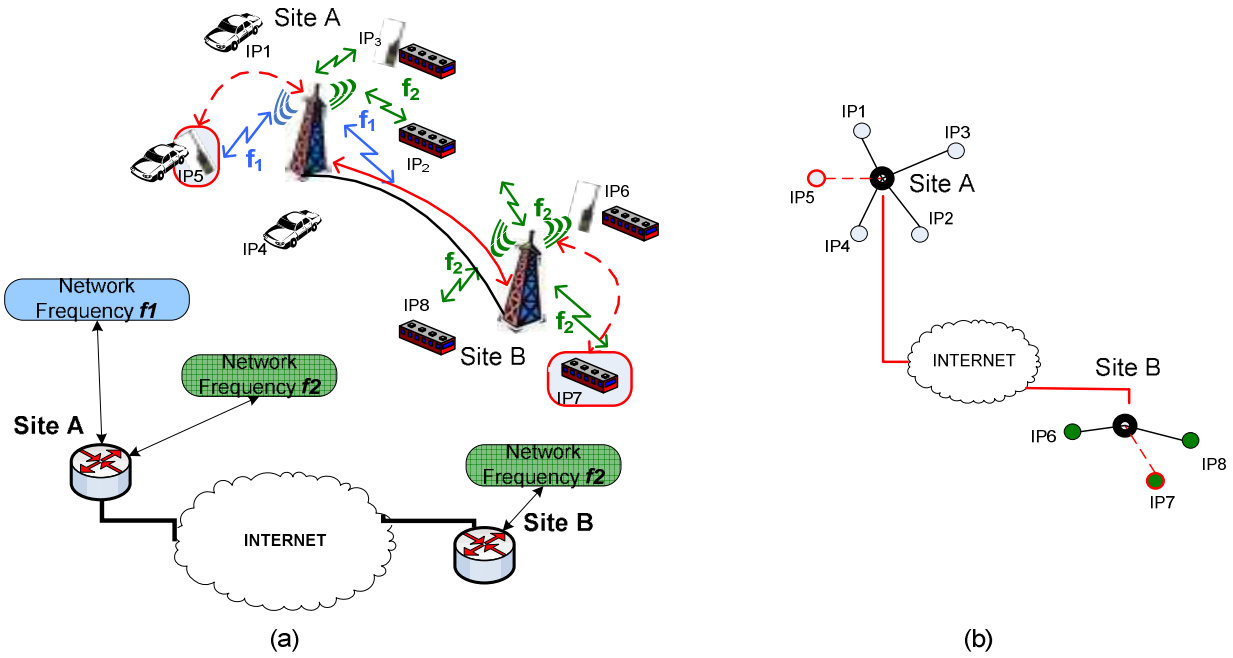

Figure 2-2: DDR Based Interoperability

2.1.2. Multiuser Support

LMR networks support a number of topologies including simplex links to trunking channels. Multiuser support in LMR networks is manifested in form of user/talk groups [1], [6]. One of the ways to form a talk group is by allocating different frequency bands to distinguish between groups. The frequency channel assignment can be either static (pre-configured) or dynamic (trunked). The number of concurrent talk groups in this case is limited by the number of channels available. Another way of forming talk groups is by using different signaling mechanisms like separate squelch tones. A number of solutions like the Continuous Tone-Coded Squelch System (CTCSS) and Digital Coded

Squelch (DCS) exists which use different signaling mechanisms to implement tone based talk groups. The disadvantage of this approach is that it often manufacturers often make their signaling mechanism proprietary, which renders radio sets from different manufactures incompatible. This is not limited to radio handsets, but even the LMR infrastructure. A real world example is Worcester city's police department and the Massachusetts State Police. Both, of these police departments use the same radio handsets and frequency bands. However a radio on the Worcester police network cannot communicate with a radio on State Police network as they use different signaling mechanisms.

A DDR based LMR network provides an easy solution to this problem. As mentioned in Chapter 1, each mobile radio has a unique IP address [2], [4]. Thus a peer-to-peer network can be formed easily by using IP subnets. Radios belonging to same subnets will be able to talk with each other, forming a talk group. Forming a multicast and broadcast domain is equally easy by use of IP filtering. IP based addressability can be used in conjunction with any existing trunking/signaling technology which makes it possible to interoperate with existing infrastructure.

2.1.3. Store and Forward Network using DDRs

Two DDRs can be connected with a short length of Ethernet cable as shown in Figure 2-3 to form a rather sophisticated store-and-forward switch. The DDRs in Figure 2-3 don't have to be interoperable, but the radios on either end of the RF links do. Because packet transmission is governed by a contention access protocol as mentioned in Section 1.2.3, the two radios in Figure 2-3 can operate on the same frequency. By placing store-and-forward switches in strategic locations, close enough together to insure good signal-to-noise ratio (SNR) between switches, a VoIP message, or data, can be relayed great distances or through buildings, or over an inhospitable path without human intervention. Such an application is of great advantages in radio hostile environments like inside mines or over sparsely populated areas where the only available connectivity is through VHF/UHF LMR infrastructure [8].

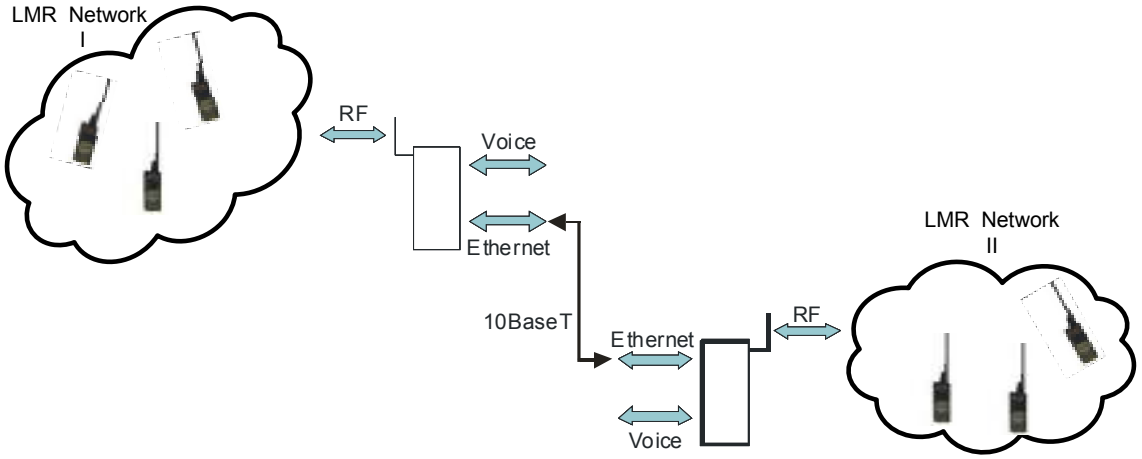

Figure 2-3: Store and forward network using DDR

2.2. First Generation (DDR I)

The DDR project was started at the Center of Advanced Integrated Radio Navigation (CAIRN) Lab, WPI in 2005. This work grew out of a U.S. Army (TATRC) and U.S. Air Force (AFMESA) grants that involved using a VHF/UHF LMRs to transmit critical medical telemetry data from the vehicles of opportunity (ambulance) in remote/hostile geographical areas to the local triage facilities. The objective was to design and build a prototype OFDM modem which is capable of transmitting and receiving data over an UHF/VHF radio link using a standard Ethernet connection and commercial off the shelf (COTS) analog radios. The protocols developed to facilitate data transfer between modems were tailored for communications between the Disaster Relief and Emergency Medical Services (DREAMS) systems.

DREAMS is an telemedicine application developed by Texas A&M University and University of Texas at Huston. It is an advanced telemedicine project designed to speed diagnosis and treatment of critically injured patients. The software developed for the system is capable of both monitoring and communicating critical and non-critical patient information. The DREAMS system is capable of establishing a communication link between the paramedic and physician station using a variety of wireless and wired technologies like cell phones, satellite radio and Ethernet. The OFDM modem developed extended these communication capabilities over VHF/UHF radio links. Figure 2-4 shows the implementation setup for a DDR I modem family device. For more details on DREAMS and DDR I please refer to [4], [12] .

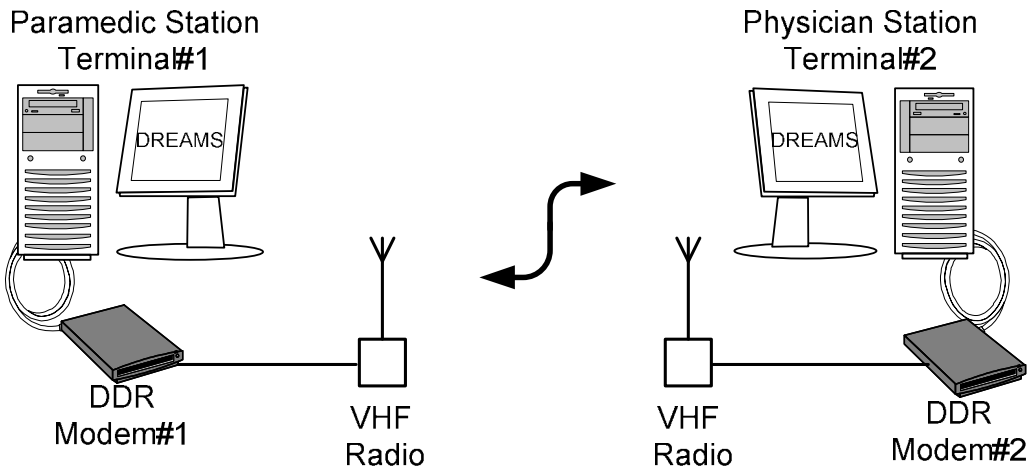

Figure 2-4: DDR I system setup

DDR I modem is comprised of three distinct components: a network card, a baseband modulator/demodulator and a radio interface card. A Netburner SB74 card provided Ethernet connectivity while a 56L307 Motorola DSP EVM was used to modulate data into a baseband OFDM signal. In order to retrofit with a variety of radio interfaces, a reconfigurable daughter card was built which provided interface to a wide range available LMR radios. Figure 2-5 shows the block diagram of modem with its internal and external interfaces. A data terminal interfaces with the DDR I modem using a RJ45 interface. Internally, the communication between the network card and DSP is carried out using RS232 interface. The DSP and Daughter card are connected with each other using an audio codec.

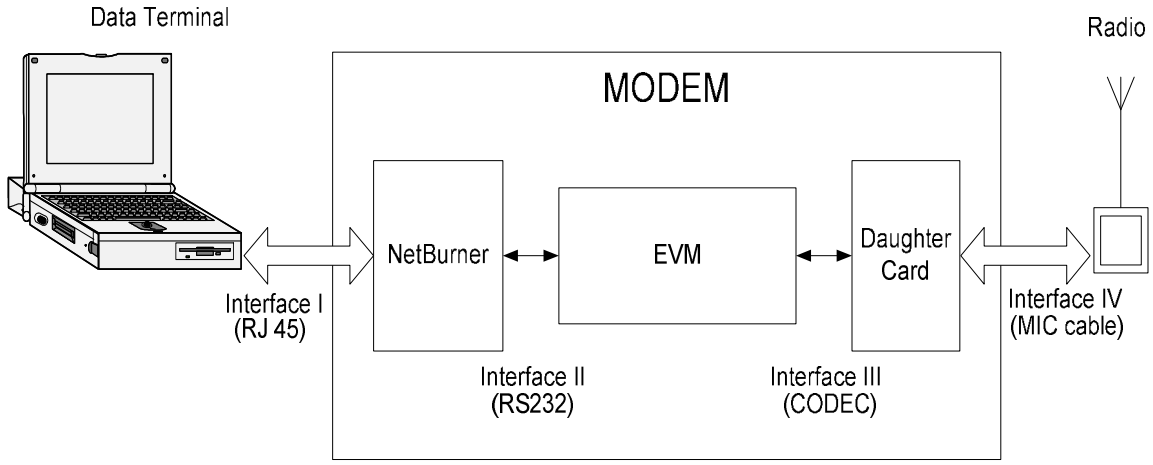

Figure 2-5: DDR I Modem Block Diagram

2.2.1. Limitations

The DDR I modem was capable of transmitting digital data at data rates of up to 12 kbps using a fixed audio bandwidth of 2 KHz. The throughput of DDR I radio was limited due to design constraints such as unknown Push-to-Talk transient delays and the Inter-frame delays of the PHY layer [4]. Furthermore the DDR I modem was designed to transmit data traffic alone and the only way to transmit voice was using a Voice over IP (VOIP) type implementation. The latency associated with data transfers varied depending upon the data priority. The minimum latency associated with data was 300 ms and the maximum value could be as much as 1 second. Needless to say DDR I is not suitable for voice transmissions which have latency requirements in order of 150 ms [13]. In addition to these system limitations, the first generation of DDRs also had physical limitations like the form factor of the device. Since these first generation devices were to be housed in a vehicle and at a EMED's base, there were no restrictions on the dimensions of the modem. Also there was no real-time support to address the problem of distortion of the baseband waveform during transmission due to saturation of the microphone amplifiers. The only way to avoid saturating the FM radio was to ensure that the maximum signal value was lower than the saturation point of the input amplifiers. The same problem existed in receiver as there was no Automatic Gain Control (AGC) implemented. To avoid saturating the codec at the modem, the volume knob was kept well below the maximum output capability of the FM Radio. Thus a tradeoff was made when the DDR I modem was set up between dynamic range of the input signal and quantization noise at the output of the codec [14]. All these factors meant that the performance of DDR I was limited.

2.3. Second Generation (DDR II)

The second generation of DDR radios operates at peak data rates of 14 kbps using an audio bandwidth of 2 KHz. In addition to its default setup, there are provisions to increase the audio bandwidth from 2 KHz to 3 KHz, thereby extending peak data rate to about 21 KHz[1]. It also supports integrated voice/data transmissions. The block diagram for a generic DDR II modem is shown in Figure 2-6.

[1] Using 128 QAM

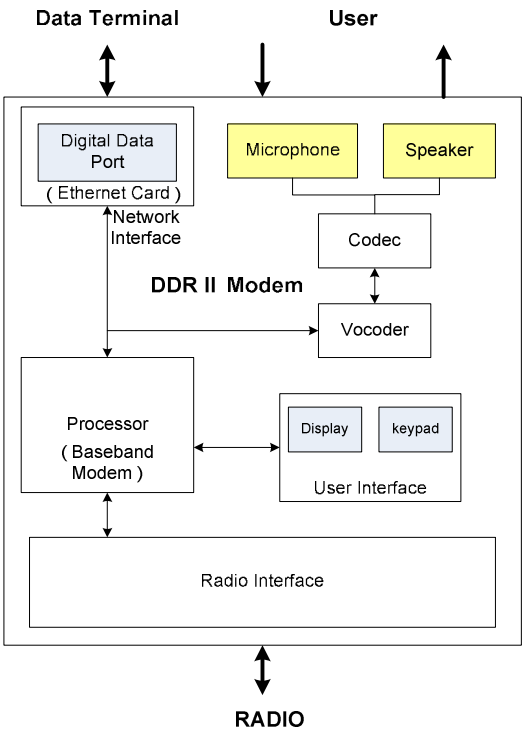

Figure 2-6: DDR II Block Diagram

As seen in the Figure 2-6, the DDR II has three external interfaces. A digital data port serves as a network interface and is used to transmit data to and from the modem and an interfaced data terminal. Here the term data terminal is associated with any device with a network card such as a laptop or a biomedical instrumentation machine which is capable of generating a digital data encapsulated in an IP datagram. The digital data port uses a standard RJ 45 connector. The microphone and speaker assembly which interfaces to a vocoder via codec is used to record/ play voice transmissions. Any information to be transmitted (either data or voice) first needs to be modulated into a baseband signal. The processor implements the modulator/demodulator functionalities of the modem. The digital data to be transmitted is derived from the digital data port while the vocoder sources the voice signals to be transmitted. A user interface provides a mechanism for entering channel, frequency information as an alternative to using the main radio interface in an event that the main radio is inaccessible. A radio interface connects a conventional FM radio to the DDR II modem. This interface module supports a wide range of proprietary FM radio interfaces like an RJ 45 type connector or a $1/8^{th}$ audio plug.

2.3.1. System Architecture

Figure 2-7 shows a typical DDR II setup for transmitting data and voice. The data communication between the terminal and the modem is carried out using Ethernet packets. The communication is directed between the modem and the terminal interfaced with it using the IP addresses of the respective entities. All the data packets which are to be transmitted by the terminal are sent to the IP address of the modem and similarly, all the packets which are received by the modem are sent to the IP address of the connected terminal. The purpose of this setup is to ensure that the applications are not required to keep a track of the IP addresses of other terminals in the system.

There are two ways of assigning IP addresses. One approach is to code the IP address into the modems. This is referred to as static IP allocation. Another approach, which is more flexible, is to dynamically assign IP addresses using the Dynamic Host Routing Protocol (DHCP). For dynamic IP assignment to work, the terminal interfaced with the modem must support DHCP capabilities. The digital data port includes a network card which extracts data payload from Ethernet frames received or encapsulates received data into an Ethernet frame payload. This constitutes the data path shown in Figure 2-7.

For transmitting analog voice signals a conventional speaker/microphone pair is used. Both the speaker and microphone entities are connected to a vocoder. The primary function of this vocoder is to compress the digitized voice signal before being transmitted for efficient utilization of resources. The voice path has been highlighted separately in Figure 2-7. Built-in support for VOIP is not included in the second generation of DDR [16], [17]. Transmission of voice using the IP protocol will traverse the same path as digital data. The baseband is generated by the processor for both, data and voice inputs. Thus the processor implements the Physical (PHY) layer and Medium Access layer (MAC) functionalities. The rest of the components can be seen as I/O subsystems. The radio interface ensures audio signal amplitude compatibility between the baseband modem and external radio.

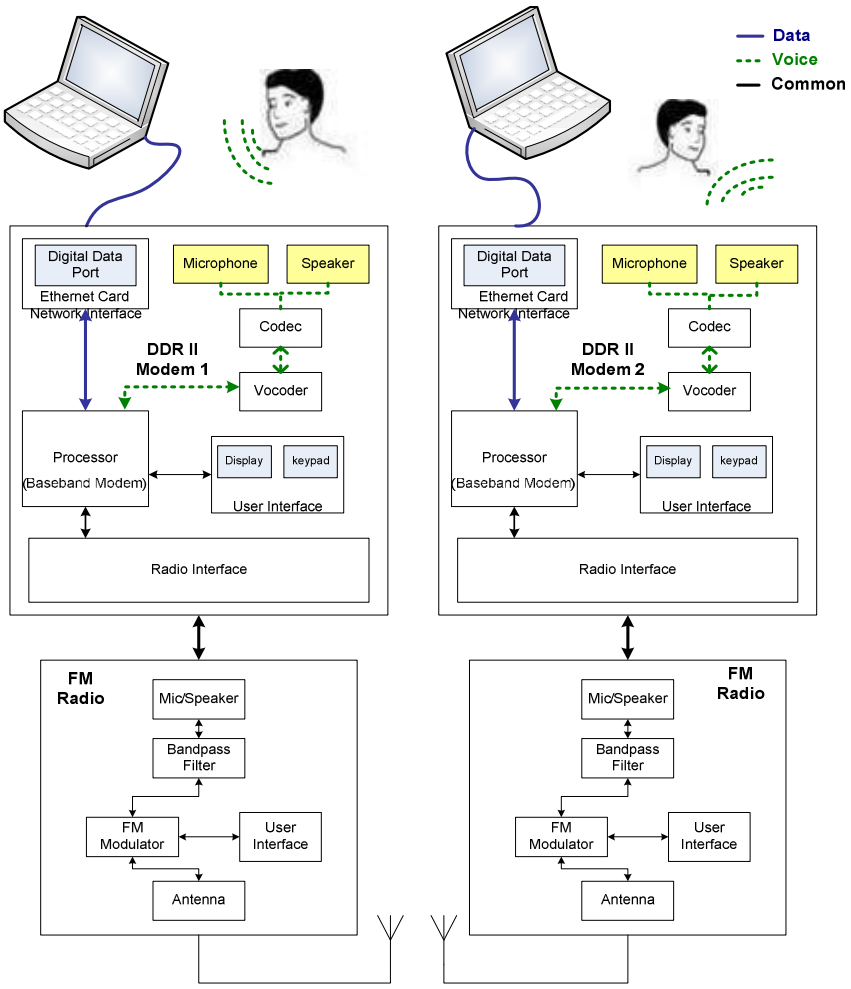

Figure 2-7: Implementation of DDR II modems

The DDR II modem like its predecessor follows the Open Systems Interconnections (OSI) model [18]. The Ethernet card is responsible for packaging the application data into standard network layer protocols like TCP/IP or UDP/IP. The baseband modem acts like a layer two device and therefore deals only with the implementation of the physical and data link layers. The data from the upper layers is repackaged into frames called MAC layer protocol data units (MPDUs). Each MPDU may extend over a number of upper layer packets. DDR II uses a variant of Carrier Sense Multiple Access (CSMA) protocol as a channel access mechanism. This description is valid only for data path. For voice transmissions, the modem acts like a bit pipe only responsible for modulation/demodulation of voice signals. Details of the MAC layer implementation will be discussed in Chapter 6.

The physical layer acts as an interface between the data link layer and the channel. The channel in this context refers to the radio link used by the radios. Each MPDU is broken down into a

number of PHY layer protocol data units (PPDUs). The size of each PPDU is fixed. For more details please refer to [4],[12]. The DDR II uses OFDM to generate baseband audio data. The modulation schemes supported are BPSK and M-ary QAM (M=16, 64, 128). It uses a rate ½ convolutional encoding to provide forward error correction (FEC). Use of OFDM presents a spectrally efficient means of transmitting data. Details of use of OFDM over FM channels are discussed in Chapter 3 and 4.

2.3.2. Hardware Architecture

Figure 2-8 shows the hardware implementation of DDR II radios. As seen in the figure, DDR II is a hybrid architecture consisting of both COTS and custom hardware. Based on functionality, it can be divided into two sub-systems; one which implements I/O functions and a second which performs the signal processing. I/O functions include both voice and data channels. A Netburner SB-72 network card is used to provide the I/O subsystem for Ethernet data. As shown in the figure, a network card consists of an Ethernet PHY layer frame extractor and a Motorola ColdFire series microprocessor. The microprocessor implements the Ethernet protocol stack. In case of voice, signals a TLV320AIC12k codec in conjunction with an Advanced Multiband Extraction (AMBE) vocoder, constitutes an I/O subsystem. The AMBE vocoder supports various bit rates from 2 kbps to 9.6 kbps [15]. In the current implementation bit rate of 9.6 kbps is used with rate ½ FEC. Both the Motorola ColdFire and AMBE vocoder is connected to an Atmel ATmega128L microcontroller. The Motorola ColdFire processor interfaces with the microcontroller using a serial port which uses the RS-232 protocol while the vocoder uses general purpose I/O (GPIO) pins. The microcontroller acts as an arbiter of channel access between data and voice. In the current implementation, voice transmissions have a higher priority than data transmissions [19],[20].

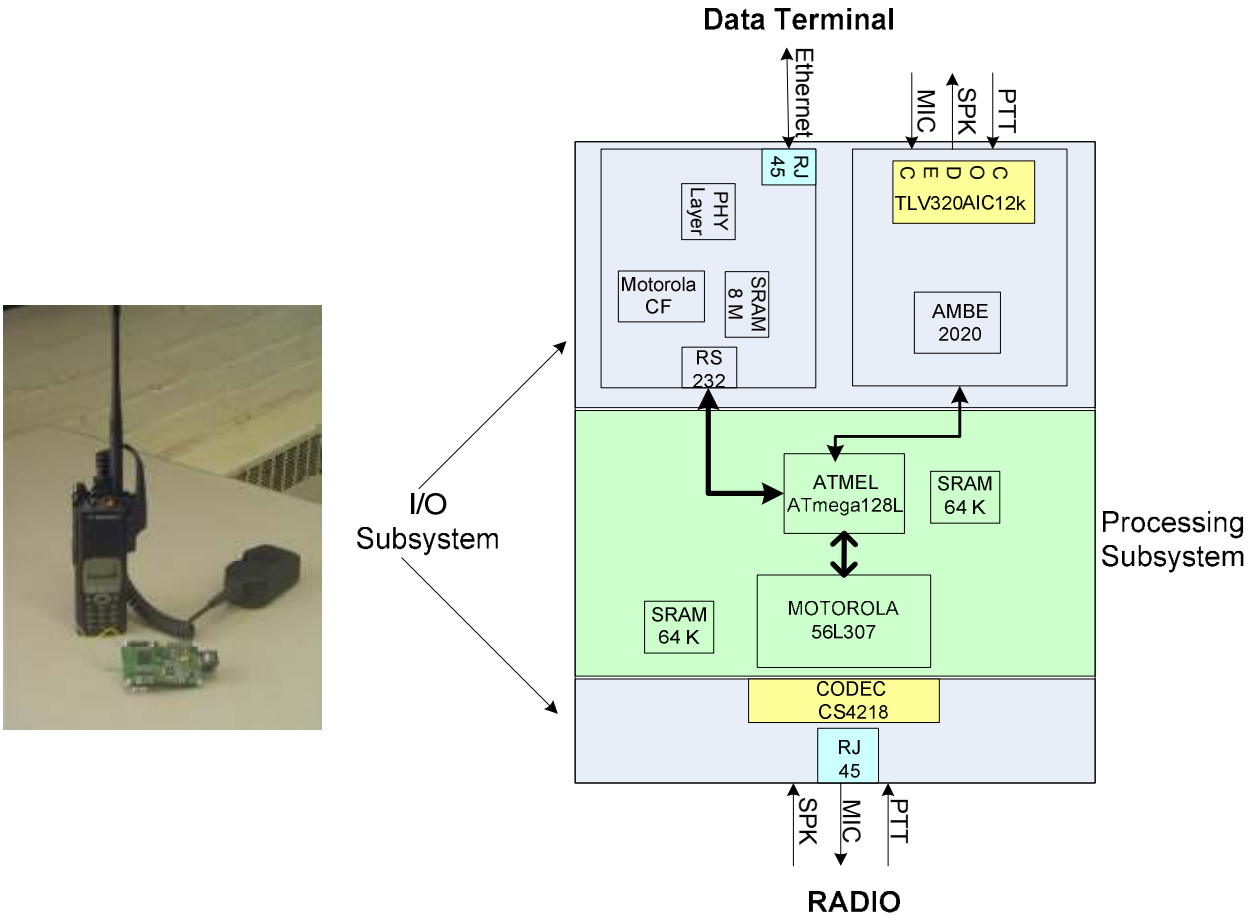

Figure 2-8: Hardware Implementation

The microcontroller is responsible for reformatting the data and voice signals into a native MPDU format which is then sent to the Motorola 56L307 DSP for modulation. The Motorola 56L307 implements the modulation and demodulation functions of the modem. Together with the ATMEL microcontroller it forms the processing subsystem. The DSP also interfaces with another codec (CS4218) which primarily acts as an A/D and D/A conversion interface to the radio. In addition to the microphone and speaker interface there exists a Push-To-Talk (PTT) interface. The primary objective of this signal is to assert and de-assert the push-to-talk line on the FM radio. For voice signals the user provides PTT input while for data signals the microprocessor itself asserts this input. The PTT signal is one of the important interface signals as most conventional analog FM radios are operated in a half duplex mode. When the PTT signal is de-asserted the FM radio acts as a receiver and when the PTT signal/switch is asserted, the FM radio transmits an FM signal.

2.3.3. Software Architecture

The DDR I and DDR II both use the same software framework, the key difference being support for voice transmissions. The microcontroller processes transmit requests from both data and voice paths and also acts as an arbiter for channel access in the event that both data and voice are available for transmission. The modems have three distinct operating modes as shown in the state diagram in Figure 2-9, the "listen" mode (State 0), the "receive" mode (State 1) and the "transmission" mode (State 2). Due to the half duplex nature of the radio link, the modem never receives and transmits at the same instant. The details on the implementation of the software architecture for the microcontroller and the entire voice/data channel are beyond the scope of this dissertation. For details on implementation of modulation/demodulation modules, inter-module communications and handshaking protocols please refer to [4],[12],[15]- [20].

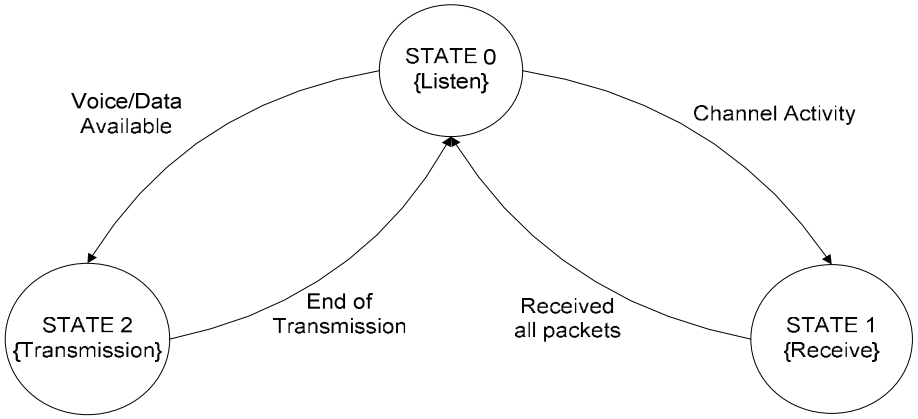

Figure 2-9: Modem states

2.4. Differences between DDR I and DDR II

In addition to different hardware implementations, DDR II implements a more complete set of software defined radio enhancements than the DDR I handsets. Software differences include changes to support a variable physical layer frame size and automatic gain control. These enhancements impact both the physical layer and MAC layer performances resulting in a better bit error rate (BER) and higher throughput. Some of the important changes are presented in the following sections.

2.4.1. Baseband Amplitude Adjustment

One of the important differences between DDR I and DDR II modems is amplitude control of the generated baseband audio signal. The transmitter and the receiver of a conventional FM radio are sensitive to the amplitude of the baseband signal. In case of the transmitter, a high amplitude baseband signal will be clipped, resulting in a harmonic distortion of the baseband signal which leads to a deterioration in system performance. This is referred to as to modulation sensitivity and is explained in Chapter 5 [21]. There are two ways to ensure that the input baseband signal is not clipped. For one approach, the maximum amplitude of the generated signal is compared with the standard optimum value. Depending upon the signal amplitude, the baseband signal is scaled. This assumes that the optimum value for the interfaced radio is known beforehand. The second approach is use a calibration mode. In this mode the transmitter transmits a known sequence of data.

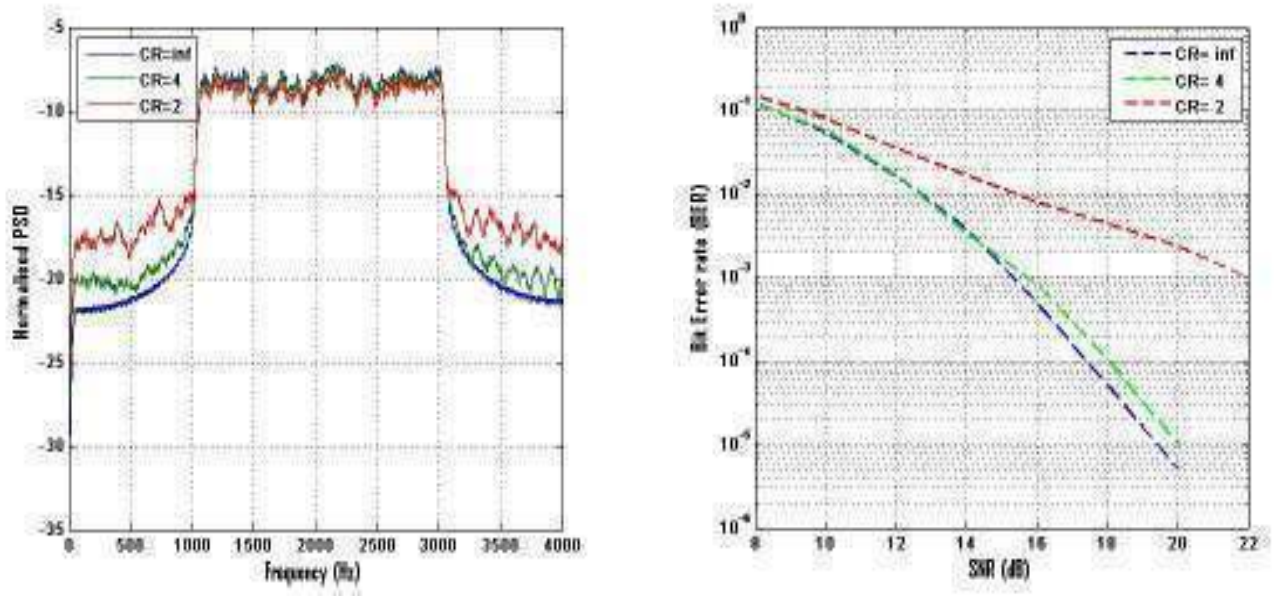

(a) (b)

Figure 2-10: Effects of clipping (a) spectrum of baseband signal (b) BER performance

The received signal is demodulated by the receiver and the resulting BER is communicated back to the transmitting station. This feedback mechanism allows the transmitter to adjust the baseband signal until an acceptable BER is achieved. Figure 2-10, shows the impact of clipping on spectrum of audio baseband signal and the resulting degradation in BER for a DDR II modem. The term *CR* stands for clip ratio which is defined as ratio of clipping amplitude to the RMS values of signal ($CR = A_c/\sigma_x$).

2.4.2. Baseband Signal Generation

Both the first and second generation of DDR radios use OFDM to generate an audio baseband signal. In the case of DDR I, the baseband OFDM symbol is a complex signal with the real part corresponding to in-band (I) channel data and imaginary part corresponding to the quadrature-band (Q) channel data. In order to ensure that no information is lost, the baseband OFDM symbol has to be upconverted to a suitable passband. The need for upconversion arises due the frequency characteristics of the radio which is designed for the transmission of voice signals. The frequency response of the radio can be equated roughly to that of a bandpass filter with cut off frequencies at 300 Hz and 3.3 KHz [4]. The upsampling process involves interpolating the signal followed by lowpass filtering. The resulting complex signal then undergoes I/Q modulation with an audioband carrier frequency of 2 KHz. For embedded systems, use of a filtering process followed by upconversion can be expensive in terms of processor cycles (≈ 8500 MACS/symbol for DDR I). In the DDR II the need for upconversion is eliminated by generating a real passband signal at the output of OFDM modulator block itself. This is achieved by using a higher size IFFT operation such that it covers the entire audio frequency spectrum. Since the IFFT code is highly optimized, the total time and processor cycles expended in generating the baseband OFDM signal for DDR II is much lower (≈ 1500 MACS/symbol) than that required for DDR I. The mathematical representation of the real OFDM signal is presented in Chapter 4.

2.4.3. Variable Audio Bandwidth

In the case of DDR I, the audio bandwidth was restricted to 2 KHz. Modifying the bandwidth would require multiple filter coefficient banks [4]. In the case of DDR II, due to the OFDM modulation scheme implemented (as described in Section 2.4.2), it is easier the provide support for variable bandwidth configurations. This can be accomplished by selectively loading the required sub-carriers which will be explained in Chapter 4.

2.4.4. Automatic Gain Control

The BER observed for a received signal depends upon the signal to noise ratio (SNR) at the audio baseband [21]. In a DDR system the baseband SNR depends upon the received signal strength, volume settings of the FM radio and the input saturation voltage of the codec on the radio interface

card. The SNR at the input of FM radio depends upon the signal power which is function of channel characteristics. The optimum setting for the volume control depends upon both the received signal power and the saturation voltage of the codec. In DDR I radios, the volume setting was fixed such that under good signal power conditions the output audio signal did not saturate the codec input. Thus, a tradeoff was made between the dynamic range of the input signal and the quantization noise at the output of the codec [14]. However, this resulted in a SNR that was lower than the optimum value for most of received signal. Figure 2-11, plots the impact of decreased dynamic range at codec input on the quantization noise at codec output, depending upon the bit resolution of the codec. In DDR II radios, the low noise amplifier (LNA) in the input codec is used as a gain block to obtain a higher baseband SNR. The modem computes the energy of the baseband signal and varies the input gain settings of the codec using the implemented codec APIs, thus providing an automatic gain control mechanism. For details on the APIs refer to the code documentation [19],[20].

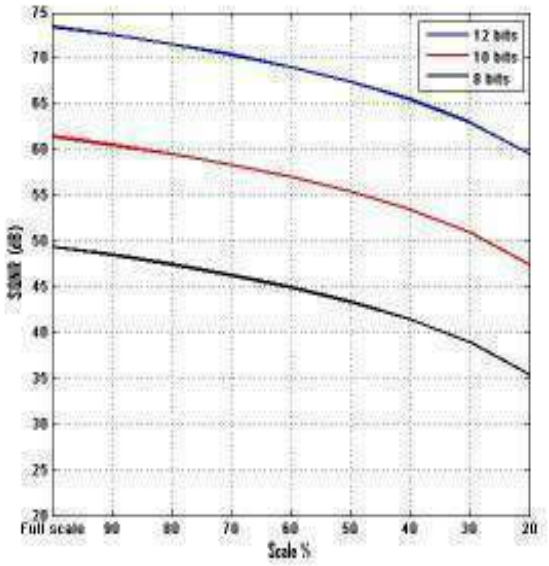

Figure 2-11: Effects of decrease in dynamic range of input signal at codec on signal-to-quantization-noise ratio (SQNR).

2.4.5. Channel Accesses for Voice/Data traffic

In order to ensure fair access to the channel and to ensure that no single radio would occupy the channel for extended durations, the number of MPDUs per transmission in DDR I modem was limited to a certain maximum number. This was possible because the modem was catering to only

data traffic and had complete control over the traffic. However, for DDR II, in case of voice transmission the user assumes the role of channel arbiter and hence there can be no limit to the number of MPDUs transmitted per PTT cycle. Further, to ensure minimum latency for voice channel, there are no random backoff delays associated with voice transmissions. This means that the channel access mechanism is user-based for voice transmissions [16],[17]. In DDR I, the handshaking protocols between various components assumed data traffic. To provide support for voice signals in DDR II, these handshaking protocols were extended to include voice frame exchanges [15]-[17].

2.5. Chapter Summary

DDR technology is a high data rate, audioband, IP based modem technology for next generation LMR networks. The second generation of DDR technology supports peak data rates of 4/8/12/14 kbps using 2 KHz of audio bandwidth with provisions to increase the audio bandwidth up to 3KHz. It also supports a full TCP/IP and UDP/IP protocol suit for data transmission. It provides novel solutions to the problems of interoperability, multiuser support and store-and-forward capabilities. In this chapter we introduced the first generation of DDR technology and discussed some of the limitations. This was followed by a detailed description of the system, hardware and software architecture for the 2nd generation DDR modems. Important improvements in this 2nd generation were also highlighted.

References

[1] J. Matthews and W. Michalson, "Distributed Digital Radios (DDR) and WLAN Interoperability", IEEE Conference on Technologies for Homeland Security, May 07.

[2] A.Navalekar, W.Michalson and J. Matthews, "Apparatus and Methods for addressable communication using voice-grade radios", Utility Patent, Publication No: WO/2007/002772, April, 2007.

[3] A.C. Navalekar and W. Michalson, "High Data rate Audioband OFDM/FM Modem", Provisional Patent, Serial No. 60/717812, Sep 05.

[4] A.C. Navalekar, " Design of High Data Rate Audioband OFDM Modem", Master's Thesis, Worcester Polytechnic Institute, 2006.

[5] A. Odima, L Oborkhale and M.Kah, "The trends in broadband wireless network technologies", The Pacific Journal of Science and Technology, May 2007.

[6] R. Desourdis *et al.* , "Emerging Public Safety wireless communication systems", Artech House 2002.

[7] S. Valcourt *et al*, "System Engineering of of Datacasting for Public Safety Vehicles", IEEE Conference on Technologies for Homeland Security, May 07.

[8] L. Miller, "Wireless Technologies and the SAFECOM SoR for Public Safety Communications", National Institute of Standards, 2005.

[9] A.C. Navalekar, H.K. Parikh, W.R. Michalson and J.W. Matthews, "OFDM based Highdata rate Audioband Modem" , ATA Annual Conf. Denver, CO 2005.

[10] A.C. Navalekar, W.R Michalson and J.W. Matthews, "OFDM based Integrated Transceiver System (OBITS) Modem" , ATA Annual Conf. San Diego, CA 2006.

[11] A.C. Navalekar, W.R Michalson and J.W. Matthews, "VHF/UHF Interoperability Demo", American Ambulance Association Annual Convention, Las Vegas, NV 2005.

[12] G. Hammouri, "OBITS Modem: Netburner Daughter Card Interface" , CAIRN Lab, WPI 2005.

[13] _____ , "Including VOIP over WLAN in a seamless Next- Generation Wireless Enviornment", Texas Insturments, White Paper.

[14] J. Proakis and D. Manolakis, "Digital Signal Processing", 4th Edition, Prentice Hall, 2006

[15] T. Pollard , " System Hardware and Software specifications for Atmel Bridge", CAIRN Lab, WPI 2006.

[16] T. Pollard and A.C. Navalekar, " Inter-Module Communications Specifications" , CAIRN Lab, WPI 2006.

[17] T. Pollard and A.C. Navalekar, "Modem Simulator Specifications", CAIRN Lab, WPI 2006.

[18] A. Tanenbaum, "Computer Networks", 4th Edition, Prentice-Hall,2002

[19] A.C. Navalekar, \\farad.ece.wpi.edu\cairn\P4_Depot\OBITS , CAIRN Lab, WPI.

[20] T. Pollard, \\farad.ece.wpi.edu\cairn\P4_Depot\AMBE_Card_Rev1, CAIRN Lab, WPI.

[21] K. Pahlavan and A. Levesque, " Wireless Information Networks", 2nd Edition, Wiley Publications 2005.

[22] D. Sakrison, "Commication Theory: Transmission of Waveforms and Digital Information", Wiley Publications, 1968.

3. FM System Analysis

3.1. Introduction

As mentioned in Chapter 1, many legacy networks like LMR and AMPS used FM modulation due to the constant signal envelope and a higher immunity to noise as compared to AM signals. FM systems have been studied extensively in past [1], [2], [3]. Various aspects of FM systems like the bandwidth of FM signals, performance of different data modulation schemes and performance in presence of fading have been documented in literature [4]-[9]. The use of OFDM for digital communication over mobile radio FM channels was studied in [10], [11]. OFDM transmission over LMR networks was first proposed in [12].

In a DDR system, an OFDM signal is used as a baseband modulating signal which, in turn, generates an FM signal. Most of the performance studies available for OFDM/ FM systems evaluate the performance of OFDM over FM systems in presence of Rayleigh fading and different data modulation schemes [10]-[13]. These analyses assumed that the amplitude of baseband signal is below the clipping threshold of the FM transmitters and hence no non-linear distortion is introduced in the baseband signal.

The clipping of baseband signals is of great importance in OFDM systems due to their high peak-to-average ratio (PAR) [14], [15]. A number of PAR reduction techniques for OFDM signal have been proposed [16], [17], [18]. However, to the best of author's knowledge the impact of clipping of a high PAR OFDM signal on an FM system has not been well-studied [19], [20]. In the case of DDR systems, characterizing the non-linear distortion of OFDM signals in FM systems will help mitigate any performance degradation resulting from clipping and will aid in improving the data rate and BER performance of DDR II which is one of the objectives behind the development of second generation DDR technology, as mentioned in Chapter 1.

The PAR problem for an OFDM waveform will be introduced in Chapter 4. The frameworks developed in Chapter 3 and 4 will be used in Chapter 5 to develop a scaling algorithm to mitigate the impact of distortion of a high PAR OFDM on the BER performance of DDR system. In this chapter, an analytical framework is developed for calculating the signal-to-noise ratio at the FM receiver and its relationship with the bandwidth of an FM signal. Section 3.2 introduces frequency modulation technology followed by a discussion on FM signal bandwidth in Section 3.3. Sections 3.4 and 3.5

briefly describe the FM transmitter and receiver structures. The expression for SNR of an FM receiver is derived in Sections 3.6 and 3.7.

3.2. Frequency Modulation

In frequency modulation the frequency of the carrier is modulated according to the strength of the modulating signal. Furthermore, the amplitude and phase of the signals remain constant while the frequency shifts back and forth about the center frequency. For a true FM signal, the variation in carrier frequency is a function of the amplitude of the modulating signal alone [2]. The frequency of the modulating signal determines the rate at which the frequency changes take place, but exerts no influence on the extent of the changes [1],[2]. The mathematical representation of an FM signal is given by 3-1.

$$z(t) = A_c \cos(\omega_c t + {}^{\omega_d}\!/_{k'} m_i(t)) \qquad \textbf{3-1}$$

where $m_i(t) = {}^{1}\!/_{k''} \int_0^t m(\tau) d\tau$, ω_c is the carrier frequency, $f_d = \omega_d/2\pi$ is the maximum frequency deviation, k' is a normalization constant and $m(t)$ represents the baseband modulating signal. Substituting value of $m_i(t)$ and $k_m = k'k''$ in 3-1, we get

$$z(t) = A_c \cos(\omega_c t + {}^{\omega_d}\!/_{k_m} \int_0^t m(\tau) d\tau) \qquad \textbf{3-2}$$

The instantaneous frequency, f_i, can be calculated as shown below

$$f_i = \frac{1}{2\pi}\frac{d}{dt}(\omega_c + {}^{\omega_d}\!/_{k_m} \int_0^t m(\tau) d\tau) \qquad \textbf{3-3}$$
$$= {}^{1}\!/_{2\pi}[\omega_c + {}^{\omega_d}\!/_{k_m} (m(t))]$$

From 3-3, we observe that the frequency deviation of the carrier, $\Delta f = f_c - f_i$, is proportional to the baseband modulating signal ($\Delta f \propto m(t)$). Consider a sinusoidal baseband signal given by

$$m(t) = A_m . \cos(\omega_m . t) \qquad \textbf{3-4}$$

where f_m represents the baseband sinusoid frequency and A_m is the amplitude of the baseband signal. Without loss of generality assume A_m is unity, under these assumptions, 3-2 reduces to

$$z(t) = A_c \cos(\omega_c t + \frac{\omega_d}{\omega_m} . \sin(\omega_m . t)) \qquad \textbf{3-5}$$
$$= A_c \cos(\omega_c t + \beta . \sin(\omega_m . t))$$

where $\beta=f_d/f_m$ is referred to as the modulation index. For a sinusoidal baseband signal, the modulation index, β, relates the bandwidth of the FM signal to the strength and frequency of the modulating signal as will be seen in Section 3.3

3.3. Bandwidth Calculation

Consider an FM signal, *z(t)* given by 3-1. The spectrum of *z(t)* is not simply determined by the spectrum of the baseband signal, *m(t)*. This is because an FM signal is a non-linear function of *m(t)*. Depending upon the nature of the modulating baseband signal it is possible to approximate the bandwidth of an FM signal [4],[6]. The most commonly derived expression for FM bandwidth assumes a sinusoidal baseband signal. Consider the FM signal given by 3-5

$$\begin{aligned} z(t) &= A_c \cos(\omega_c t + \beta \sin(\omega_m t)) \\ &= \mathrm{Re}\{A_c e^{j\omega_c t} e^{j\beta \sin(\omega_m t)}\} \end{aligned} \quad \textbf{3-6}$$

Consider the term $f(t)= e^{j\beta \sin(\omega_m t)}$ in 3-6 . The exponential Fourier series for $f(t)$is given by 3-7.

$$f(t) = \sum_{n=-\infty}^{\infty} D_n e^{jn\omega_0 t} \quad \textbf{3-7}$$

$$\begin{aligned} D_n &= \frac{1}{T_0}\int_{T_0} f(t) e^{-jn\omega_0 t} dt = \frac{1}{T_0}\int_{T_0} e^{j\beta \sin(\omega_m t)} e^{-jn\omega_0 t} dt \\ &= J_n(\beta) \end{aligned}$$

Where the coefficients $J_n(\beta)$ are Bessel functions of the first kind and are of order n. From 3-7 and 3-8, we can obtain an expression for *z(t)* as shown below

$$\begin{aligned} z(t) &= \mathrm{Re}\{A_c e^{j\omega_c t} e^{j\beta \sin(\omega_m t)}\} = \mathrm{Re}\{A_c e^{j\omega_c t} \sum_{n=-\infty}^{\infty} J_n(\beta) e^{jn\omega_m t}\} \\ &= \mathrm{Re}\{A_c \sum_{n=-\infty}^{\infty} J_n(\beta) e^{j(\omega_c + n\omega_m)t}\} \end{aligned} \quad \textbf{3-8}$$

Using the frequency shifting property $e^{j\omega_0 t} f(t) \xrightarrow{F} F(\omega-\omega_0)$, the Fourier transform of 3-8 can be calculated as shown below

$$Z(\omega) = \sum_{n=-\infty}^{\infty} \frac{A_c J_n(\beta)}{2} [\delta(\omega + \omega_c + n\omega_m) + \delta(\omega - \omega_c - n\omega_m)] \quad \textbf{3-9}$$

From 3-9, we observe that the number of sidebands is infinite and the bandwidth required to encompass a sinusoidally modulated FM signal is also infinite. However in practice, for a given value

of modulation index, β, a large fraction of the total power lies within some finite bandwidth [2]. This is because, except for $J_o(\beta)$, each $J_n(\beta)$ diminishes as n increases as seen in Figure 3-1. A good approximation for the bandwidth of FM signal, $z(t)$, is given by the Carson's Rule [2] shown below:

$$B = 2(\Delta f + f_m) \quad \textbf{3-10}$$

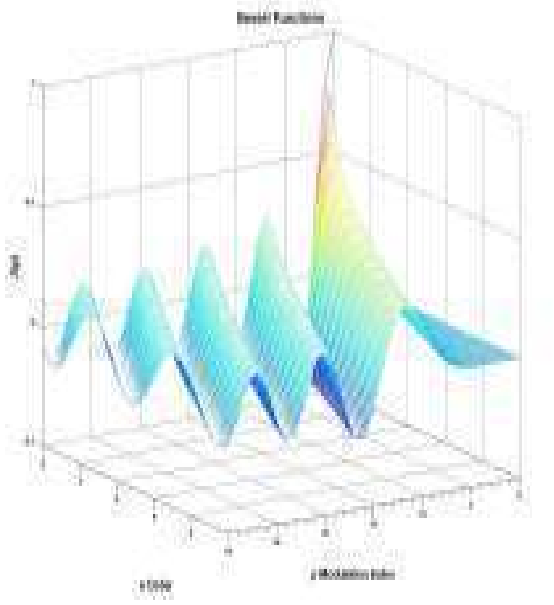

Figure 3-1: Bessel functions $J_n(\beta)$

Many FM systems use modulating signals which are not simple sinusoids. For example, LMR systems mostly transmit voice signals which can be modeled as bandpass signals between 300 Hz and 3.3 KHz. In DDR systems, the baseband signal is an OFDM waveform which can be considered as the superposition of orthogonal sinusoids [10], [13]. It has been proven in [14], [15] that for higher values of IFFT size (N), a baseband OFDM signal can be modeled as a Gaussian process with zero mean. [4], [6] give a mathematically rigorous derivation for the RMS bandwidth of an FM signal generated by a generalized Gaussian Random Process (GRP). For DDRs, we are interested in only a small subset of GRPs with zero-mean and with constant and finite second order statistics (Wide Sense Stationary). In Appendix A, we present a new method for the derivation of RMS bandwidth under the aforementioned assumptions. The objective of the derivation is to provide a mathematical validation for the bandwidth of an OFDM/FM signal. In this section only the important results are highlighted.

Consider an FM signal modulated by a Gaussian baseband signal.

$$\begin{aligned} z(t) &= A_c \cos(\omega_c t + u(t)) \\ &= A_c \operatorname{Re}\left\{ v(t) e^{j\omega_c t} \right\} \end{aligned} \quad \textbf{3-11}$$

where $u(t) = \omega_d / k_m \int_0^\tau m(\zeta)d\zeta$, $v(t)=e^{j\,u(t)}$ and $m(t)$ represents the zero-mean, WSS Gaussian process with variance σ^2_x. We can compute power spectral density (psd) for $z(t)$ by calculating the autocorrelation $R_z(\tau)$ and then using the Wiener-Kinchin theorem [21] to calculate $S_z(f)$ followed by computing the RMS bandwidth $\bar{f}_v$ as given below

$$R_z(\tau) = (A_c^2/2)\cos(\omega_c\tau)e^{-(\sigma_Q^2(\tau)/2)} \qquad \textbf{3-12}$$

$$\bar{f}_v^2 = f_d^{\,2}/k_m^2\, R_x(0) \Rightarrow \bar{f}_v = f_d\sigma_x/k_m$$

From 3-12, we observe that the RMS bandwidth of the FM signal, $\bar{f}_v$ depends on the maximum frequency deviation f_d, proportionality constant k_m and RMS value of the modulating baseband signal, σ_x. Thus, for a constant ratio f_d/k_m, the RMS bandwidth will depend upon the RMS value of the modulating signal.

3.4. FM Transmitter Structure

An FM transmitter converts the modulating baseband signal into a frequency modulated RF output signal. The most common method of generating an FM signal is referred to as the direct method. In the direct method, the frequency of the oscillator is varied directly by the modulating signal while the indirect method the modulating frequency modifies the phase of the carrier waveform. A typical block diagram for an FM transmitter using Direct Method is shown in Figure 3-2.

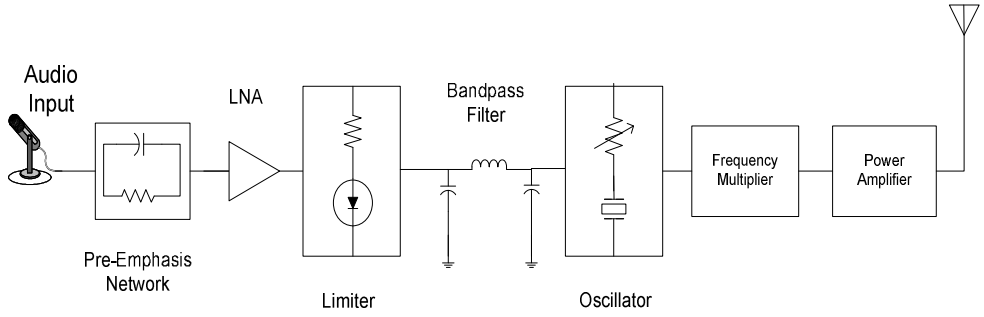

Figure 3-2: FM transmitter (Direct FM)

The microphone audio signal is feed to a pre-emphasis network, which amplifies signal power at higher frequencies. This compensates for poorer signal-to-noise ratios at the higher frequencies due

to low pass filtering which occurs in the FM receiver [2]. The pre-emphasized signal is then amplified by a low noise amplifier and passed through a peak limiter circuit. The main purpose of the peak limiter circuit is to clip the strength of modulating signal so as to limit the maximum deviation to f_d [3].

Figure 3-3a, shows the non-linear response observed for an ICOM IC-T7H LMR. It can be seen that the maximum input signal amplitude is about 100 mV (≈ 200 mV_{p-p}). If input signal amplitude exceeds this value, it is clipped. The clipping process generates audio harmonics which must be filtered before they modulate the oscillator. This is achieved by the bandpass filter which has a pass band between 300 Hz – 3.3 KHz corresponding to the audio frequencies of interest. Figure 3-3b shows the frequency response observed for the ICOM IC-T7H radio. The audio signal is then applied to the varactor of the oscillator resulting in a frequency of oscillation proportional to the strength of modulating signal. The output of the oscillator is then upconverted to the required carrier frequency. This frequency modulated waveform is then amplified before being transmitted. The frequency spectrum of the FM signals must fall within the FCC transmit mask for Narrowband FM channels as shown in Figure 3-4a. Figure 3-4b shows the spectrum of the FM signal at the output of a DDR. As seen from figure the signal generated by DDR satisfies the FCC regulations.

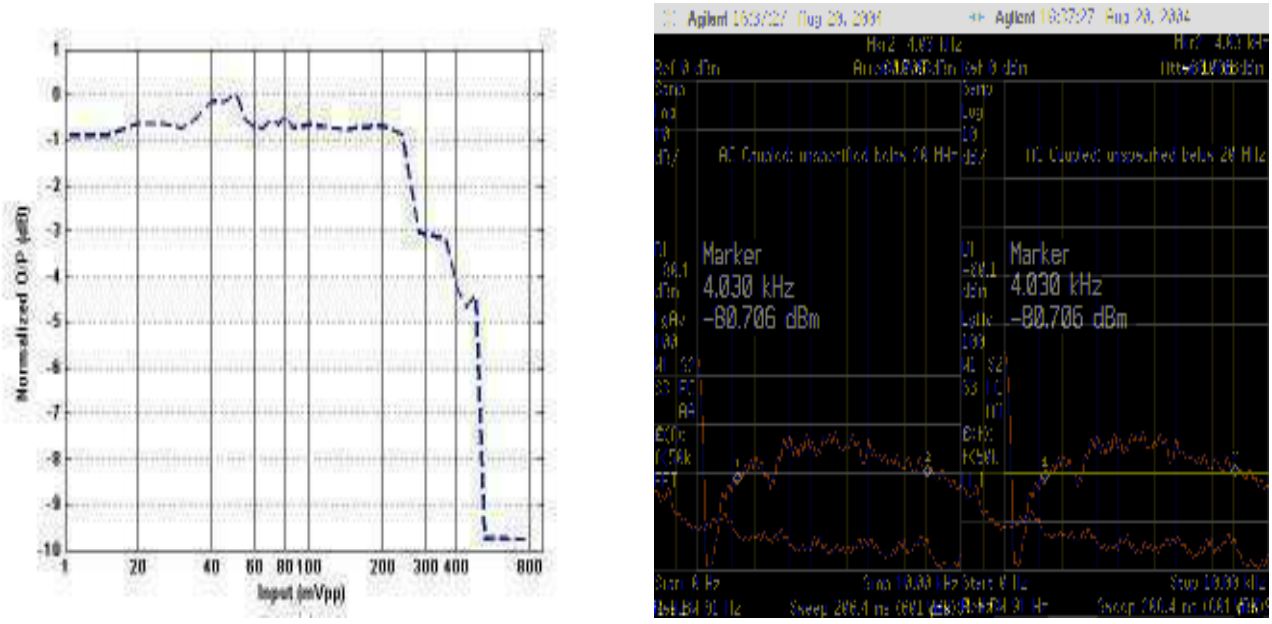

(a) **(b)**

Figure 3-3: (a) Non-linear response in ICOM T7H FM transmitter, (b) Frequency respone observed for ICOM T7H

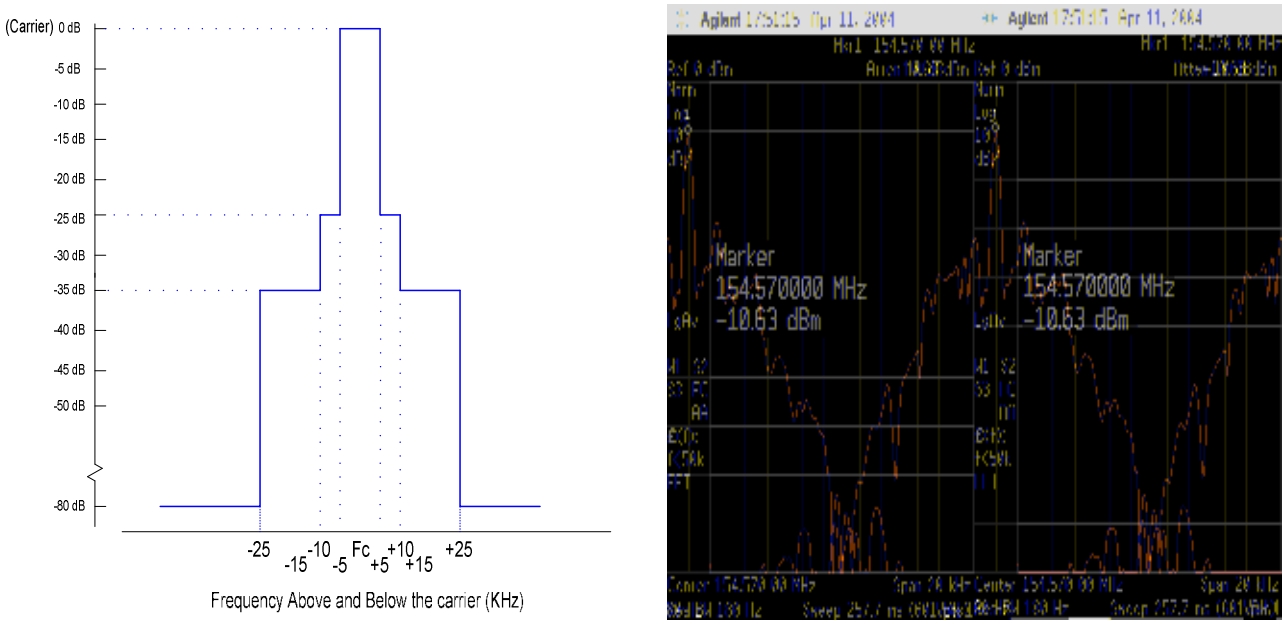

(a) **(b)**

Figure 3-4: (a) FCC spectrum mask for Narrowband FM channel (b) FM signal generated by DDR

3.5. FM Receiver

One of the simplest ways of recovering the modulating signal from a frequency-modulated carrier is shown in Figure 3-5 [2],[3]. An FM modulated carrier wave is applied to the frequency selective network whose transfer function, $|H(j\omega)|$, is frequency dependent. The output of the frequency selective network is then fed to an envelope detector to obtain the demodulated baseband signal.

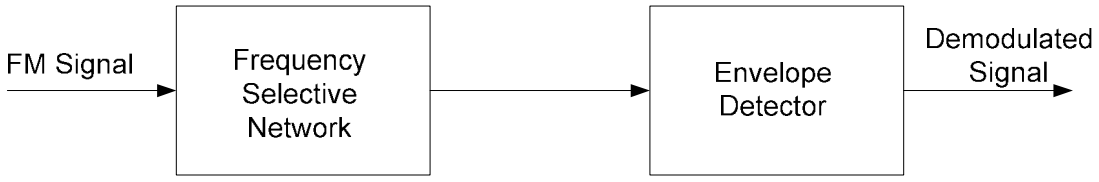

Figure 3-5: Basic FM demodulator

Figure 3-6 shows example of a frequency selective network. Suppose that the time constant of the RC-network is adjusted such that the transfer function $|H(j\omega)|$ about the carrier frequency is linear and has a slope $d|H(j\omega)|/df = \lambda/A_L$. Then a change of Δf in the instantaneous frequency of the input would translate into equivalent change in the amplitude of the carrier. If the output waveform of such

a RC-network is feed to an envelope detector, the baseband modulating signal can be obtained back. Such type of a frequency demodulator is referred to as an FM discriminator. In addition to FM discriminators there are different implementations of FM demodulators, for example demodulator based on phased locked loop and frequency demodulator using feedback [2].

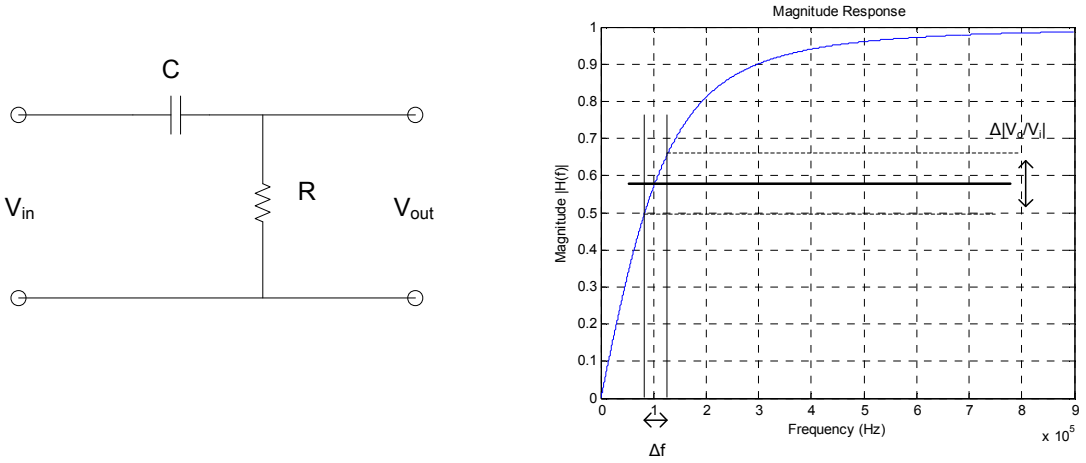

Figure 3-6: Frequency Selective Network

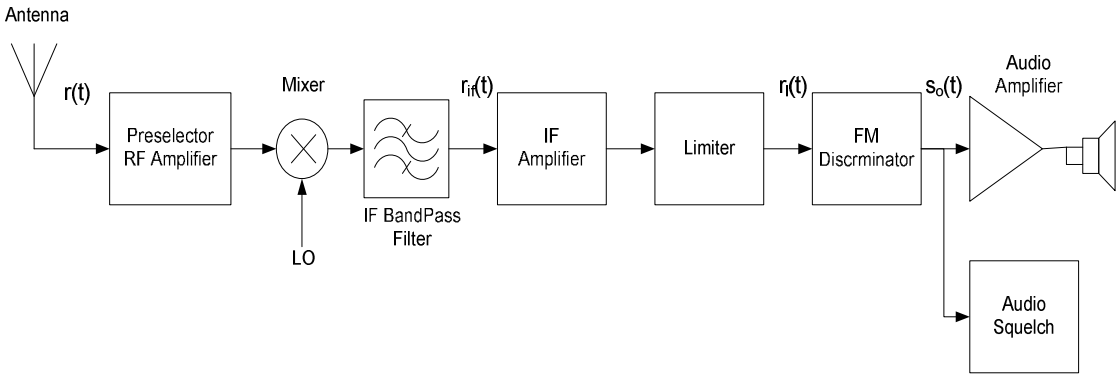

Figure 3-7: Simplified block diagram of a typical FM receiver

The block diagram of a typical FM receiver is shown in Figure 3-7. As seen in the figure a typical FM receiver is a heterodyne receiver with a single IF stage. Typical values for IF frequency vary between 200 KHz to 400 KHz. The downcoverted IF FM signal is first bandlimited and then passed trough an IF stage amplifier. It is then sent to a limiter which limits the IF signal envelope [2],[3]. The IF signal is then feed to an FM discriminator. The output of the FM discriminator is the modulating signal. The mathematical representation of FM discriminator is given in Section 3.5.1. It

will be required in calculate the signal power and noise power at the output at the output of the FM receiver.

3.5.1. Mathematical representation of FM Discriminator

As described in 3.5, the discriminator consists of two components. The first component is a frequency selective network which has a transfer function $|H_f(j\omega)|$ that is frequency dependent. The output of this network varies linearly with frequency over a range of excursions of the instantaneous frequencies. Thus when a constant amplitude FM signal is passed through such a network the output produced not only varies in frequency but also exhibits amplitude variation. The baseband signal can be recovered by passing this amplitude modulated waveform through an envelope detector which is a low pass filter [2],[3].

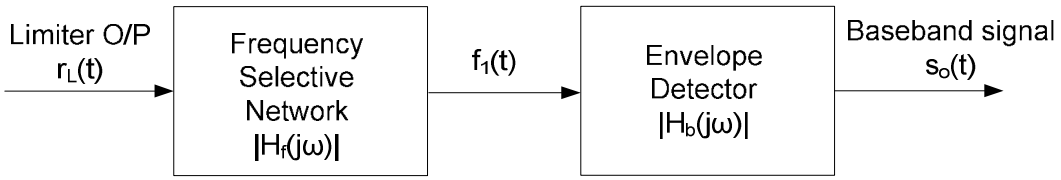

Figure 3-8: Mathematical representation of discriminator

The frequency to amplitude conversion required to obtain frequency demodulation needs $|H_f(j\omega)|$ which varies linearly with ω over only a limited range and its slope may be positive or negative. In addition the phase variation of H_f is of no consequence [1],[3]. The simplest transfer function which satisfies such a requirement is that of an ideal differentiator given in 3-13.

$$H_f(j\omega) = j\,\omega\lambda / A_L \qquad \textbf{3-13}$$

where λ is a slope constant and A_L is the amplitude at the output of limiter.
Suppose that the voltage $r_L(t)$, as seen in Figure 3-8, is applied to the converter is given by 3-14.

$$r_L(t) = A_L \cos(\omega_i t + \phi(t)) \qquad \textbf{3-14}$$

where A_L is the limited amplitude and $\omega_i t + \Phi(t)$ represents the instantaneous phase.
The output of the frequency selective network $f_1(t)$ is related to input $r_L(t)$ by the 3-15.

$$f_1(t) = \frac{\lambda}{A_l}\frac{d}{dt} r_L(t) \qquad \textbf{3-15}$$

Substituting 3-14 in 3-15 we obtain 3-16 shown below

$$f_1(t) = \frac{\lambda}{A_L}\frac{d}{dt} A_L \cos(\omega_i t + \phi(t)) \qquad \textbf{3-16}$$

$$= -\lambda(\omega_i + \frac{d}{dt}\phi(t)) \sin(\omega_i t + \phi(t))$$

The envelope detector is a baseband filter which rejects the dc component and passes the signal component without distortion. The output of the envelope detector is given 3-17.

$$s_o(t) = \lambda(\omega_i + \frac{d}{dt}\phi(t)) \qquad \textbf{3-17}$$

$$= \lambda\omega_i + \lambda\frac{d}{dt}\phi(t)$$

Comparing 3-2 and 3-14, and substituting $\varphi(t)$ in 3-17, the output of the discriminator $s_o(t)$ is proportional to the modulating signal $m(t)$ as seen in 3-18.

$$\phi(t) = \omega_d \Big/ k_m \int_0^t m(\tau)d\tau \qquad \textbf{3-18}$$

$$s_o(t) \propto m(t)$$

For a sinusoid modulating signal as shown in 3-4 and 3-5, the output of the FM discriminator shown in 3-18 can be written as

$$s_o(t) = \lambda\beta\omega_m \cos(\omega_m t) = \lambda\omega_d \cos(\omega_m t) \qquad \textbf{3-19}$$

It is a commonly accepted fact that the output of the FM discriminator is the baseband modulating signal as seen in 3-17 and 3-18 [1], [2]. However the author was not able to find a mathematical proof for a baseband signal consisting of multiple sinusoids in literature. Such an analysis is non-trivial and can be extended to an OFDM baseband signal. The derivation for the output of FM discriminator for a baseband OFDM signal is given in Appendix B.

3.6. Calculation of output signal power (S_o) and output noise power (N_o)

A DDR is an OFDM/FM system. The BER observed by the DDR modem will depend upon the SNR value at the output of the FM receiver. The SNR at the output of an FM discriminator can be derived using the assumptions made in Section 3.5. Let the received FM signal, $r(t)$ be given by

$$r(t) = h_c(t) * z(t) \qquad \textbf{3-20}$$

where $h_c(t)$ represents the channel response of the FM channel. The objective of the analysis is to show the relationship between non-linear distortions introduced by clipping of baseband signal in FM transmitter to the SNR observed at the FM receiver. To that effect, we will assume that the channel response is accurately known and the received signal can be equalized without any loss of information, i.e $r(t)= z(t)$ and the noise is AWGN with psd η. Consider the FM discriminator structure shown in Figure 3-8. In order to calculate the output signal/noise power, we assume that the baseband and IF filter have responses $H_b(f)$ and $H_f(f)$ as defined below:

$$H_b(f) = \begin{cases} 1; & |f| \le W \\ 0; & otherwise \end{cases} \qquad \textbf{3-21}$$

$$H_f(f) = \begin{cases} 1; & |f - f_c| \le BW \\ 0; & otherwise \end{cases}$$

where W represents the maximum bandwidth of the modulating signal and BW represents the fixed bandwidth of IF signal. As an example, for narrowband FM audioband channel typical values of W and BW will be 4 KHz and 15 KHz respectively. It has been proved in [1],[5] that, when the SNR ratio is high, the noise at the input of the discriminator does not affect the output signal power. Under this assumption the output signal power can be calculated from 3-18, as shown below:

$$S_0 = |\bar{s}_o(t)|^2 = (\lambda^2 \omega_d^2 / k_m^2)|\overline{m}(t)|^2 \qquad \textbf{3-22}$$

$$= (\lambda^2 \omega_d^2 / k_m^2)\sigma_x^2 = 4\pi^2 \lambda^2 f_v^2$$

where σ_x represent the RMS value of the baseband signal, f_v represents the RMS frequency bandwidth of FM signal. In order to output noise power, N_o consider Figure 3-9.

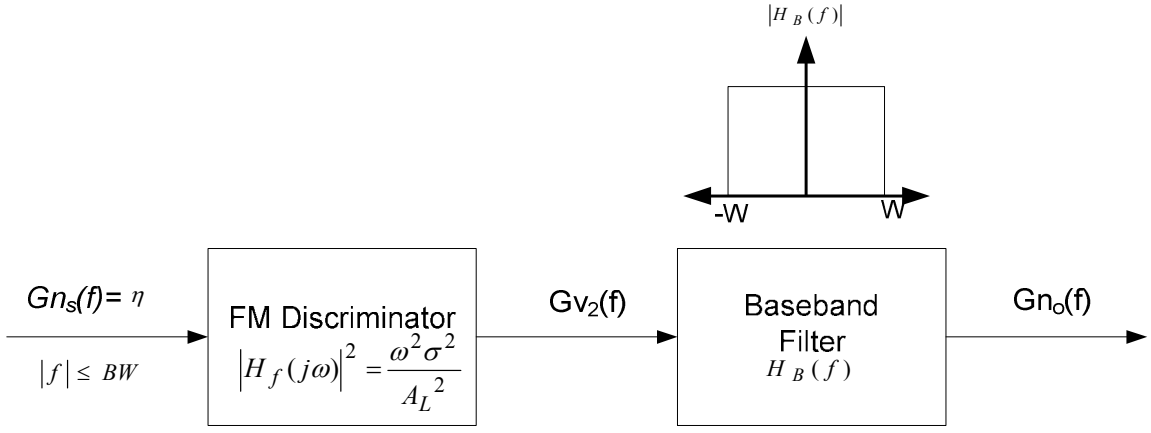

Figure 3-9: Power spectral density of noise

The power spectral density of $n_s(t)$ is given in 3-23.

$$G_{ns}(f) = \eta \quad for \quad |f| \le BW$$
$$= 0; \quad otherwise \tag{3-23}$$

As in the earlier derivation for signal power, the noise power at the output can be considered independent of the demodulated baseband signal at the FM discriminator output [1], [5]. Using the discriminator transfer function shown in Figure 3-9, for high SNR, the power spectral density of noise at the output of the discriminator can be computed as shown in 3-24.

$$G_{v2}(f) = \frac{\lambda^2 \omega^2}{A_L^2} \eta \tag{3-24}$$

The noise power output at the output of the baseband filter N_o can be computed as shown in 3-25.

$$N_o = \int_{-W}^{W} G_{v2}(f) df = \int_{-W}^{W} \frac{\lambda^2 (2\pi f)^2}{A_L^2} \eta df \tag{3-25}$$
$$= \frac{8\pi^2}{3} \frac{\lambda^2 \eta}{A_L^2} W^3$$

As seen in the above equation the output noise power, N_o depends upon the bandwidth of the envelope filter, the noise psd η and the transfer function of the frequency selective network ($H_f(f)$) in the FM discriminator.

3.7. SNR at the output of FM receiver

The SNR at the output of FM discriminator can be calculated using 3-22 and 3-25 as shown below:

$$SNR_o = S_o / N_o = 4\pi^2 \lambda^2 f_v^2 \Big/ \frac{8\pi^2}{3} \frac{\lambda^2 \eta}{A_L^2} W^3 \tag{3-26}$$
$$= (3A_L^2 / 2W^3)(f_v^2 / \eta)$$

As seen in 3-26, the SNR at the output depends on the RMS bandwidth of FM signal, psd of AWGN noise η, the clipping amplitude of the IF limiter A_L and bandwidth of lowpass filter W. Figure 3-10 shows the SNR at the output of an FM receiver using a narrowband FM channel, for different bandwidths for the lowpass filter and fixed noise psd η. From the figure, we observe that as the RMS bandwidth f_v increases, the SNR also increases. Using the relationship between RMS bandwidth of

FM signal and RMS value of baseband modulating signal given in Section 3.3, this indicates that the SNR at FM receiver increases as the RMS value of modulating signal increases. The initial SNR values observed depend upon both the signal power and noise power which is dependent upon the bandwidth of the lowpass filter as seen in 3-25. Also note that the maximum value of instantaneous FM bandwidth will be limited to the maximum deviation f_d, permitted for the channel in use. For narrowband FM channels f_d is 5 KHz while for wideband channels the limit is 75 KHz.

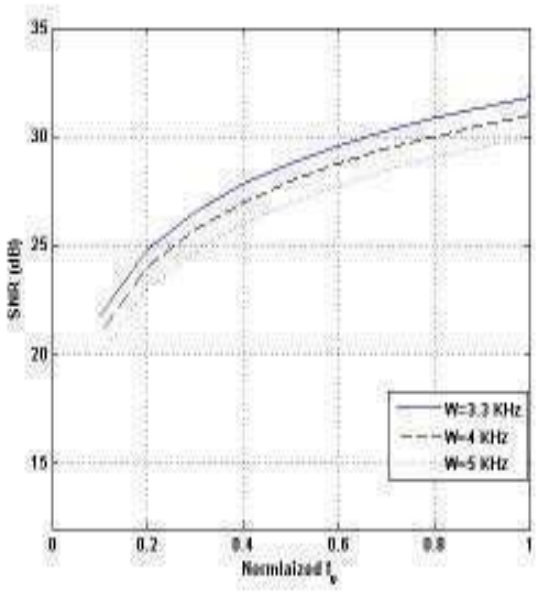

Figure 3-10: SNR at output of FM discriminator.

3.8. Chapter Summary

DDRs use frequency modulation for transmission of voice and data signals over narrowband FM channels. In this chapter we described the generation and demodulation of an FM signal. An analytical framework was developed to obtain an expression for the SNR at an FM receiver. We also derived the relationship between RMS bandwidth of FM signal and the RMS value of baseband modulating signal followed by the relationship between the RMS bandwidth and SNR at FM receiver. From the analysis, we can conclude that higher the RMS value of baseband modulating signal greater is the RMS bandwidth of FM signal and consequentially the SNR at FM receiver. A maximum SNR is obtained when the RMS bandwidth of FM signal is equal to the maximum deviation permitted by the channel.

References

[1] D. Sakrison, "Commication Theory: Transmission of Waveforms and Digital Information", Wiley Publications, 1968.

[2] H. Taub and D. Schilling, "Principles of communication systems", 2nd Edition, Mc-Graw Hill, 1986.

[3] K. Clarke and D. Hess, "Communication Circuits: Analysis and Design", 2nd Edition, Kreiger Publishing, 1994.

[4] N. Abramson, "Bandwidth and spectra of phase- and frequency modulated waves", IEEE Trans. On Comm. Systems, 1963.

[5] O'Keefe, "Spectrum spreading of FM signals by additive dispersal signals", PhD Thesis, Worcester Polytechnic Institute, 1975.

[6] J. Stewart, "The power spectrum of a carrier frequency modulated by Gaussian Noise", Proc. Of IRE, 1954.

[7] K. Chung, "Generalized Tamed FM and its application for mobile radio communications", IEEE Journal on selected areas in Comm., July 1984.

[8] H. Arnold and W. Bodtmann, "Performance of FSK in frequency-selective Rayleigh Fading", IEEE Trans. on Comm., April 1983.

[9] K. Hirade, M. Ishizuka, F. Adachi and K. Ohtani, "Error-Rate Performance of Digital FM with differential detection in Land Mobile Channels", IEEE Trans. on Vehicular Tech., August 1979.

[10] E. Casas and C. Leung, "OFDM for digital communication over mobile radio FM channels-Part I", IEEE Trans. on Comm., May 1991.

[11] L. Cimini, "Analysis and simulation of a digital mobile channel using orthogonal frequency division multiplexing", IEEE Trans. on Comm. Vol 33, Jul 1985.

[12] M. Ridder-de Groote, et al. "Analysis of new methods for broadcasting digital data to mobile terminals over an FM channel", IEEE Trans. on broadcasting, March 1994.

[13] A.C. Navalekar, "Design of High Data Rate Audioband OFDM Modem", Master's Thesis, Worcester Polytechnic Institute, 2006.

[14] D. Dardari, V. Tralli and A. Vaccari, "A theoretical characterization of nonlinear distortion effects in OFDM systems" , IEEE Trans. on Comm. , Oct 2000.

[15] S. Thompson, J. Proakis and J. Seidler, " The effectivess of signal clipping for PAPR and total degradation reduction in OFDM systems", IEEE Globecomm, 2005.

[16] X. Wang and T. Tjhung, "Reduction of PAPR of OFDM systems using companding techniques", IEEE Trans. on Broadcasting, Sep 1999.

[17] R. Nee and A. Wild, "Reduction of peak to avearge power ratio of OFDM", IEEE VTC 1998

[18] R. Rajbanshi, " OFDM-based cognitive radio for DSA Networks", Thesis PhD, Kanas State University, 2007.

[19] A.C. Navalekar and W.R. Michalson, " A new approach to improve the BER perfoamnce of a high PAPR OFDM signal over FM based Land Mobile Radios", IEEE WTS, Pomona, CA 2008.

[20] A.C. Navalekar and W.R. Michalson, " A Linear Scaling Technique (LST) for improving BER perfoamnce of a high PAR OFDM signal over LMR networks", *submitted* (*first revision)*, IEEE Trans. on Broadcasting, 2009.

[21] A. Papoulis and U. Pillai, " Probability, Random variables and stochatic processes", Mc-Graw Hill, 4th Edition, 2002.

4. OFDM System Analysis

4.1. Introduction

Orthogonal Frequency Division Multiplexing (OFDM) is used in high data rate wireless local area networks (WLAN) like 802.11a/g, wide area networks (WAN) like 802.16 and wired systems like DSL [1], [2]. OFDM can be interpreted as a hybrid of multi-carrier modulation (MCM) and frequency shift keying (FSK). A MCM technique involves transmitting data over multiple carriers simultaneously as opposed to FSK which uses a single carrier tone [3], [4]. In OFDM the spacing between adjacent subcarriers is kept lower than the coherence bandwidth (B_c) of the channel making it robust to frequency selective fading and multipath. This also makes OFDM resilient to narrowband interference and deep fades [5], [6].

The tradeoff for OFDM's multipath robustness comes in many forms and is well documented [7]. For example, due to close spacing of subcarriers, OFDM requires precise frequency synchronization and is highly sensitive to inter-carrier-interference (ICI) [4], [8]. Another important drawback of OFDM is the high peak-to-average ratio (PAR). The PAR problem in OFDM has been studied extensively in literature [9], [10]. One of the major impacts of high PAR is a sensitivity to non-linearities found in communication systems. For AM systems, the power amplifier in the transmitter is an example of a non-linear device. For OFDM over FM systems like the DDR, the limiter circuit in the transmitter, as the one discussed in Chapter 3, introduces a non-linearity. Distortion due to these non-linearities introduces ICI and out-of-band spectral growth in an OFDM signal which leads to performance degradation [11], [12]. One of the ways of avoiding this performance degradation is to minimize the amplitude of the baseband signal to ensure that the system operates in its linear region. This approach, in case of AM systems, will result in low power efficiency for the power amplifier (PA) while in case of FM systems it will result in lower SNR at the FM receiver. Another way to avoid performance degradation is to use PAR reduction techniques like companding, constellation extension and pilot reduction carriers [13], [14], [15].

In this chapter we develop a framework to explore the PAR issue for the OFDM baseband signal used in the DDR system. The PAR problem for an OFDM signal is introduced in Section 4.2. An expression for an OFDM baseband signal at the output of the DDR is derived in Section 4.3 followed

by expressions for Peak and Average power in Sections 4.4 and 4.5. The statistical characteristics of the OFDM signal and its impact on OFDM/FM systems are discussed in Sections 4.6 and 4.7.

4.2. Peak-to-Average Power Ratio (PAPR) and Crest Factor (CF) of an OFDM signal

One of the ways to implement OFDM modulation/demodulation is by using Discrete Fourier Transform pairs (IDFT/DFT) [4], [16]. The implementation of an Inverse Discrete Fourier Transform (IDFT) which corresponds to OFDM modulation is given by 4-1.

$$x(n) = \frac{1}{N} \sum_{k=0}^{N-1} X(k) e^{\frac{j2\pi kn}{N}} \quad ;0 \le n < N \quad ,0 \le k < N \qquad \textbf{4-1}$$

A Discrete Fourier Transform (DFT) which emulates OFDM demodulation is given in 4-2.

$$X(k) = \sum_{n=0}^{N-1} x(n) e^{\frac{-j2\pi kn}{N}} \quad ;0 \le n < N \quad ,0 \le k < N \qquad \textbf{4-2}$$

where N represents the number of sub-carriers, k represents the discrete frequency index, n represents the discrete sample index, $X(k)$ represents the data corresponding to k^{th} sub-carrier and $x(n)$ represents the time domain signal. Due to orthogonal placement of sub-carriers, OFDM presents a spectrally efficient high data rate transmission technology. The summation of orthogonal carriers, as shown in 4-1, can result in large discrepancies between the peak value and the average value of the resulting time domain OFDM signal. The worst case scenario occurs when the data modulating the subcarriers ($X(k)$) are selected such that all the sinusoids align in phase. The two most common ways of characterizing the variation in amplitudes are Peak-to-Average Power Ratio (PAPR) and Peak Envelope Ratio (PEP) or Crest Factor (CF) [9], [10]. The term PAPR refers to the ratio between the peak power and the average power of the OFDM signal while CF refers to the ratio between the peak amplitude of the OFDM signal to the rms power.

Figure 4-1, shows an example of a PAPR variation for a BPSK modulated OFDM signal. In Figure 4-1.a, a high PAPR value for the OFDM signal is obtained by modulating 32 subcarriers by identical BPSK symbols, for e.g. $\{X_0=1, X_1=1, \ldots X_{31}=1\}$. Figure 4-1.b shows a low PAPR value for an OFDM signal generated by random BPSK data. We observe that the PAPR value varies from 24dB to 4dB depending upon the randomness of BPSK data. The PAPR and CF can be defined mathematically as shown in 4-3.

$$CF = \frac{\max_n |x(n)|}{\sqrt{\sigma_x^2}}; \quad PAPR = \frac{\max_n |x^2(n)|}{\sigma_x^2} \qquad \text{4-3}$$

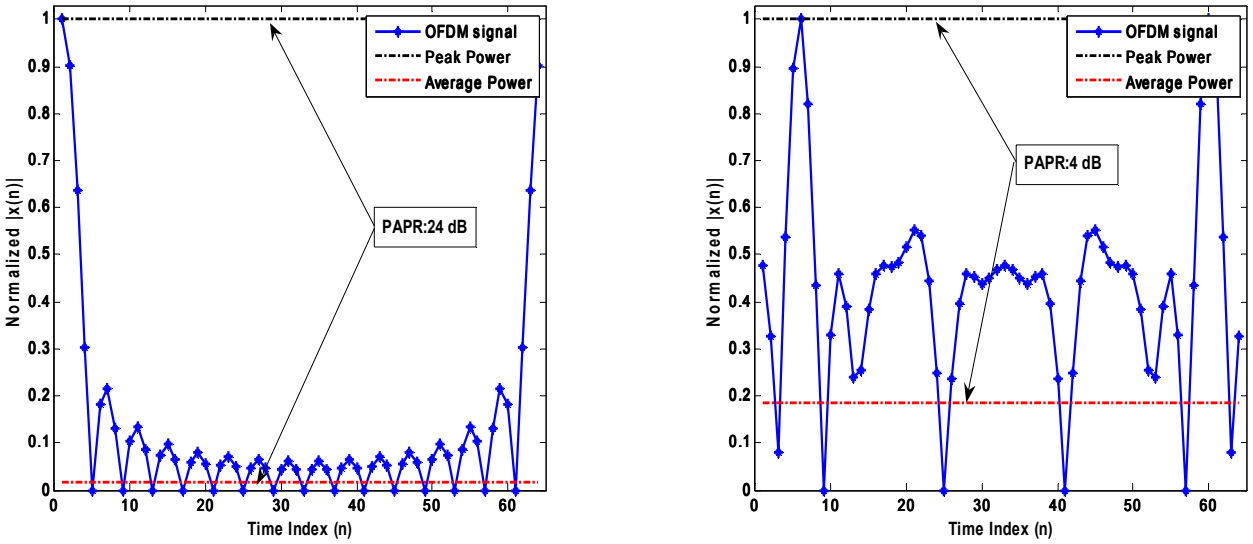

Figure 4-1: PAPR ratios for OFDM signal (a) Fixed data (b) Random Data

The theoretical limits on maximum and minimum values of PAPR and CF depend on the implementation of the OFDM modulation i.e. how the time domain signal *x(n)* is generated. Theoretical calculations for limits on PAPR and CF for complex OFDM symbols can been found in [10] while derivations for non-contiguous and oversampled OFDM are given in [15]. As explained in Chapter 2, DDR II uses real OFDM symbols. Generation of a real OFDM signal requires significantly fewer computations as described in Section 2.4.2. In order to calculate the PAPR/CF values we obtain the expression for the real OFDM baseband signal, its maximum value and its rms value as shown in Sections 4.3, 4.4 and 4.5.

4.3. Derivation for an IFFT real sequence output:

In order to generate a real sequence at the IFFT output, the complex input data to the IFFT should have Hermitian symmetry as shown in 4-4, and the data corresponding to the DC subcarrier must be real [17].

$$X_{N-k} = X_k^*; \quad k = 0,\ldots,\frac{N}{2}-1 \qquad \text{4-4}$$

Assume that $X_k = a_k - j\, b_k$, ,where X_k represents the data that modulates the k^{th} sub-carrier, a_k and b_k are the I/Q constellation mappings for the implemented data modulation scheme and X_0 , $X_{N/2}$ are real numbers. Now substitute the value of X_k obtained into 4-1.

$$x(n) = \frac{1}{N}\{X_0 + X_1 e^{\frac{j2\pi 1n}{N}} + X_2 e^{\frac{j2\pi 2n}{N}} + \cdots\cdots + X_{N/2} e^{j\pi n} + X_{\frac{N}{2}-1} e^{\frac{j2\pi(\frac{N}{2}-1)n}{N}} + \cdots$$
$$\cdots + X_{N-2} e^{\frac{j2\pi(N-2)n}{N}} + X_{N-1} e^{\frac{j2\pi(N-1)n}{N}}\} \qquad \textbf{4-5}$$

Let $e^{j2\pi kn/N} = W_N^{kn}$, thus 4-5 reduces to 4-6.

$$x(n) = \frac{1}{N}\{X_0 + X_{N/2} e^{j\pi n}\} + \frac{1}{N}\{X_1 w_N^{1n} + X_2 w_N^{2n} + \cdots\cdots$$
$$+ X_{\frac{N}{2}-1} w_N^{(\frac{N}{2}-1)n} + \cdots + X_{N-2} w_N^{(N-2)n} + X_{N-1} w_N^{(N-1)n}\} \qquad \textbf{4-6}$$

Using Hermitian symmetry of twiddle factor W_N^{kn} ($W_N^{(N-k)n} = W_N^{*kn}$) and input data X_k given in 4-4, we get 4-7.

$$x(n) = \frac{1}{N}\{X_0 + X_{N/2} e^{j\pi n}\} + \frac{1}{N}\{(X_1 w_N^{1n} + X_1^* w_N^{*n}) +$$
$$(X_2 w_N^{2n} + X_2^* w_N^{*2n}) + \cdots\cdots + (X_{\frac{N}{2}-1} w_N^{(\frac{N}{2}-1)n} + X_{\frac{N}{2}-1}^* w_N^{*(\frac{N}{2}-1)n})\} \qquad \textbf{4-7}$$

Substituting identities from 4-8 into 4-7 we can get the expression for real sequence *x(n)* as shown in 4-9.

$$\mathrm{Re}(z) = \frac{1}{2}\{z + z^*\} \qquad \textbf{4-8}$$
$$X_k = a_k - jb_k \;; \quad W_N^{kn} = \cos(\frac{2\pi kn}{N}) + j\sin(\frac{2\pi kn}{N})$$
$$\mathrm{Re}(X_k W_N^{kn}) = a_k \cos(\frac{2\pi kn}{N}) + b_k \sin(\frac{2\pi kn}{N})$$

$$x(n) = \frac{1}{N}\{X_0 + X_{N/2} e^{j\pi n}\} + \frac{2}{N}\sum_{k=1}^{\frac{N}{2}-1} a_k \cos(\frac{2\pi kn}{N}) + b_k \sin(\frac{2\pi kn}{N}); \quad n = 0,\ldots, N-1 \qquad \textbf{4-9}$$

Without loss of generality, it can be assumed that $X_0, X_{N/2}=0$, the expression for OFDM signal reduces to the equation shown in 4-10.

$$x(n) = \frac{2}{N} \sum_{k=1}^{\frac{N}{2}-1} a_k \cos(\frac{2\pi kn}{N}) + b_k \sin(\frac{2\pi kn}{N}); \quad n = 0,..., N-1 \qquad \textbf{4-10}$$

From 4-10, we observe that the OFDM signal, *x(n)* is real.

4.4. Average Power of the OFDM Signal

In order to calculate the average power of OFDM signal (σ^2_x), we first calculate $E[x^2(n)]$ for 4-9, as shown in 4-11 [18].

$$\sigma_x^2 = E[x^2(n)] = E[(\frac{1}{N}\{X_0 + X_{N/2}e^{j\pi n}\} + \frac{2}{N}\sum_{k=1}^{\frac{N}{2}-1} a_k \cos(\frac{2\pi kn}{N}) + b_k \sin(\frac{2\pi kn}{N}))^2] \qquad \textbf{4-11}$$

$$= \frac{1}{N^2}\{E[(X_0 + X_{N/2}e^{j\pi n})^2 + 4(\sum_{k=1}^{\frac{N}{2}-1} a_k \cos(\frac{2\pi kn}{N}) + b_k \sin(\frac{2\pi kn}{N}))^2 + \ldots$$

$$+ 4(X_0 + X_{N/2}e^{j\pi n})(\sum_{k=1}^{\frac{N}{2}-1} a_k \cos(\frac{2\pi kn}{N}) + b_k \sin(\frac{2\pi kn}{N}))]\}$$

Expanding 4-11 and using identities in 4-12, we get 4-13.

$$\textit{for} \quad k \neq j \qquad \textbf{4-12}$$

$$E[\{\sum_k \sum_j a_k a_j \cos(\frac{2\pi kn}{N})\cos(\frac{2\pi jn}{N})\}] = E[\sum_k \sum_j b_k b_j \sin(\frac{2\pi kn}{N})\sin(\frac{2\pi jn}{N})] = 0$$

$$\textit{Also} \quad \forall \quad k, j$$

$$E[2\sum_k \sum_j a_k b_j \cos(\frac{2\pi kn}{N})\sin(\frac{2\pi jn}{N})] = 0$$

$$\sigma_x^2 = E[x^2(n)] = \frac{1}{N^2}E[X_0^2 + X_{N/2}^2] + \frac{4}{N^2}E[(\sum_k a_k^2 \cos^2(\frac{2\pi kn}{N}) + \sum_k b_k^2 \sin^2(\frac{2\pi kn}{N}))] \qquad \textbf{4-13}$$

$$= \frac{1}{N^2}E[X_0^2 + X_{N/2}^2] + E[\frac{4}{N^2}\{\frac{1}{2}\sum_k (a_k^2 + b_k^2) + \sum_k a_k^2 \cos(\frac{4\pi kn}{N}) - \sum_k b_k^2 \sin(\frac{4\pi kn}{N})\}]$$

$$= \frac{1}{N^2}[X_0^2 + X_{N/2}^2] + \frac{4}{N^2}\{\sum_{k=1}^{\frac{N}{2}-1} \frac{1}{2}E[(a_k^2 + b_k^2)]\}$$

The term $E[(a^2_k+b^2_k)]$ represents the average energy in the signal constellation corresponding to the modulation scheme implemented, E_s [19]. The relationship between symbol energy, E_s and sub-carrier energy, E_{sc} is shown in 4-14.

$$\begin{aligned} E_{sc} &= E[\{a_k \cos(\frac{2\pi kn}{N}) + b_k \sin(\frac{2\pi kn}{N})\}^2] \\ &= E[a_k^2 \cos^2(\frac{2\pi kn}{N}) + b_k^2 \sin^2(\frac{2\pi kn}{N}) + 2a_k b_k \cos(\frac{2\pi kn}{N})\sin(\frac{2\pi jn}{N})] \\ &= \frac{1}{2}E[a_k^2 + b_k^2] = \frac{1}{2}E_s \end{aligned} \quad \textbf{4-14}$$

Substituting 4-13 in 4-14, we get an expression for the average power of the OFDM signal.

$$\sigma_x^2 = E[x^2(n)] = \frac{1}{N^2}[X_0^2 + X_{N/2}^2] + \frac{2}{N^2}(\frac{N}{2} - 1)E_{sc} \quad \textbf{4-15}$$

For $X_0, X_{N/2}=0$, the expression for σ^2_x reduces as shown in 4-15.

$$\sigma_x^2 = E[x^2(n)] = \frac{2}{N^2}(\frac{N}{2} - 1)E_{sc} = \frac{(N-2)}{N^2}E_s \quad \textbf{4-16}$$

As seen in 4-16, the average power of the OFDM signal depends on the number of sub-carriers, N, and the average symbol energy, E_s. The average symbol energy is a function of the modulation scheme and the size of the signal constellation.

4.5. Peak value of OFDM Signal

The real sequence output of the IFFT assuming $X_0, X_{N/2}=0$, is given by 4-10. Consider a fixed instant of OFDM symbol, at $n=r$, the output of IFFT is given by

$$x(r) = \frac{2}{N}\sum_{k=1}^{\frac{N}{2}-1} a_k \cos(\frac{2\pi kr}{N}) + b_k \sin(\frac{2\pi kr}{N}) \quad \textbf{4-17}$$

We can represent the RHS in 4-17 as a product of two vectors x and l as shown below:

$$\sum_{k=1}^{\frac{N}{2}-1} a_k \cos(\frac{2\pi kr}{N}) + b_k \sin(\frac{2\pi kr}{N}) = x.l \quad \textbf{4-18}$$

$$where \quad x = [a_1, b_1, a_2, \cdots\cdots, a_{\frac{N}{2}-1}, b_{\frac{N}{2}-1}] \quad ;$$

$$l = [\cos(\frac{2\pi 1r}{N}), \sin(\frac{2\pi 1r}{N}), \cos(\frac{2\pi 2r}{N}), \cdots\cdots, \cos(\frac{2\pi(N/2 - 1)r}{N}), \sin(\frac{2\pi(N/2 - 1)r}{N})]$$

Now using Cauchy-Schwartz inequality for norm of vectors, $|x.l| \le \|x\|.\|l\|$ into 4-18, we get 4-19 [18], [19].

$$x(r) \le \left| a_1^2 + b_1^2 + a_2^2 + b_2^2 + \cdots\cdots + a_{\frac{N}{2}-1}^2 + b_{\frac{N}{2}-1}^2 \right|^{1/2} \cdot \left| \cos^2\left(\frac{2\pi 1 r}{N}\right) + \sin^2\left(\frac{2\pi 1 r}{N}\right) + \cdots\cdots + \cos^2\left(\frac{2\pi(N/2-1)r}{N}\right) + \sin^2\left(\frac{2\pi(N/2-1)r}{N}\right) \right|^{1/2} \quad \textbf{4-19}$$

Thus, the upper bound for the maximum value of the OFDM signal will be as shown in 4-20.

$$\max_n |x(n)| \le \frac{2}{N} \left| a_1^2 + b_1^2 + a_2^2 + b_2^2 + \ldots\ldots + a_{\frac{N}{2}-1}^2 + b_{\frac{N}{2}-1}^2 \right| \left(\frac{N}{2}-1\right)^{1/2} \quad \textbf{4-20}$$

From 4-20, we observe that the maximum value of the OFDM signal depends on the number of sub-carriers, N and values of a_k,b_k which depend on the modulation scheme implemented. From 4-16 and 4-20, we can observe that both the average power and maximum value for a real OFDM signal and, consequentially, the PAPR and CF values, depend on the modulation scheme implemented. As mentioned in Chapter 2, DDRs support BPSK, QPSK, 16 QAM, 64 QAM and 128 QAM. We will derive expressions for the maximum and average power for M-ary PSK and M-ary QAM modulation.

4.5.1. M-ary PSK

The average symbol energy E_s for M-ary PSK modulation scheme can be calculated as shown in 4-21.

$$E_s = E[P_k] = \frac{1}{M}\sum_{k=1}^{M} a_k^2 + b_k^2 = \frac{1}{M}\sum_{k=1}^{M} A_p^2 = A_p^2 \quad \textbf{4-21}$$

where a_k b_k represents the I/Q points of the signal constellation associated with M-ary PSK. Using 4-21 and 4-16, the average power of an OFDM signal with M-ary PSK or M-ary QAM modulation is given in 4-22.

$$\sigma_x^2 = E[x^2(n)] = \frac{(N-2)}{N^2} A_p^2 \quad \textbf{4-22}$$

M-ary PSK is a constant envelope modulation scheme and hence the energy of each constellation point in M-ary PSK is equal to A^2_p [3],[19]. Thus, the peak value for an OFDM M-ary PSK signal will be as shown in 4-23.

$$\max_n |x(n)| \le \frac{(N-2)}{N} A_p \qquad \textbf{4-23}$$

Substituting the values for peak and average power into the definition for CF and PAPR, we get the expressions shown in 4-24.

$$CF = \frac{\max_n |x(n)|}{\sqrt{\sigma_x^2}} = (N-2)^{1/2}; \quad PAPR = \frac{\max_n |x^2(n)|}{\sigma_x^2} = (N-2) \qquad \textbf{4-24}$$

From 4-24, we see that in the case of M-ary PSK, both the PAPR and CF are dependent only on the number of sub-carriers. As the number of sub-carriers increases, the theoretical value of PAPR/CF also increases.

4.5.2. M-ary QAM

In order to calculate the average energy E_s for an M-ary QAM modulation scheme, assume that the QAM constellation points are selected so as to maintain symmetricity i.e. the points are selected from $\{+/- mA_Q, +/- mA_Q,\}$ for m=1,3 … $\sqrt{M}-1$ [3],[19]. In this case, the average energy E_s can be calculated as shown in

$$E_s = E[P_k] = \frac{1}{M}\sum_{k=1}^{M} a_{mk}^2 + b_{mk}^2 = \frac{2}{M}\sum_{k=1}^{M} a_{mk}^2 = \frac{8A_Q^2}{M}\sum_{k=1}^{M/4} a_m \qquad \textbf{4-25}$$
$$= \frac{8A_Q^2}{M}(\sqrt{M/4})\sum_{k=1}^{\sqrt{M/4}} (2m-1)^2 = \frac{2A_Q^2(M-1)}{3}$$

Thus, the average power of OFDM signal for M-ary QAM modulation scheme can be computed by substituting 4-25 into 4-16 as shown below:

$$\sigma_x^2 = E[x^2(n)] = \frac{2(N-2)}{3N^2} A_Q^2 (M-1) \qquad \textbf{4-26}$$

The peak value for the OFDM signal is given in 4-20. We observe that the peak value will be maximized if each of the constellation point has the maximum possible energy. Thus, the peak value for OFDM M-ary PSK signal will be as shown in 4-27.

$$\max_n |x(n)| \le \frac{\sqrt{2}(N-2)}{N}(\sqrt{M}-1)A_Q \qquad \textbf{4-27}$$

Substituting the values for peak and average power into the definitions for CF and PAPR, we get the expressions shown in 4-28.

$$CF = \frac{\max_n |x(n)|}{\sqrt{\sigma_x^2}} = \frac{\sqrt{3}(N-2)^{1/2}((\sqrt{M}-1))}{(M-1)^{1/2}}; \quad PAPR = \frac{\max_n |x^2(n)|}{\sigma_x^2} = \frac{3(N-2)(\sqrt{M}-1)^2}{(M-1)} \qquad \textbf{4-28}$$

From 4-28, we observe that the PAPR and CF values depend on both the number of sub-carriers, N, and size of the signal constellation, M. Figure 4-2, shows the maximum CF and PAPR values for different M-ary PSK and M-ary QAM modulation schemes. We can observe that the PAPR and CF values for a fixed IFFT size increase for higher modulation schemes. Also, for the same modulation scheme, the PAPR and CF values increase for higher IFFT sizes. However, the amount of increase in PAPR/CF values decreases for higher IFFT sizes.

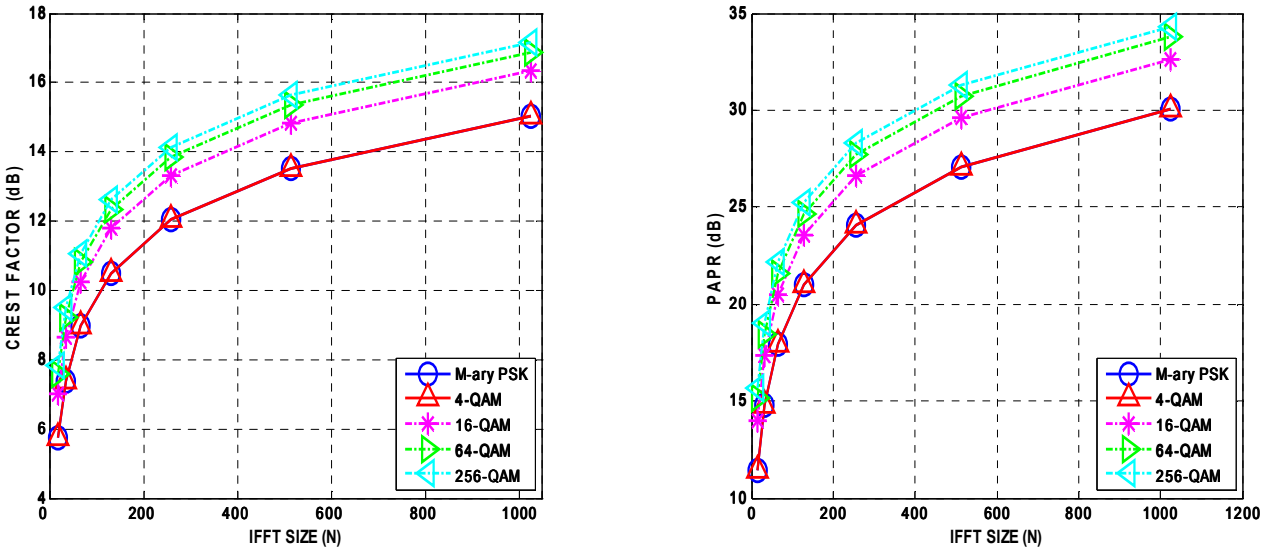

Figure 4-2: Maximum Crest Factor (CF) and PAPR Ratios

4.6. Statistical Characteristics of OFDM

Consider a real sequence output of an IFFT, assuming $X_0, X_{N/2}=0$, given by 4-10. Assume that the symbols $\{a_k, b_k\}$ are independently and identically distributed (i.i.d) [20]. Then, for a sufficiently large number of subcarriers, N, by using central limit theorem (CLT) the N-point IFFT output follows Gaussian distribution with zero mean and a standard deviation equal to σ^2_x ($\approx N(0, \sigma^2_x)$). The output power will follow non-central chi-square distribution (χ^2) with one degree of freedom (*d.f.=1*) and parameter value (λ) of $1/\sigma^2_x$ and the PAPR ratio (y) will follow a chi-square distribution with one degree of freedom as seen in 4-29 [21],[22].

$$x(n) \sim N(0, \sigma_x^2); \quad P(x \le r) = \frac{1}{\sigma\sqrt{2\pi}} \int_{-\infty}^{r} e^{-x/2\sigma^2} dx$$
$$y \sim \chi^2(1); \quad P(y \le \mu) = \frac{1}{\sqrt{2\pi}} \int_{-\infty}^{\mu} y^{-1/2} e^{y/2} dx \qquad \textbf{4-29}$$

Thus, the probability that the envelope exceeds a threshold r is given in 4-30.

$$P(x > r) = \frac{2}{\sigma\sqrt{2\pi}} \int_{r}^{\infty} e^{-x/2\sigma^2} dx = 2Q(\frac{r}{\sigma_x}) \qquad \textbf{4-30}$$

Similarly, the probability that the PAPR at n^{th} sample exceeds a threshold (γ) can be calculated as shown in 4-31.

$$P(\frac{x_n^2}{\sigma_x^2} > \gamma) = P(\frac{x_n}{\sigma_x} > \sqrt{\gamma}) = P(x_n > \sigma_x\sqrt{\gamma}) = 2Q(\sqrt{\gamma}) \qquad \textbf{4-31}$$

Thus, the probability that the PAPR exceeds the threshold can be extended over N instances as shown in 4-32.

$$P(PAPR\{x(n)\} > \gamma) = 1 - (1 - 2Q(\sqrt{\gamma})^N \qquad \textbf{4-32}$$

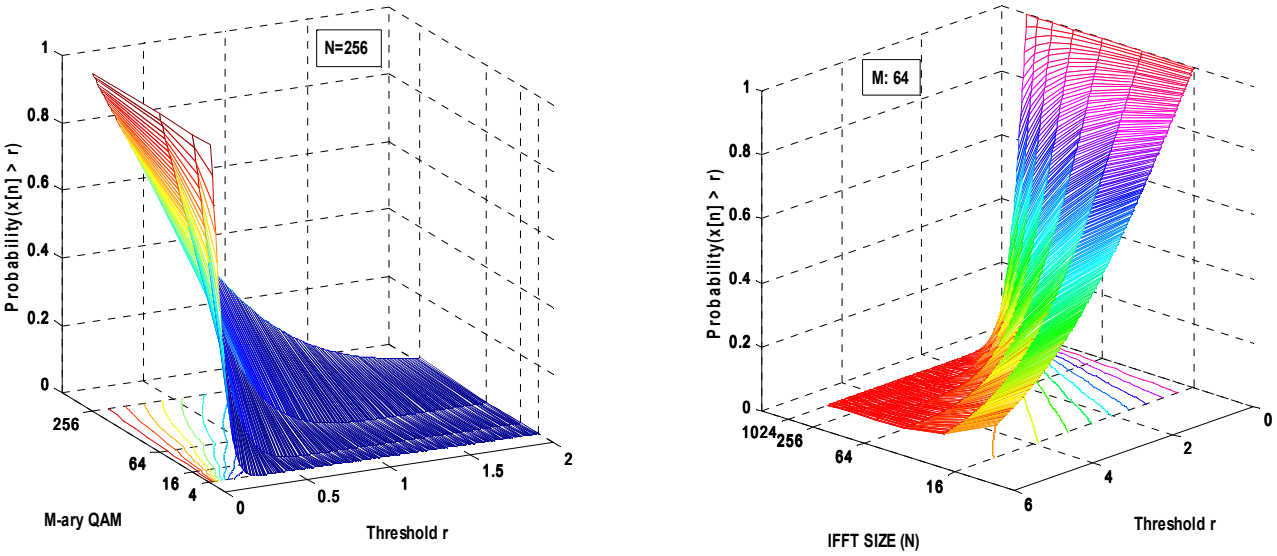

Figure 4-3: Complementary CDF plot for CF ratio (a) Fixed IFFT Size (b) Fixed Modulation Scheme

Figure 4-3, shows the complementary cumulative distribution function (ccdf) for the CF. In Figure 4-3.a, we observe that for a fixed IFFT size (*N=256*), for higher-order modulation schemes the probability that $|x(n)| < r$, where r is the threshold, is higher than that for the lower-order modulation schemes. From Figure 4-3.b, we observe that the CF decreases as the IFFT size increases for a fixed-order modulation scheme (*M=64*). Figure 4-4, shows the ccdf for PAPR for different IFFT size and 64-QAM modulation.

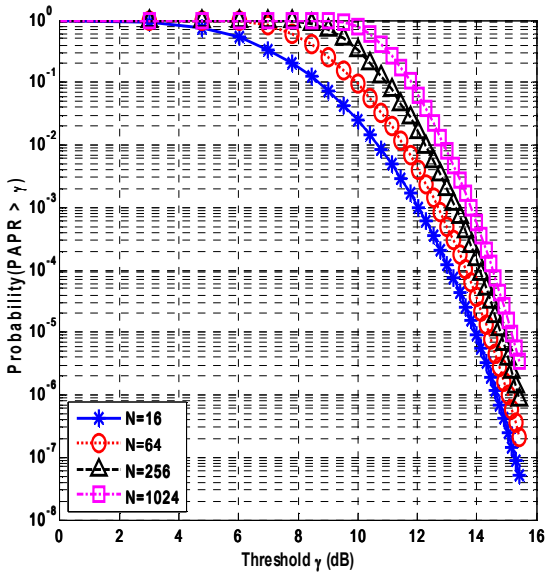

Figure 4-4: CCDF for PPAR Ratio

We observe that as the size of IFFT increases, the probability that the PAPR ratio will exceed the threshold (γ) also increases [10], [15]. Another use of Figure 4-4 is to obtain the input power backoff (IBO) value. An IBO value is a measure of how far the input power must be reduced to obtain the desired output linearity and power [23]. For example, suppose that we want to make sure that only 1 out of 10,000 OFDM symbols have any non-linear distortion, for an IFFT size of 256 and 64 QAM modulation scheme. In this case, from Figure 4-4, we can observe that the PAPR equivalent for an IBO of 10^{-4} is about 14 dB. In other words the clipping voltage should be at least 7 dB higher than the rms value of the signal. For an OFDM signal with high PAPR ratio, this requirement will severely limit the dynamic range of the input signal.

4.7. Impact of PAR on performance of OFDM/ FM systems

As described in Chapter 3, the SNR at the output of FM receiver depends on the rms bandwidth of the FM signal, the psd of the AWGN noise and the bandwidth of the lowpass filter. The rms bandwidth, in turn, depends on the rms value of the baseband modulating signal. For an OFDM system, the IBO value and its PAPR equivalent are selected according to linearity requirements as mentioned in Section 4.6. The threshold, γ, imposes a limit on the PAPR and consequentially on the rms value of the baseband signal. The smaller the IBO value is, the higher PAPR requirement is, which results in lower rms baseband values.

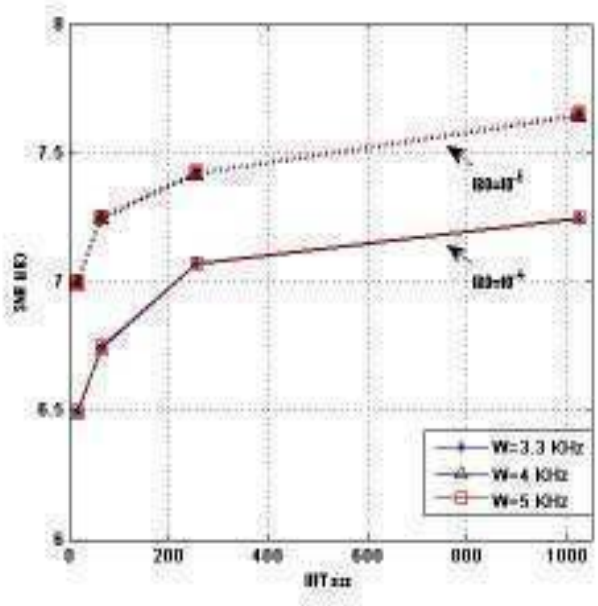

Figure 4-5: Decrease in SNR due to PAPR restrictions for different lowpass filter bandwidths

In the case of an OFDM over FM system, a lower rms value will result in a lower rms bandwidth for the FM signal. This would translate into a lower SNR at the FM receiver as seen in Section 3.6. Figure 4-5 shows the decrease in SNR observed for IBO values of 10^{-4} and 10^{-5}, for different bandwidths (W) of lowpass filter at the FM receiver. It can be seen that the decrease in SNR observed for the required PAPR values is greater for wider bandwidth filters. This is because the total noise power, given by equation 3.25, increases as bandwidth of filter increases. The difference between the observed SNR value and the maximum achievable SNR (corresponding to the maximum rms value) also depends upon the size of IFFT, N. As N increases, the probability that the PAPR ratio exceeds a given threshold, γ also increases. Hence, a greater loss in SNR is observed for higher IFFT sizes, as seen in Figure 4-5. Furthermore, the difference in SNRs also depends upon the IBO values. The lower the IBO value is, the higher the PAPR requirement is and the larger the decrease in SNR observed at at FM receiver will be. This observation is important given the high theoretical bound on values of PAPR/CF for OFDM symbols using M-ary PSK and M-ary QAM modulation schemes as discussed in Section 4.5. Thus, we can conclude that low IBO values not only result in lower non-linear distortion, but they also result in a lower SNR at the FM receiver.

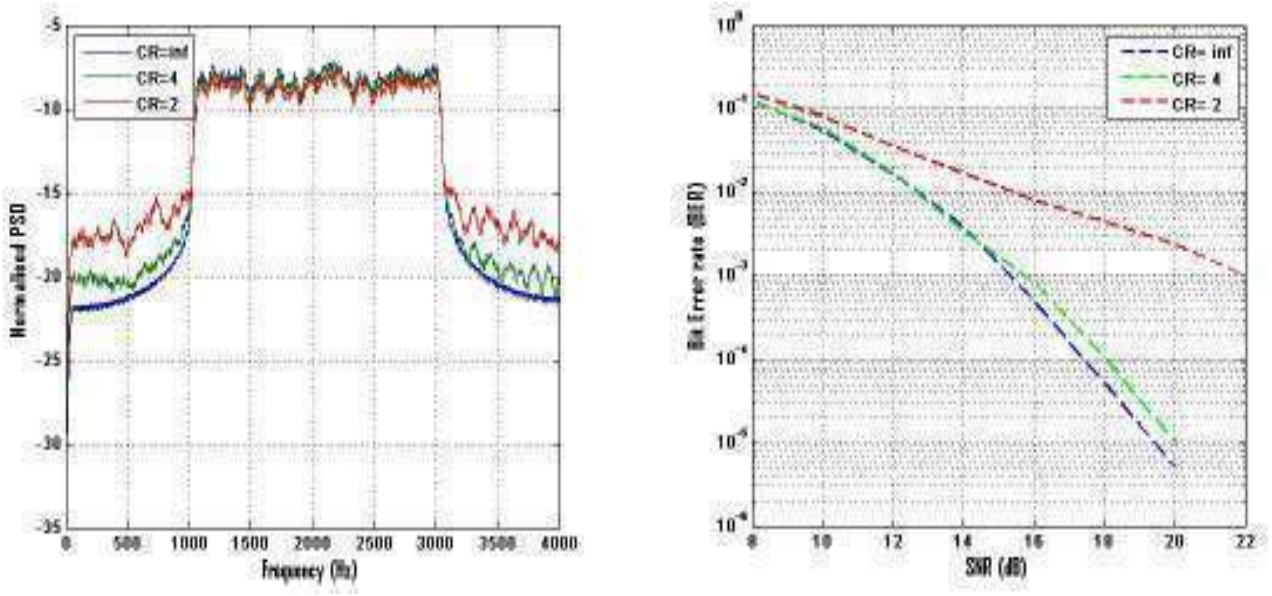

(a) (b)

Figure 4-6: Impact of clipping on performance of OFDM over FM systems

Another effect of high PAR values is the impact of clipping or non-linear distortion on the performance of an OFDM/FM system. A convenient way to characterize the non-linear distortion is by using Clip Ratio (*CR*). The term *CR* is defined as the ratio between the clipping amplitude and the rms value of the signal i.e $CR=A_c/\sigma_x$. A lower *CR* value indicates that the clipping amplitude, A_c, is close to the rms value of the signal with $CR=1$ indicating $A_c = \sigma_x$. Figure 4-6 shows the impact of clipping on the spectrum of an OFDM baseband signal and the resulting degradation in BER for an IFFT size of N=256 using 64 QAM modulation. As the value of *CR* decreases, the BER value increases due to an increase in the non-linear distortion which results from clipping the baseband signal. In Figure 4-6, a *CR* value of infinity ($CR=\infty$) indicates no distortion, while a CR value of 2 indicates that the clip amplitude is 3 dB higher than the rms value. Note that a high value of *CR* also indicates a higher IBO. Thus, based on the analysis in the previous paragraph, we can conclude that a trade off is required between the reducing the non-linear distortion of an OFDM signal and increasing the SNR at the FM receiver.

4.8. Chapter Summary

Multi-carrier modulation is a very attractive technology for next generation wireless broadband networks. OFDM is a type of MCM technique which provides robust multipath performance and high spectral efficiency. However, it suffers from high PAR depending upon the correlation between input sequences. In this chapter we presented the definitions of PAPR and CF, expressions for peak and rms values of OFDM symbols followed by theoretical bounds on PAPR and CF values for M-ary PSK and M-ary QAM modulation schemes. We also presented the statistical characteristics of OFDM signals. Using the statistical analysis and the theoretical bounds on PAPR/CF values, the impact of a high PAR OFDM signal on the performance of an OFDM over FM system was highlighted. We concluded that an OFDM/FM system with low non-linear distortion (low IBO) will result in low SNR at the FM receiver while a system with higher SNR will introduce greater non-linear distortion. In both cases the BER performance of the OFDM/FM system is degraded. Hence, a tradeoff is required between reducing non-linear distortion of the OFDM symbol and raising the SNR at the FM receiver.

References

[1] A. Odima, L Oborkhale and M.Kah, "The trends in broadband wireless network technologies", The Pacific Journal of Science and Technology, May 2007.

[2] R. Van Nee and R. Prasad, "OFDM for wireless multimedia communications", Artech House, 1999.

[3] K. Pahlavan and A. Levesque, " Wireless Information Networks", 2nd Edition, Wiley Publications 2005.

[4] J. Heiskala and J. Terry, "OFDM wireless LANs: A Theoretical and Practical Guide", Sams Publishing, 2001.

[5] B. Saltzberg, "Performance of an effcicient parallel data transmission system", IEEE Trans. on Comm. Vol 15, 1967.

[6] L.J. Cimini, "Analysis and simulation of a digital mobile channel using orthogonal frequency division multiplexing" , IEEE Trans. on Comm. Vol 33, 1985.

[7] H. Sari, et al., "Transmission Techniques for digital terrestrial TV broadcasting" , IEEE Comm. Magzine, Feb 1995.

[8] Y. Li and J. Cimini, " Bounds on the Interchannel Interference of OFDM in Time-Varying Impairiments", IEEE Trans. on Comm. Vol 49, 2001.

[9] D. Dardari, V. Tralli and A. Vaccari, "A theoretical characterization of nonlinear distortion effects in OFDM systems" , IEEE Trans. on Comm. , Oct 2000.

[10] J. Tellado, "Multicarrier Modulation with Low PAR: Applications to DSL and Wireless", Kluwer Academic Publishers, 2000.

[11] S. Thompson, J. Proakis and J. Seidler, " The effectivess of signal clipping for PAPR and total degradation reduction in OFDM systems", IEEE Globecomm, 2005.

[12] X. Li and J. Cimini, "Effects of clipping and filtering on the performance of OFDM", IEEE Comm. Lett., Vol 2, 1998.

[13] X. Wang and T. Tjhung, "Reduction of PAPR of OFDM systems using companding techniques", IEEE Trans. on Broadcasting, Sep 1999.

[14] B. S. Krongold and D. Jones, “An active-set approach for OFDM PAR reduction via Tone reservation”, IEEE Trans. on Sig. Proc., Vol 52, 2004.

[15] R. Rajbanshi, “ OFDM-based cognitive radio for DSA Networks”, Thesis PhD, Kanas State University, 2007.

[16] S. Weinstein and P. Ebert, “Data transmission by Frequency Division Multiplexing using the Discrete Fourier Transform” , IEEE Trans. on Comm. Vol 19, 1971.

[17] J. Proakis and D. Manolakis, “Digital Signal Processing”, Prentcie Hall 4th Edition. 2006.

[18] A. Leon-Garcia, “Probability and random processes for electrical engineering”, Prentice Hall 2nd Edition, 1993.

[19] J. Proakis, “Digital Communications”, McGraw Hill 4th Edition, 2000.

[20] A. Papoulis and S. Pillai, “Probability, Random Variables and Stochastic Processes” , McGraw Hill, 2002.

[21] S. Wei, D. Goeckel and P. Kelly, “A mordern extreme value theory approach to calculating the distribution of the peak-to-avergae power ratio in OFDM systems“, IEEE Int. Conf. on Comm., NY, 2002.

[22] H. Yu, M. Chen and G. Wei, “Distribution of PAR in DMT systems”, IEEE Electron. Lett. Vol 32, 2003.

[23] T. Nechiporenko and H. Nguyen, “Optimal Clipping Value for PAR Reduction of OFDM”, IEEE WCNC 2007.

5. Linear Scaling Technique (LST)

5.1. Introduction

The performance of OFDM for digital communication over mobile FM channels has been studied extensively [1], [2]. These studies evaluated the performance of an OFDM/FM system in presence of Rayleigh fading and different data modulation schemes [1]-[4]. Most of these analyses assumed that the amplitude of baseband signal was below the clipping threshold of FM Transmitter and that no non-linear distortion was introduced [4], [5]. As seen in Chapter 4, the clipping of a baseband signal generated using OFDM modulation is of great importance due to its high PAPR value. A high PAPR OFDM baseband signal will result either in a low SNR or a high non-linear distortion at the FM receiver. Both of these artifacts can significantly deteriorate the BER performance of an OFDM/FM system.

There are several solutions proposed in the literature that could be used to reduce the PAPR in OFDM systems [6]-[15]. These solutions include the use of error control coding, interleaving and constellation shaping techniques [10], [11], [12]. Most of these solutions are based on iterative approaches which possess high computational complexity. Several non-iterative algorithms based on Newman phases, Subcarrier Phase adjustments, Narahashi and Nojima phases which compute phase adjustments independent of input data sequences are also available [9], [13], [14]. However these approaches do not guarantee PAPR reduction and also suffer from large communication overheads which results in a decrease of data throughput for an OFDM system [9].

In this chapter we propose a new PAPR reduction method called Linear Scaling Technique (LST). The LST is based on calculating the tradeoff between maximizing the SNR at the FM receiver and minimizing the nonlinear distortion of OFDM baseband signal at the FM transmitter [15]. One of the important advantages of LST is that it has no implementation overhead and a minimum throughput overhead [16]. Performance improvements of up to 6 dB are obtainable using LST, depending upon the IFFT size and modulation scheme implemented. The rest of the chapter is organized as follows. The system model used for analysis is given in Section 5.2 followed by the characterization of non-linear distortion introduced by FM transmitter in Section 5.3. The LST is described in Section 5.5.

The results of simulation, analysis and experimental testbed are given in Sections 5.6, 5.7 and 5.8. Finally the implementation of LST algorithm is discussed in Section 5.9.

5.2. System Model

The system model considered for the OFDM/FM system analysis is shown in Figure 5-1. This model is applicable to a DDR system described in Chapter 2. As seen in the figure the data to be transmitted is represented by the mapped data vector *X*. The OFDM modulator converts this raw data vector into a baseband modulating signal *x(n)*. Without loss of generality, assume that the OFDM signal is real and has no dc offset. In this case the signal can be represented as

$$x(n) = \frac{2}{N} \sum_{k=1}^{\frac{N}{2}-1} a_k \cos(\frac{2\pi kn}{N}) + b_k \sin(\frac{2\pi kn}{N}); \quad n = 0,..., N-1 \qquad \textbf{5-1}$$

where *N* represents the number of sub-carriers, *k* represents the discrete frequency index, *n* represents the discrete sample index and a_k, b_k are constellation mappings for the implemented data modulation scheme. The derivation of the expression above was given in Chapter 4. This OFDM baseband signal is used to modulate the carrier frequency f_c to generate a FM signal *z(t)* given by 5-2 which is then transmitted over a LMR channel.

$$z(t) = A\cos(\omega_c t + u(t)) \qquad \textbf{5-2}$$

In 5-2 $u(t) = {2\pi f_d}/{k_m} \int_0^\tau m(\zeta)d\zeta$, f_d is the peak deviation of the FM signal and *m(t)* represents the continuous time version of a discrete time OFDM baseband signal, *x(n)*. The input to the FM receiver is represented by received signal *r(t)* given by

$$r(t) = h_c(t) * z(t) + w(t) \qquad \textbf{5-3}$$

where $h_c(t)$ represents the channel impulse response (CIR) and *w(t)* represents continuous time AWGN. For our analysis we assume that the CIR is accurately known and the received signal can be equalized such that the only channel impairments introduced are due to AWGN. The FM demodulated signal is given by *y(n)=x(n)+w(n)* where *w(n)* represents the discrete time AWGN samples. The output of OFDM demodulation is represented by vector *Y*.

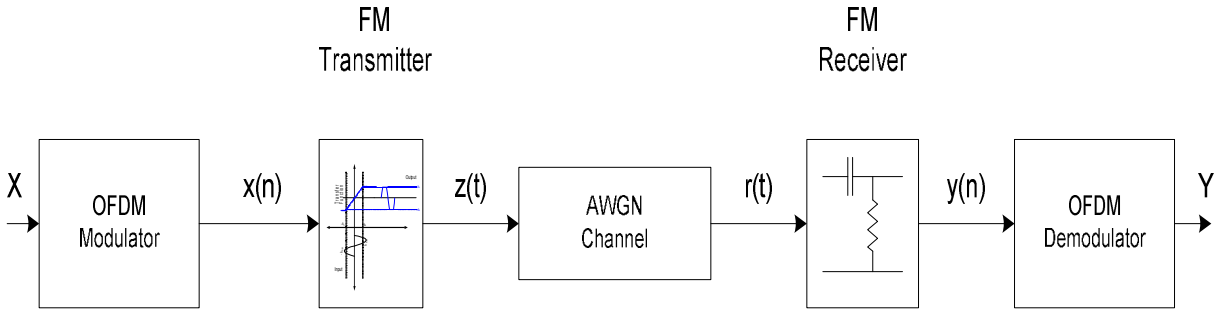

Figure 5-1: OFDM/FM system model

In order to obtain to compute the tradeoff between the SNR at FM receiver and the non-linear distortion of baseband signal at FM transmitter, we first characterize the non linear distortion as shown in Section 5.3. This analysis is then used to correlate the effect of distortion on SNR at the FM receiver in Section 5.4.

5.3. Non-linear Distortion Model

As discussed in Chapter 3, in practical FM systems, the permissible value of peak deviation f_d is predefined in order to minimize co-channel interference between two adjacent FM channels. The FM transmitter imposes the restriction on peak deviation by using a clipper circuit followed by a splatter filter as shown in Figure 3.2. Figure 5-2a shows the voltage response observed for an ICOM IC T7H radio, using a 1 KHz modulating signal [17]. From the figure it can be observed that any input signal with peak amplitude greater than 100 mV (≈ 200 mV_{p-p}) is clipped. There are number of ways of modeling non-linear devices like clipper circuits and high-power amplifiers (HPA) based on the AM/AM and AM/PM conversion characteristics of the device [18]. Commonly used models include Soft limiter model (SL) or Solid State Power Amplifier model (SSPA) or Travelling-wave Tube (TWT) model. The term AM/AM distortions refers to the change in magnitude of an input signal while the term AM/PM refers to the changes in phase of an input signal, resulting from the non-linearity [18], [20].

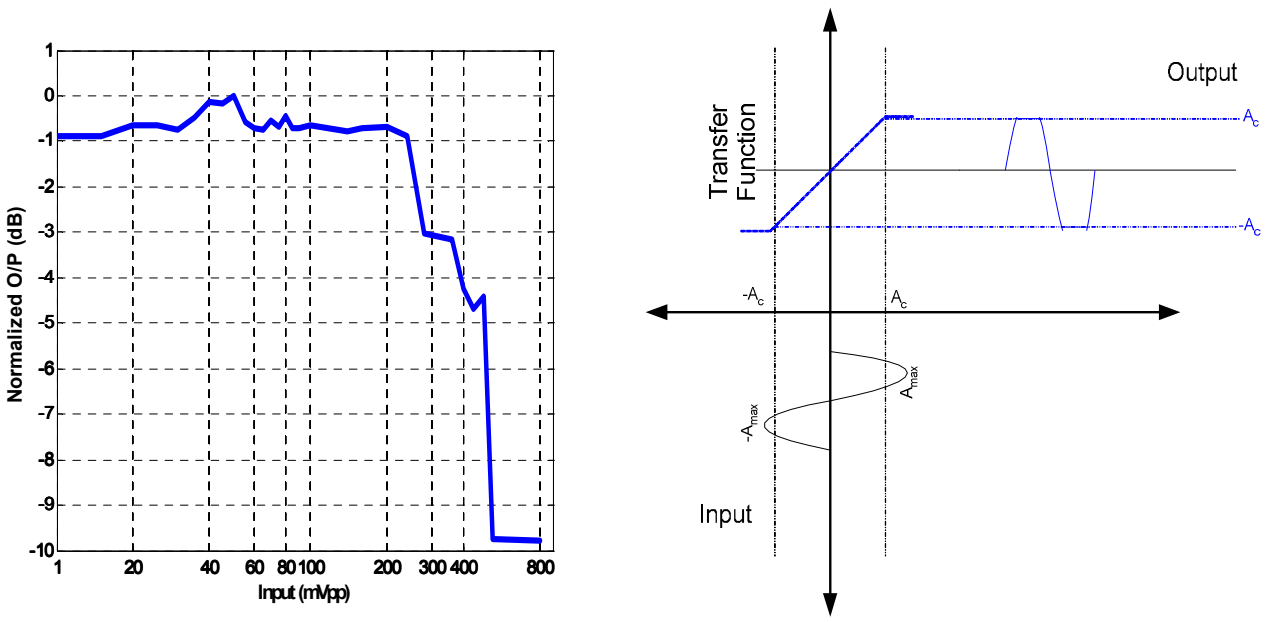

(a) (b)

Figure 5-2: Non-linear distortion (a) Response for ICOM IC T7H (b) Transfer function of soft limiter (SL)

A clipping device is commonly modeled as a nonlinear, memory-less device such as a soft limiter (SL) with a non linear function, *g(.)*. The transfer function for a SL is shown in Figure 5-2b. From the figure we observe that whenever the input signal amplitude exceeds the clipping amplitude A_c, the output waveform is distorted. It is important to note that this analysis assumes that the nonlinear function is non-expansive, i.e. $|g(x)| \leq |x|, \forall x$ and follows saturation property, i.e. $|g(x)| \leq A, \forall x$. This means that the clipper device does not result in any amplification of the input signal and that the output signal is bounded. This is consistent with the non-linear response observed in Figure 5-2.a. A non-liner device which results in amplification of input signals is better modeled as a HPA. Consider a input signal, *x(n)* represented in polar coordinates as

$$x = |x| e^{j \arg(x)} = \rho e^{j\phi} \qquad \textbf{5-4}$$

In the above equation the input signal *x(n)* is referenced as *x* without explicit reference to the discrete time samples. As mentioned before, a memoryless non-linear device can introduce distortion in amplitude and phase of the output signal characterized by AM/AM and AM/PM conversion functions. Using the polar coordinate representation of input signal, the distorted output of a SL can be represented as

$$x^g = g(x) = F[\rho] e^{j(\phi + \Phi[\rho])} \qquad \textbf{5-5}$$

where $F[\rho]$, $\Phi[\rho]$ represents the AM/AM and AM/PM conversion characteristics respectively while x^g represents the non-linear output. For a SL we consider only the amplitude distortion of the input signal. Hence $F[\rho]$ and $\Phi[\rho]$ are given by [18]

$$F[\rho] = \begin{cases} \rho; & \rho < A_c \\ A_c; & \rho > A_c \end{cases} \qquad \textbf{5-6}$$
$$\Phi[\rho] = 0$$

The nonlinear output, x^g can be represented as a sum of two uncorrelated signal components by using the Bussgang's Theorem; $x^g = g(x) = l^g x + d$, where d represents the nonlinear distortion and l^g is a proportionality constant [21]. The constant l^g is selected to minimize the mean square error (MSE) term $E[|g(x) - l^g x|^2]$. In this case it can be proved that the distortion term d will have minimum energy and will be uncorrelated with the input sequence, x [18], [19]. Furthermore, for SL the constant $l^g \rightarrow 1$ for sufficiently higher values of clipping amplitude A_c. Thus the output of SL can be approximated as shown

$$x^g = g(x) = x + d \qquad \textbf{5-7}$$

Equation 5-7 represents the non-linear distortion of the OFDM baseband signal by the FM transmitter. Note that it is assumed that the distortion d from a single OFDM symbol does not affect other received OFDM symbols. This can be easily ensured by making sure that the cyclic prefix (CP) in OFDM symbol is greater than the channel delay spread there by minimizing the Inter-symbol Interference (ISI) [22]. Assuming that no other distortion is introduced by the FM transmitter, the output at the FM demodulator is given by the sum of baseband signal, distorted signal and noise as

$$y(n) = x(n) + d(n) + w(n) \qquad \textbf{5-8}$$

5.4. Effects of non-linear distortion on SNR at FM receiver

As seen in Chapter 3, the SNR at the output of a FM receiver depends upon the rms bandwidth of FM signal, f_v, and the psd of AWGN noise, η, while f_v depends upon the rms value of baseband signal, σ_x. The signal power (S_o) at the output of FM receiver for a non-distorted baseband signal was derived in Section 3.5. The expression in equation 3-22 can be re-written in terms of the output of a non-linear device as

$$S_o = |\bar{y}(t)|^2 = E[(\lambda \omega_d x^g / k_m)^2] = (2\pi\lambda f_d)^2 / k_m \, E[(x^g)^2]$$
$$= (2\pi\lambda f_d)^2 / k_m \, E[(x+d)^2] = (2\pi\lambda f_d)^2 / k_m \, [\sigma_x^2 + \sigma_d^2] \quad \textbf{5-9}$$

where λ, k_m are proportionality constants, f_d is the maximum frequency deviation, x^g represents the output of the non-linear device as described in the previous section and σ_x^2, σ_d^2 represent the average power of baseband signal and the distortion signal respectively. In order to calculate the effect of distortion, d on the SNR of the received signal, we first need to obtain the average power of the distortion signal. As discussed in Chapter 4, for a sufficiently large value of N, an OFDM baseband signal, $x(n)$, can be approximated by a Gaussian distribution, that is, $x \sim N(0,\sigma^2_x)$. In this case, the average power of the distortion can be calculated as shown below:

$$\sigma_d^2 = E\{|d|^2\} = \int_{-\infty}^{\infty} (x - x^g) f(x) dx$$
$$= \frac{2}{\sigma_x \sqrt{2\pi}} \int_{A_c}^{\infty} (x - A_c)^2 e^{-x^2 / 2\sigma_x^2} dx$$
$$= \sigma_x^2 [-\sqrt{\frac{2}{\pi}} \delta e^{-\delta^2/2} + (1+\delta^2) erfc(\frac{\delta}{\sqrt{2}})] \quad \textbf{5-10}$$

where A_c represents the clip level and δ represents the Clip Ratio ($CR = A_c / \sigma_x$). As discussed in Chapter 4, a CR value is the measure of distortion introduced due to clipping of the baseband signal. For example, a δ=1 in case of a Gaussian variable, such as OFDM signal, would indicate that 31 % of the signal is distorted. As the value of CR decreases, the amount of distortion in the baseband increases as evident from 5-10 . It is also important to note that although the OFDM baseband samples, $x(n)$, are independently and identically distributed (i.i.d.) and Gaussain, the distortion samples $d(n)$ are i.i.d. alone and not necessarily Gaussian [18], [23]. The output noise power (N_o) depends upon the bandwidths of IF and baseband filters in FM receiver as described in Chapter 3. Assuming an ideal filter response and baseband bandwidth represented by W Hz, the noise power is given by

$$N_o = \frac{8\pi^2}{3} \frac{\lambda^2 \eta}{A_L^2} W^3 \quad \textbf{5-11}$$

where λ, A_L represent proportionality constants and η represents the psd for AWGN. The BER performance of an OFDM/FM system would depend upon the ratio of signal power to noise power given by 5-9 and 5-11. For a clipped signal, in addition to AWGN, the distortion will further lead to performance degradation as seen in Chapter 4. Using 5-9 and 5-11 we can obtain the expressions for the Signal-to-Noise plus Distortion Ratio (SNDR) as below

$$SNDR = \frac{\frac{(2\pi f_d)^2}{k_m^2}\sigma_x^2}{\left[\frac{(2\pi f_d)^2}{k_m^2}\sigma_d^2 + \frac{8\pi^2\eta W^3}{3A_L^2}\right]} = \frac{f_v^2}{[f_d^2\sigma_d^2 + \Psi_N]}; \quad where \quad \Psi_N = \left(\frac{2\eta W^3 k_m^2}{3A_L^2}\right) \qquad \textbf{5-12}$$

In the above equation, ψ_N represents the total output noise power at the baseband which depends upon proportionality constants k_m and A_L, baseband bandwidth W and psd of AWGN signal. It is important to note that the distortion samples *d(n)* are uncorrelated with AWGN samples *w(n)*. From 5-12, we observe that the SNDR value depends upon the rms bandwidth of FM signal, maximum peak deviation and average distortion and noise power.

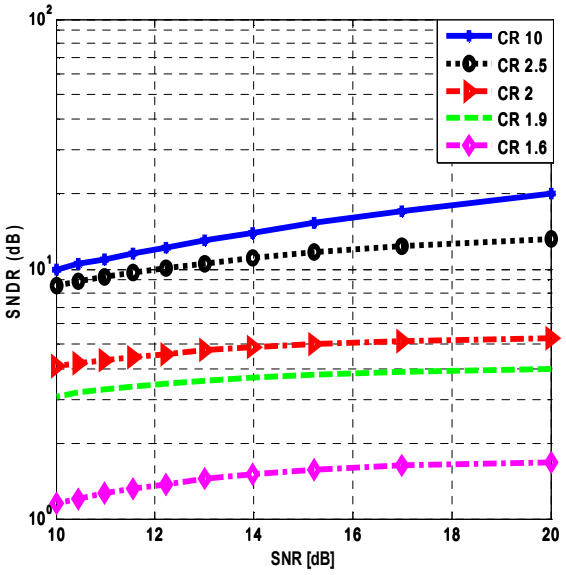

Figure 5-3: Comparison of SNDR and SNR at FM receiver

Figure 5-3 shows the SNDR and SNR values, in dB, as a function of different CR values. From the figure we observe that for higher CR values (>10) negligible amount of baseband signal is clipped

and hence only distortion in the baseband signal is due to AWGN samples i.e. SNDR ≈ SNR. However as the value of CR decreases the received baseband signal is heavily distorted i.e. SNDR << SNR. As previously mentioned the term SNDR is used to imply the presence of non-linear distortion and AWGN, while SNR reflects the SNR for an unclipped baseband signal [15]. This implies that as CR value decreases, the BER performance of the OFDM/ FM system decreases due to a decrease in SNDR value as seen in Figure 4-6b.

5.5. Linear Scaling Technique (LST)

Let the clipping amplitude of FM transmitter be represented by A_c and the maximum amplitude of baseband signal be represented by A_{max}. Then according to the definition of crest factor (CF) given in Chapter 4 and Clip Ratio given in Section 5.4, the expressions for CF and CR can be re-written as

$$CF = A_{\max}/\sigma_x \; ; \quad CR = A_c/\sigma_x \tag{5-13}$$

Let us define a quantity, Backoff Ratio (χ), as a ratio of CR and CF (CR/CF). Then using 5-13, χ can be expressed as shown:

$$\chi = CR/CF = \frac{A_c/\sigma_x}{A_{\max}/\sigma_x} = \frac{A_c}{A_{\max}} \tag{5-14}$$

From 5-14 we observe that for χ=1, the clipping amplitude will be equal to the maximum amplitude of the modulating signal, for any value of $\chi < 1$, the modulating signal will be clipped, and for $\chi \geq 1$ the modulating signal will be unclipped. Consider an OFDM baseband signal *x(n)* at the input of FM transmitter with a constant bandwidth *W* Hz and maximum amplitude $A_{max}=A_c$. For such a signal, the value of Backoff ratio is χ=1 i.e. there is no baseband signal distortion. Using 3-12 and 3-26 it can be shown that the rms bandwidth $\sqrt{f^2_v}$, and *SNR* for the received baseband signal, in this case, will be:

$$\sqrt{f_v^2} = f_d \sigma_x \; ; \quad SNR = f_v^2/\Psi_N \tag{5-15}$$

Now if the baseband signal *x(n)*, was scaled by a positive gain factor α (> 1) the Backoff Ratio for the resulting signal will be less than unity ($\chi < 1$) and hence the signal will be clipped. Using 3-12 and

5-12 the rms bandwidth and SNDR for the received baseband signal can be computed as shown below:

$$x'(n) = \alpha x(n); \quad \sigma_{x'}^2 = \alpha^2 \sigma_x^2 \qquad \textbf{5-16}$$

$$\sqrt{f_{v'}^2} = \alpha f_d \sigma_x = \alpha \sqrt{f_v^2};$$

$$SNDR = f_{v'}^2 \Big/ [f_d^2 \sigma_d^2 + \Psi_N] = \alpha^2 f_v^2 \Big/ [f_d^2 \sigma_d^2 + \Psi_N]$$

From 5-15 and 5-16, it can be observed that the output noise power Ψ_N at the FM receiver will remain constant, as it is not affected by scaling of the OFDM baseband signal in FM transmitter. Thus theoretically, in the absence of clipping distortion, the SNR of the unclipped baseband signal, at the FM receiver, should increase by a factor α^2. However, as the value of χ decreases the effects of distortion will start becoming prominent and degrade the overall performance. Note that the performance improvement obtained also depends on the output noise power, and that this analysis does not include the distortion occurring due to ICI between the orthogonal carriers in OFDM signal. Only the additive noise aspect of non-linear distortion is considered for the derivation. A more robust analytical expression will have to account for these effects.

Figure 5-4 shows the improvement in SNDR obtained for different values of CR, and different values of unclipped SNR using the equation shown in 5-12. For very low-noise power levels (SNR > 70 dB), introduction of any distortion will degrade the performance (SNDR < SNR). As the rms value, σ_x increases due to the scaling factor α, the CR value corresponding to the modified modulating signal decreases. The SNDR for higher noise powers (SNR < 40 dB) increases initially at higher CR values as the signal power increases due to linear-scaling factor, and the distortion is negligible. For lower CR values, where the clipping level is near the rms value of the modulating signal, the distortion contributes substantially to offset the gain achieved by increasing signal power, and hence the SNDR is lower than the corresponding SNR. Thus we can conclude that the SNDR value depends upon the scaling factor, extent of non-linear distortion and noise psd [16].

It is also important to note that as the scaling factor increases, the backoff ratio decreases. This is because as α increases, maximum amplitude of the baseband signal A_{max} also increases. The rms value of the baseband signal at the output of clipper circuit also increases. However the maximum amplitude A_{max} is limited to the clipping amplitude A_c. In other words the scaling of baseband signal in conjunction with clipping results in a decrease of PAPR for the OFDM modulating signal. Figure 5-5 shows the reduction in PAPR for different values of backoff ratio. From the figure we observe

that for backoff ratio greater than unity there is no decrease in PAPR value. This is because for $\chi \geq 1$, $A_c > A_{max}$ and hence no signal is clipped. However as value of χ decreases further the amount of baseband signal clipped increases and hence PAPR reduces.

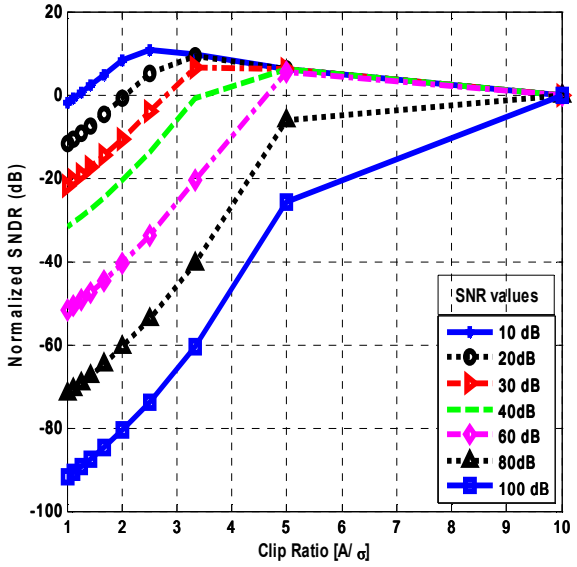

Figure 5-4: Effects of scaling on SNDR at FM receiver

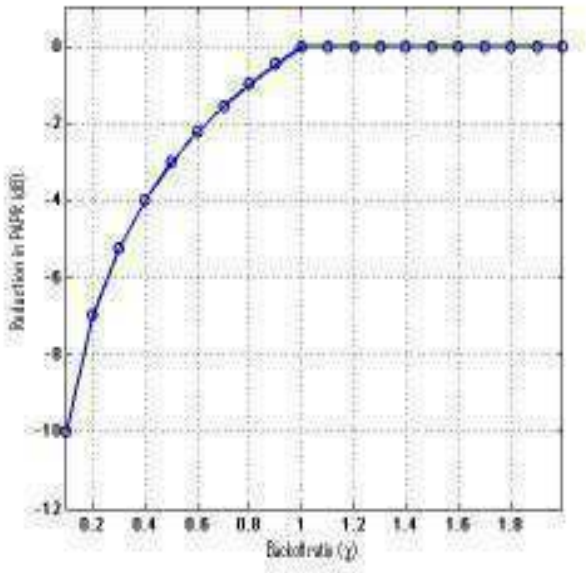

Figure 5-5: Reduction in PAPR for OFDM baseband signal due to LST

From the discussion in this section it can be concluded that for lower/moderate SNR values (SNR < 40 dB) the performance of an OFDM/FM system can be improved by scaling the baseband signal at

the FM transmitter at the expense of some non-linear distortion. This also reduces the PAPR value of the OFDM baseband signal. Note that the extent of improvement and the optimum backoff ratio varies according to the noise power as seen in Figure 5-4.

5.6. Simulation Results

As mentioned in the previous section, the amount of SNR improvement depends upon the optimum backoff ratio. From 5-13 we observe that for a constant CR value, the backoff ratio would depend upon the corresponding CF value. The IFFT size and data modulation scheme implemented affects the CF value of an OFDM baseband signal as discussed in Chapter 4. Hence for constant CR value the optimum value of χ will depend upon both, the IFFT size and data modulation scheme. Figure 5-6 and Figure 5-7 show the BER performance of an OFDM/FM system. For the simulations the maximum value of deviation was assumed to be 5 KHz and bandwidth of the modulating signal was assumed to be 2 KHz. The IFFT sizes varied between N=64, 256 and 512 while the modulation scheme implemented was M-ary QAM with constellation sizes of M=16, 64 and 256. The value of scaling factor α was varied from 1–10 linearly. For Figure 5-6, a fixed clipping amplitude (A_c) was assumed. The noise spectral density η was selected so that the SNR at maximum CR was 15 dB. This was selected to highlight the improvement obtained in BER performance. Matlab was used to simulate the OFDM/FM system performance.

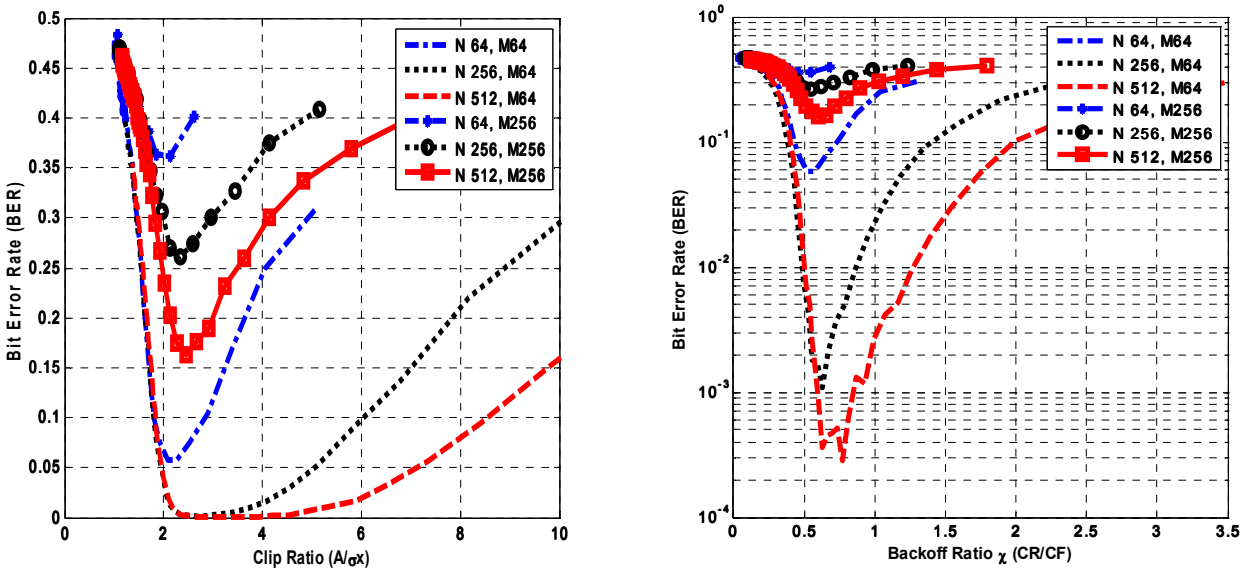

Figure 5-6: (a) BER Vs Clip Ratio (b) BER Vs Backoff Ratio

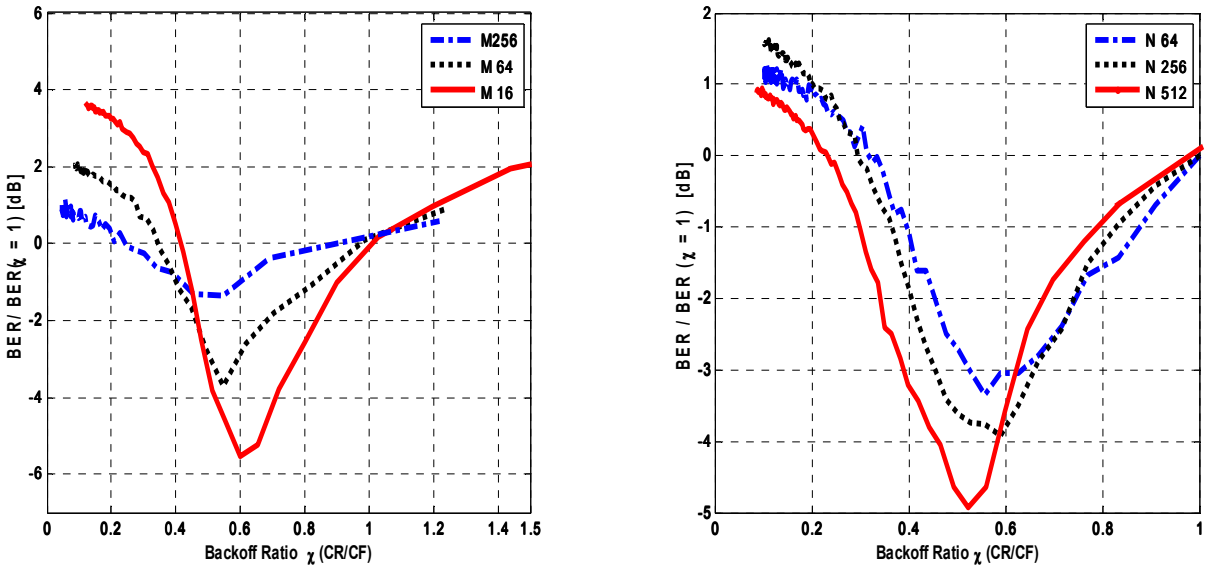

Figure 5-7: BER Vs Backoff ratio (a) Variable *M* (b) Variable *N*

For Figure 5-7, the clipping amplitude was set to the maximum amplitude of the un-scaled modulating signal i.e. A_c=A_{max} so as to obtain a backoff ratio of unity (χ=1). Again, the noise spectral density η was selected so that the SNR at maximum CR was 15 dB. Figure 5-6a shows the BER for different CR values for IFFT sizes of N=64,256 and 512 and M=64 and 256. As expected, the BER values decrease as SNDR increases initially for higher values of CR. For lower values of CR (<2), higher error rates are observed, reflecting the decrease in SNDR. In Figure 5-6b and Figure 5-7a,b we observe the BER performance with respect to the backoff ratio. The BER values at χ=1, represents the BER of the unscaled signal. Initially, as the value of χ decreases further, the BER decreases in tandem. However, for lower vales of χ, BER rises exponentially as the modulating signal is distorted heavily. Figure 5-7a shows the BER values normalized with respect to the unclipped BER for fixed IFFT size (N=256). We observe that for lower modulation schemes, the improvement obtained in BER values is more than that obtained for higher values. This is because the probability that amplitude of the OFDM signal is greater than the clipping threshold ($P(x[n]>r$) increases for higher modulation schemes as described in Chapter 4. Figure 5-7b shows the normalized-BER values obtained for a fixed modulation scheme (M=64). Lower-BER values are obtained for higher-IDFT sizes. This is because the probability that amplitude of OFDM signal is greater than the clipping threshold ($P(x[n]>r$) is lower for higher modulation schemes as mentioned in Chapter 4.

5.7. Analytical Results

The SNDR information can be used to compute the BER performance for an OFDM/FM system. The BER expression for M-ary modulation scheme is given by

$$BER \approx \frac{4}{\log_2(M)}\left(1-\frac{1}{\sqrt{M}}\right)Q\left(\sqrt{\frac{3SNDR}{M-1}}\right) \qquad \textbf{5-17}$$

Using 5-15, 5-16 and 5-17 we can obtain the normalized BER performance for an OFDM/FM system as shown in Figure 5-8. It can be seen that scaling an OFDM signal at the expense of nonlinear distortion is productive only till a minima is reached. At this point, the SNR gain obtained is maximum, and further attempts to improve the performance by increasing the scaling factor, α, becomes counterproductive. This is because of the increase in degradation due to nonlinear distortion, as more of the modulating signal is clipped. The CF values observed during simulations were used in plotting the theoretical performances. Furthermore, comparing Figure 5-6 and Figure 5-7, we observe that although the plots obtained using simulations and analysis look similar, the magnitude of changes in BER values varies significantly.

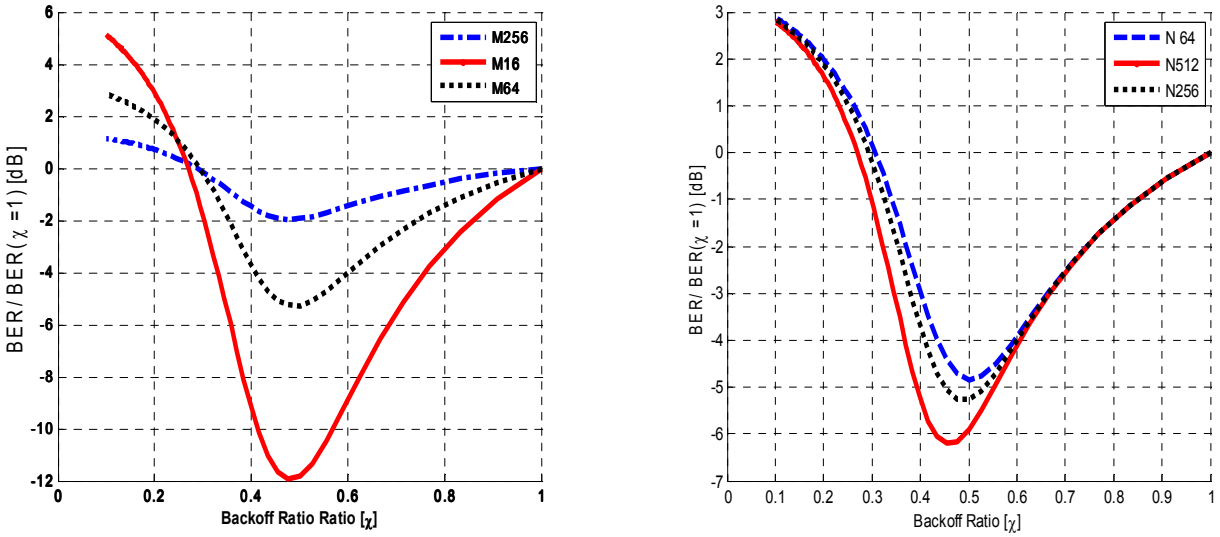

Figure 5-8: Analytical BER Vs Backoff ratio (a) Variable *M* (b) Variable *N*

One of the reasons for a better BER performance observed in case analysis as compared to results obtained by simulations is that the approximation for SNDR, as shown in 5-12, does not account for performance degradation due to in-band noise and ICI caused due to clipping operation. In other words, the theoretical approximation will account for only the additive noise aspect of distortion. As

mentioned in Section 5.4, a more robust approximation will have to account for the other factors. As opposed to the analytical expression, the simulations will be affected by ICI and in-band noise.

5.8. Experimental Results

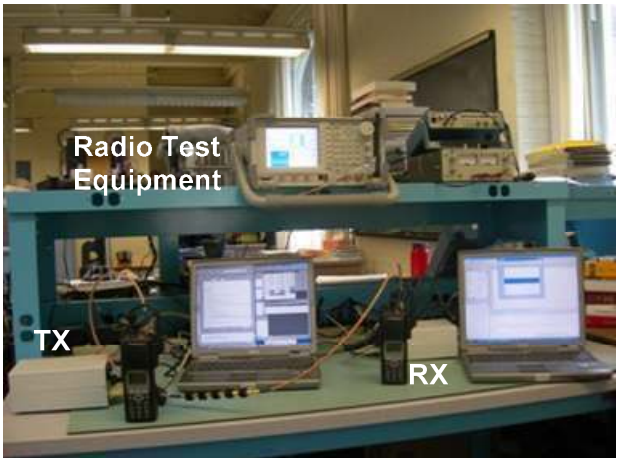

Figure 5-9: Experimental Test bed

Figure 5-9 shows the setup used for obtaining the experimental results. The setup consists of a transmitting and a receiving station which emulate a DDR system. Each station consists of a laptop and a base-band modem, which generates an OFDM audio-band signal and a LMR radio. The radio used in the current setup is a Motorola XTS 5000 portable hand-held radio [24]. The Motorola XTS 5000 radio is a dual-mode (Digital/Analog) radio. For the current test, we use the conventional analog FM-radio mode. The data to be transmitted is generated on the laptop at the transmitter end and transferred to the modem over the serial port using RS232 protocol. The modem converts the data into an OFDM signal which then drives the microphone input on to the portable radio. The amplitude of the generated OFDM signal (Vpp) is adjusted according to the transfer function, as shown in Figure 5-2a, by using the codec on the baseband modem. The modem on the receiver side synchronizes with the incoming signal and demodulates the same. A single-tap Decision Feedback Equalizer (DFE) is used to mitigate the distortion caused by the channel, so that only the nonlinear distortion due to clipping of OFDM signal can be studied. In order to minimize the effect of channel distortion and have a control over the RF SNR at the receiver, the portable radios are connected using a coaxial cable with power attenuators, as shown in Figure 5-9. The laptop on the receiver side compares the demodulated data with the transmitted data to compute the BER. Figure 5-10 shows the

results of the experimental setup. The estimated SNR at the base-band signal was 20 dB while the IFFT size, *N*, was 256 and the modulation scheme was 64 QAM.

The results of experimental tests are also compared with simulated and analytical results in Figure 5-10. Note that in case of experimental results in addition of AWGN noise in FM receiver the performance is also affected by the distortion by other non-linearities in FM transmitter/receiver chain. This is evident from the difference between the experimental results and simulation/analytical results observed in Figure 5-10. As expected the analytical results displays the best performance as it accounts for AWGN alone. Even the results of simulation only account for the non-linearity introduced by clipper circuit alone. A better equalizer implementation will be able to minimize the effects of distortion in a more efficient way and result in more accurate BER improvement representation for experimental testbed. However, from the objective of corroborating the theoretical model, the results obtained are sufficient. In addition to the difference in the extent of improvement, the value of optimum-scaling factor also varies. This is inferred from the locations at which the minima occur for each curve in Figure 5-10. For a fixed-noise power, as the amount of distortion increases, the sensitivity of the scaling factor also increases and the optimum-scaling factor shifts loser to unity.

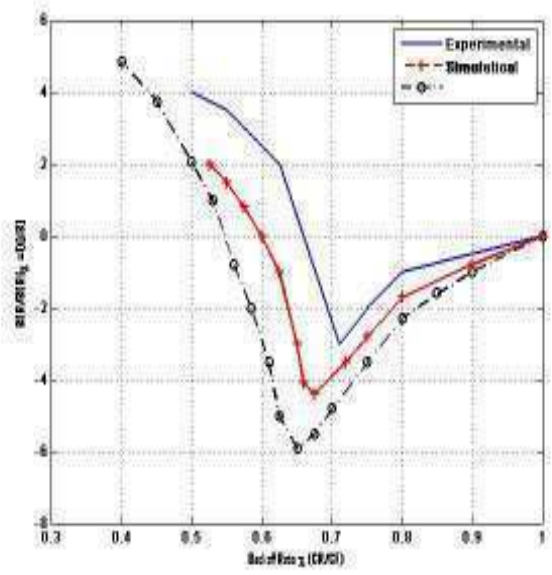

Figure 5-10: Comparison between results obtained experimentally, analytically and simulations.

In addition to the BER measurement, the rms deviation of the FM signal was also observed using Aeroflex IFR 2975 radio service monitor [25]. The observed values are tabulated in

Table 5-1. From the table we observe that the values of actual scaling factor α, and the value observed α_{obs} are approximately equal. The difference is due to the fact that clipping results in a decreased rms value of the signal. Further, we can observe that the difference is more pronounced at lower values of the Backoff ratio. This is because of the fact that as Backoff ratio decreases due to increase in scaling factor, the amount of signal clipped also increases, and hence the actual rms value of the OFDM signal does not increase proportionally.

Table 5-1: BER Vs Backoff Ratio (Experimental)

χ Backoff Ratio	α Scaling Factor	$\sqrt{f_v}$, RMS Deviation	$\alpha_{obs} = \sqrt{f_v}/\sqrt{f_v}$
1	1	1.08	1
0.88	1.125	1.19	1.1
0.8	1.25	1.31	1.21
0.76	1.32	1.37	1.26
0.72	1.37	1.43	1.32
0.65	1.51	1.54	1.42

5.9. Implementation of LST in DDR systems

As seen in preceding sections, LST achieves improvement in BER performance by scaling the baseband modulating signal thereby introducing some amount of non-linear distortion. The optimum value of backoff ratio also depends upon the IFFT size and modulation scheme. In case of DDR systems as discussed in Chapter 2, the IFFT size is constant while the modulation scheme changes. The system setup that can be used for finding the optimal backoff ratio is depicted in Figure 5-11. As

seen in above figure, the audio codec on the DDR modem is used to provide the scaling. The calibration routine is described below:

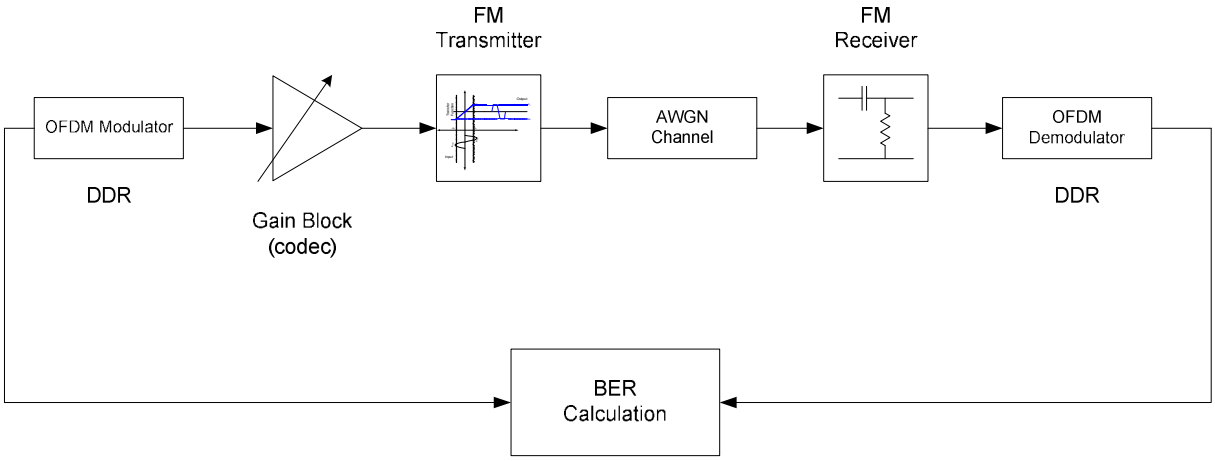

Figure 5-11: Block diagram of DDR system setup

(a)During initialization, the codec gain on the DDR which is to be calibrated is set to minimum. This is done to ensure that the baseband signal is not clipped by the FM transmitter.
(b)A known pattern of a selected modulation scheme is then transmitted from the modem. In order to ensure that the channel distortion is minimum, an AWGN channel is used during the calibration process. This can be accomplished by connecting the TX/RX pair using a coaxial cable.
(c)The BER at the FM receiver is calculated using the knowledge of the transmitted signal.
(d) The gain on the codec of Transmitting DDR is increased by a predefined amount. Repeat steps (b) through (d) till the BER observed during previous iteration is lower than the current BER value.
(e) Save this gain setting for future use and repeat steps (a)-(d) for all the modulation schemes.

Once the table consisting of optimum gain settings is tabulated, the DDR terminal is ready to be used. Every time a modulation scheme is changed, the codec gain is changed, according to the lookup table, to reflect the optimum value. Note that although the procedure described above is more suited for stationary channels, it can be repeated to obtain optimum performance at any SNR value or channel condition. This can be done by using special calibration symbols inserted in a DDR physical layer frame (PPDU) defined in Chapter 2. The BER performance, in this case, will have to be communicated back to the transmitting station by the receiver by using specific feedback frames. If the variation in channel profile is not drastic, we can converge to an optimum gain setting faster. For

example, if the SNR changes from 20 dB to 25 dB for an IFFT size of 256 and 64 QAM, the number of codec steps required to converge on to the optimum backoff ratio will be 5.This is assuming a codec step size of 0.2 dB. Another advantage of this technique is that it does not result in any computational overhead for the DDR modem. Only the gain setting on the codec has to be changed.

5.10. Chapter Summary

In this chapter we introduced a new method called LST to mitigate the performance degradation resulting from non-linear distortion of high PAPR OFDM baseband signal. The LST is based on computing the optimum clipping value of the baseband signal. We presented the results obtained using simulation, analytical derivations and from experimental testbed. It was observed that the effectiveness of LST depends upon the IFFT size and modulation scheme implemented. BER performance improvements upto 6 dB were observed. This observation can be used to increase the data rate or BER performance of DDR systems. For example, for a constant BER rate of 10^{-6}, a 128-QAM modulation scheme can be used in-conjunction with LST instead of 64 QAM, thereby compensating for the increase in SNR requirement. This would effectively increase the data rate to 14 Kbps without the use of any additional audio bandwidth. Similarly, for a constant modulation scheme of 64 QAM and IFFT size 256, the BER performance can be improved by a factor of 3 dB at SNR of 20 dB.

References

[1] E. Casas and C. Leung, "OFDM for digital communication over mobile radio FM channels-Part I", IEEE Trans. on Comm., May 1991.

[2] L. Cimini, "Analysis and simulation of a digital mobile channel using orthogonal frequency division multiplexing", IEEE Trans. on Comm. Vol 33, Jul 1985.

[3] M. Ridder-de Groote, et al. "Analysis of new methods for broadcasting digital data to mobile terminals over an FM channel", IEEE Trans. on broadcasting, March 1994.

[4] A.C. Navalekar, " Design of High Data Rate Audioband OFDM Modem", Master's Thesis, Worcester Polytechnic Institute, 2006.

[5] D. Dardari, V. Tralli and A. Vaccari, "A theoretical characterization of nonlinear distortion effects in OFDM systems" , IEEE Trans. on Comm. , Oct 2000.

[6] S. Thompson, J. Proakis and J. Seidler, " The effectivess of signal clipping for PAPR and total degradation reduction in OFDM systems", IEEE Globecomm, 2005.

[7] X. Wang and T. Tjhung, "Reduction of PAPR of OFDM systems using companding techniques", IEEE Trans. on Broadcasting, Sep 1999.

[8] R. Nee and A. Wild, "Reduction of peak to avearge power ratio of OFDM", IEEE VTC 1998

[9] R. Rajbanshi, " OFDM-based cognitive radio for DSA Networks", Thesis PhD, Kanas State University, 2007.

[10] T. Wilkison and A. Jones, "Minimization of the peak to mean envelope power ratio of multicarrier transmission schemes by block coding", IEEE VTC, Chicago, 1995.

[11] R. Bauml, R. Fisher and J. Huber, "Reducing the peak to average power ratio of multicarrier modulation by selective mapping", IEEE Electron. Lettr., Vol 32, 1996.

[12] A. Jayalath and C. Tellambura, "The use of interleaving to reduce the PAPR of OFDM schemes by scelective scrambling", IEEE Globecomm, San Fransico, 2000.

[13] D. Gimlin and C. Patisaul, "On minimizing the PAPR for the sum of N sinusoids", IEEE Trans. on Comm., Vol 41, 1993.

[14] S. Narahashi and T. Nojima, “New phasin scheme of N-multiple carriers for reducing PAPR”, IEEE Electron. Lettrs. Vol 30.,1994.

[15] A. Navalekar and W. Michalson, “A New Approach to Improve BER Performance of a High Peak-to-Average Ratio (PAR) OFDM signal over FM based LMRs”, IEEE WTS, Pomona, 2008.

[16] A. Navalekar and W. Michalson, “A Linear Scaling Technique (LST) for improving BER performance of high PAR OFDM signal over FM-based LMR”, *resubmitted*, IEEE Trans. on Broad., 2009.

[17] ICOM, “ICOM IC T7H Specific Sheet”, 2002.

[18] J. Tellado, “Multicarrier Modulation with Low PAR: Applications to DSL and Wireless”, Kluwer Academic Publishers, 2000.

[19] M. Friese, “On the degradation of OFDM signals due to peak-clippin in optimally predistorted power amplifiers”, IEEE Globecomm,Sydney, 1998.

[20] D’Andrea et al., “RF power amplifier linearization through amplitude and phase predistortion”, IEEE Trans. on Comm., 1996.

[21] J. Bussgang, “Crosscorrelation functions of Amplitude Distorted Guassian Signals”, RLE, MIT, March 1952.

[22] J. Heiskala and J. Terry, “OFDM wireless LANs: A Theoretical and Practical Guide”, Sams Publishing, 2001.

[23] A. Leon-Garcia, “Probability and random processes for electrical engineering”, Prentice Hall 2nd Edition, 1993.

[24] Motorola, “Astro XTS 5000 Specification Sheet,” 2004.

[25] Aeroflex , “Radio Test Set IFR 2975 Operations Manual” , Publication 1002-4202-2P0, Jan 2005.

6. Push-To-Talk (PTT) Delays

6.1. Introduction

The use of DDR I provided a bandwidth efficient method of communications over LMR channels as discussed in Chapter 1. In Chapters 3 and 4 we developed an analytical frame work for performance evaluation of OFDM/FM systems. This was followed by proposal of a new PAPR reduction technique, LST, in Chapter 4. The use of LST improves the Physical Layer (PHY) performance of DDR II modems which may translate into a higher data rate or better a BER performance as described in Chapter 4 [1], [2]. This enables the DDR technology to cater to hybrid applications like VOIP which have higher data rate requirements [3].

Another important factor which affects the throughput performance of a wireless network is the MAC Layer protocol. One of the important functions of MAC layer is to ensure a fair access to the wireless media [4]. There are number of ways to implement a channel access mechanism like Time Division Multiple Access (TDMA), Frequency Division Multiplexing (FDMA), and Carrier Sense Multiple Access (CSMA) [4], [5]. In case of TDMA implementation, a single frequency channel is shared between different users by dividing a single frame into a number of time slots. This allows individual nodes to share the same medium without interference. An example of a TDMA system in LMR networks will be a TETRA network [6]. FDMA, on the other hand, supports multi-node networks by allocating different frequency channels to each node. An example of FDMA system would be a P 25 system [7]. As described in Chapter 2, DDR technology uses Carrier Sense Multiple Access (CSMA) with Collision Avoidance (CA) for data transmissions to ensure fair access to a wireless channel. CSMA is a classic protocol which implements channel access mechanism by monitoring the shared medium activity [4], [8]. The performance of CSMA in wireless local area networks has been studied extensively in literature [8]-[14]. There are a number of analytical models which correlate the performance of CSMA protocol to MAC layer factors like size of contention window and schedule pipelining [9], [10]. Performances due to capture effect, propagation delays and directional antennas have also been studied for WLANs [11], [12]. In addition to decrease in throughput, a multi-node WLAN also suffers from asymmetric throughput problems arising due to several factors like Unfair Access (UA) or Unintentional Denial of Service (UDOS) [13], [14].

For LMR networks, in addition to the factors mentioned in the previous paragraph, another important parameter that affects the throughput is Push-to-Talk (PTT) delays [15]. A PTT delay refers to the delay between the instant when PTT line (switch), on a conventional LMR radio, is keyed/unkeyed and the instant when a response is observed at the radio output. These delays result in an increase in the size of collision window. A collision window refers to the time interval when transmissions from contending nodes can overlap. A typical PTT delay for a LMR node can run between tens to hundreds of milliseconds. The use of LMR networks was traditionally restricted to voice traffic, in which a user himself provided the mechanism for channel access, and hence the effects of PTT delays were greatly overlooked [16]. Since a PTT delay can protract the collision window to several hundreds of milliseconds, it not only affects the throughput of LMR networks but will also impact the performance of latency sensitive applications like VOIP. For example, PTT delays for a LMR network consisting of ICOM IC-T7H radios will introduce a latency of about 110 msec and result in 10-25 % increase in collision rate depending upon number of radios in the network [17]. Furthermore, a LMR network consisting of radios with different PTT delay profiles will exhibit asymmetric throughput problem which will impact the capacity planning for heterogeneous LMR networks [18].

In this chapter we highlight the impact of PTT delays on the throughput performance of DDR networks. Note that although the analysis conducted in this chapter is specific to CSMA/CA implementation for DDR networks, it can be extended to other LMR networks. We first present the typical PTT delay values and their distributions in Section 6.2. This is followed by brief description of the DDR MAC layer implementation in Section 6.3. A theoretical model for probability of collision for heterogeneous networks is developed in Section 6.4 followed by discussion on results of simulation and analysis in Section 6.5. The impact of PTT delays on performance of DDR networks is highlighted in Section 6.6.

6.2. PTT delays

As mentioned in the previous section, a PTT delay refers to the time difference between the instant when PTT line (switch) on a conventional analog radio is keyed and the instant when a RF carrier is observed at the antenna output. This delay is referred to as Receive-To-Transmit Switch Interval (RTSI). A similar delay occurs when the PTT line is un-keyed and is referred to as Transmit-To-Receive Switch Interval (TRSI). These delays occur due to the latency involved in switching

between transmit and receive hardware chains. The magnitude of delay depends upon the implementation of RF front end for transceivers. For example, in case of a full duplex RF front end with separate transmit and receive chains and antennas, the PTT delays would be negligible. As opposed to this a half duplex design where a single antenna is shared by transmit and receive chains, the switching mechanism will introduce delays. Typical values of switching delays can range from few microseconds, in the case of cellular phones, to several hundred milliseconds in the case of LMR radios [19].

Figure 6-1: Delays during keying and unkeying for a conventional analog radio

Figure 6-1 shows a snapshot at the antenna output observed, for a LMR radio, between the assertion and de-assertion of the PTT switch. The transition of PTT line from high level to low level indicates the keying of the radio. The corresponding RTSI delay is represented by the KEY_DELAY in the figure. Likewise, the transition of PTT line from low level to high level indicates unkeying of the radio. The resulting TRSI delay is shown by UNKEY_DELAY in the figure. We also observe that in case of RTSI delay there is no signal at the antenna output while in case of TRSI delays the channel is occupied by transient noise. This would indicate that TRSI introduces a delay in the network while RTSI, in addition to delays, result in collisions between contending nodes of a network. The impact of delays on throughput performance of CSMA networks has been studied previously and hence the analysis of TRSI delays is trivial and not discussed in this dissertation [8], [9]. However RTSI which introduces collisions, in addition to delays, warrants further investigation.

Figure 6-2, shows the RTSI Delay distribution observed for a Motorola XTS 5000 and ICOM IC-T7H radio sets. A DDR modem is used to key/unkey the LMR radios. From Figure 6-2.a, we observe that the mean value of RTSI delay for a Motorola XTS 5000 radio was approximately 83 msec and that for the ICOM IC-T7H radio was approximately 115 msec [20], [21]. The Gaussian distribution and polynomial fit for PTT delay values for Motorola XTS 5000 and ICOM IC-T7H can be seen in Figure 6-2.a. A Gaussian distributions with parameters (μ=0.08, σ^2=2.8e-6) and (μ=0.115, σ^2=4.8e-6) is used to represent RTSI delays for a XTS 5000 and ICOM T7H radios respectively in Figure 6-1.a. The Cumulative Distribution Function (cdf) for the RTSI delay values is shown in Figure 6-2.b. From the figure we can observe that the 96 percentile value for the delay distribution is 85 msec and 118 msec for XTS 5000 and IC-T7H radios respectively [22].

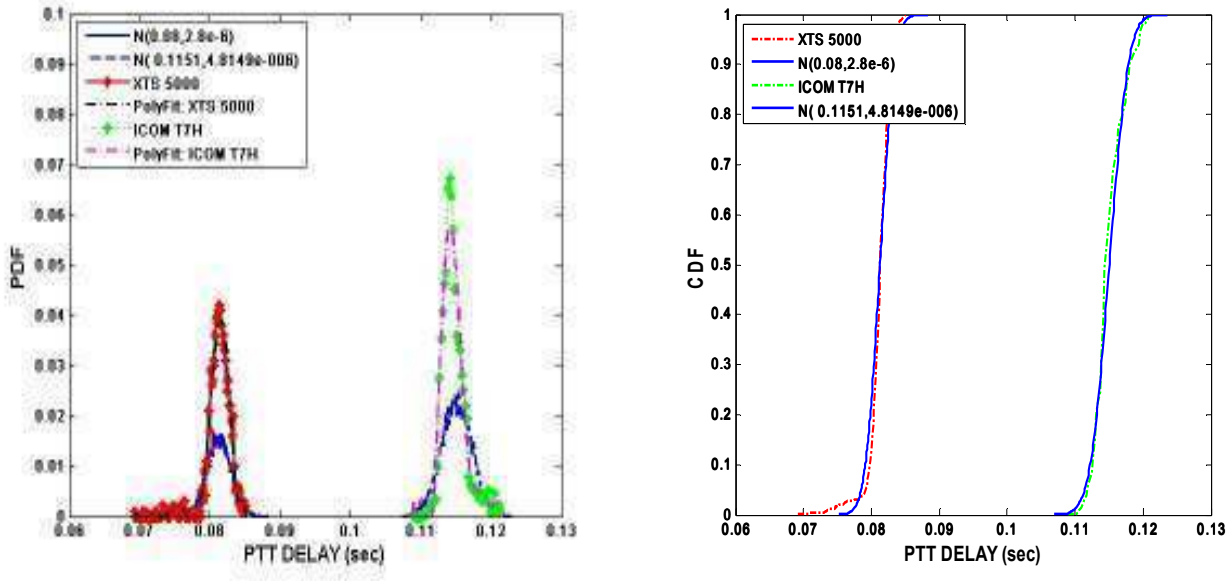

Figure 6-2: Distribution of RTSI delays for Motorola XTS 5000 and ICOM IC-T7H

6.3. CSMA/CA implementation for MAC layer

A MAC layer protocol ensures fair access to a shared resource such as a wireless channel. As discussed in Chapter 2, for voice transmissions, the users themselves enforce a de-facto contention resolution mechanism. As mentioned in the introduction, for data transmissions some variation of channel access mechanisms like Time Division Multiple Access (TDMA)/Frequency Division Multiple Access (FDMA)/ CSMA, is used. FDMA is spectrally less efficient but simpler to implement than TDMA which is more efficient but more complex to implement due to the network

synchronization requirement [4], [5]. CSMA is a classic protocol used to arbitrate channel access between contending nodes in adhoc or infrastructure based WLANs. In this method a node which has data to transmit attempts to avoid collisions by listening to the channel and only transmitting when no activity is detected on the channel [8]. Modified versions of CSMA protocols such as CSMA with Collision Avoidance (CSMA/CA), Floor Acquisition Multiple Access (FAMA) and Multiple Access with Collision Avoidance (MACA) exist [23], [24] and [25]. These protocols differ by the action (pertaining to data frame transmission) that a terminal takes after sensing the channel. However, in all cases, when a terminal learns that its transmission was unsuccessful, it reschedules the transmission according to a randomly distributed retransmission delay. At the end of delay time, the transmitter senses the channel again and if inactive begins the transmission. The time window for backoff depends upon the implemented algorithm. Most commonly used algorithms use uniform or exponential distribution. This time window is referred to as a contention interval. Using a random backoff time ensures collision avoidance. Another way to implement collision avoidance is by using a preamble or a handshaking procedure.

A CSMA algorithm can be implemented in a non-persistent or *p*-persistent form. For details on implementation of non-persistent CSMA protocol please refer to [8]. For our analysis, we consider a variation of *p*-persistent CSMA/CA protocol used by DDR modems. Any radio which has a packet to send first senses the channel to detect any existing transmissions. If the channel is occupied, the packet is identified as backlogged and queued for retransmission. The CSMA protocol is designed to reduce collision probability between multiple LMR nodes, at the point where collisions will most likely occur. Just after the channel becomes idle (as detected by carrier sensing) is when the highest probability of collision exists. This is because multiple nodes might be waiting to transmit data. To avoid collisions, each LMR node which has a backlogged packet selects a random backoff before initiating data transfer. The backoff time is selected randomly within a uniformly distributed backoff time window. In case of DDRs, the length of the window, which defines the contention interval, is constant. Thus each LMR node with a backlogged packet transmits packets with a probability p the next time channel becomes free.

From the above paragraph we can conclude that the one of the factors which would affect the performance of the CSMA protocol is the ability to sense the activity on a channel. If the channel is deemed inactive in spite of an ongoing transmission from another node, the sensing node will initiate data transfer, resulting in a collision. This would affect the throughput of the system. A similar

phenomenon is produced by RTSI delays. As seen in Figure 6-1, there is a delay between assertion of PTT line and the instant when a carrier signal is observed at the antenna o/p. Any node in the network which senses the channel in this duration (KEY_DELAY) will assume that the channel is inactive and may initiate transfer of data resulting in a collision. Such a collision can also be interpreted as an unintentional denial of service in which the packets from the primary transmitting mode are jammed by transmissions from other nodes in the networks. Also note that a DDR modem is half duplex i.e. it can either be in receive mode or transmit mode. This means that the two or more colliding nodes have no way of finding out that a collision has occurred. The time interval over which the transmissions from two or more nodes can collide is referred to as a collision window (*CW*). The impact of collisions on the performance of DDR networks is shown in Figure 6-3. In Figure 6-3.a, we plot the throughput performance of a DDR network as a function of different RTSI delays and number of nodes in absence of collisions while Figure 6-3.b shows the performance in presence of collisions. Ptolmey was used to obtain the simulation results. The contention interval for simulations was assumed to be uniformly distributed between 0 to 1 sec. Note that although the performance of a network also depends upon the duration of contention interval, a theoretical analysis of this relationship is beyond the scope of this dissertation. Only the impact of contention window size is addressed later in Section 6.6.

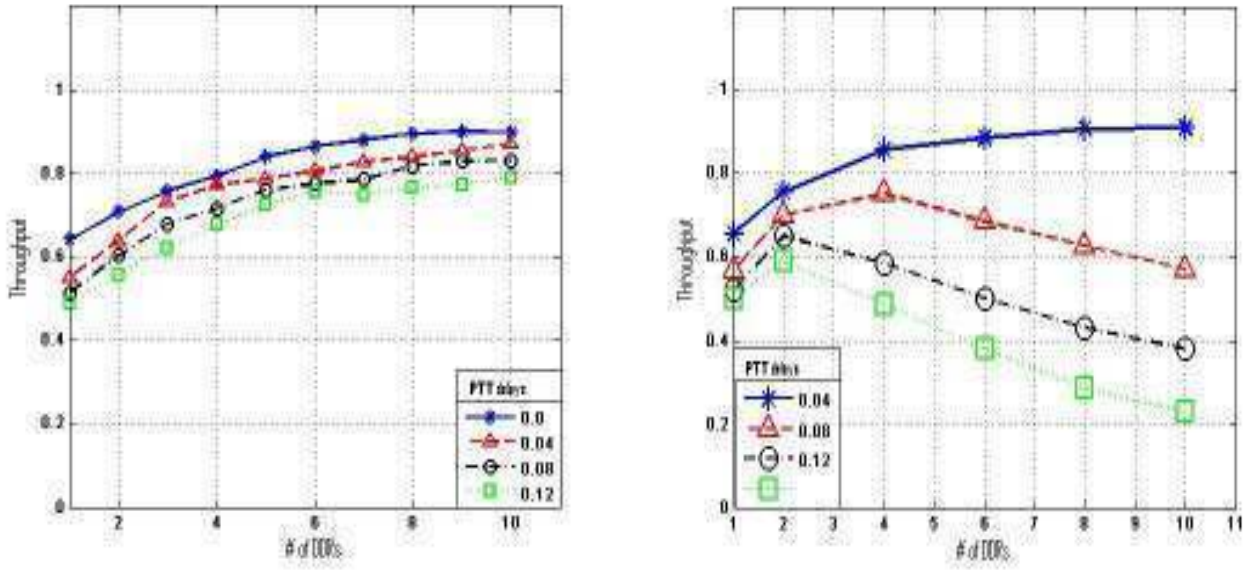

(a) (b)

Figure 6-3: Channel throughput for number of DDR nodes (a) Without Collision (b) With Collision

From Figure 6-3.a, we observe that in absence of collisions, the throughput of a network increases as the number of nodes increases. In this case it is assumed that the RTSI delays will only impact the transmission delay. However, if the collisions due to RTSI delays are considered the throughput performance degrades as number of nodes increase. This is because greater the number of nodes, higher is a probability that two or more nodes decide to transmit within the collision window. Furthermore, we observe that as the RTSI delay increases the throughput decreases further. Thus an RTSI delay affects the throughput performance in two ways; first it introduces delay in the network and secondly it increases the number of collisions in the network. In the next section we develop a theoretical model to calculate the probability of collisions for nodes with different RTSI delay profiles.

6.4. Collision Probability: Effects of RTSI Delays on CSMA/CA

As discussed in previous section RTSI delay will affect the performance of CSMA/CA algorithm since any decision about the channel availability during RTSI will yield erroneous results. For a node which has elected to transmit, the carrier sensing mechanism will be suspended during RTSI interval. Conversely, other DDR nodes sensing the channel during this RTSI, will infer that the channel is free for transmission and may start transmitting a packet. Thus RTSI protracts the collision window between contending DDR nodes, increasing the probability of collision. Figure 6-4, delineates the impact of RTSI on collision window size. As mentioned in Section 6.3, a collision within the duration of a collision window can be interpreted as an unintentional interference and will result in a denial of service (DOS) for the transmitting node.

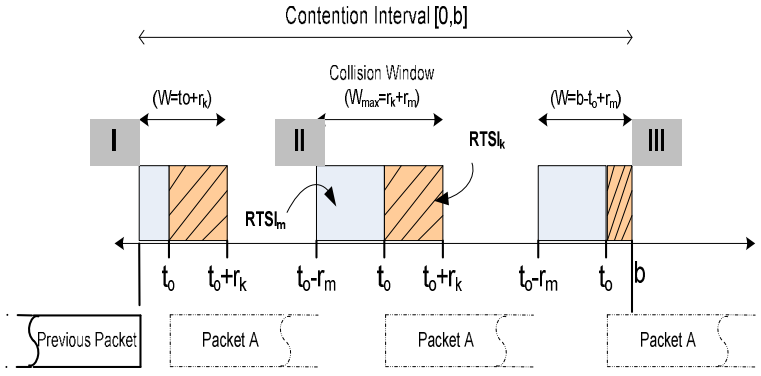

Figure 6-4: Collision window for a single node

To better understand the impact of an increase in collision window size, consider a heterogeneous DDR network consisting of two nodes with two RTSI delay profiles. Let the RTSI delays be represented by constants r_k and r_m. Assume that a Node k decides to transmit at an instant t_0 as shown in Figure 6-4. Now due to RTSI, the other node in the network will sense this channel activity only after t_0+r_k seconds. If the Node m is scheduled to transmit packet between the interval $\{t_0, t_0+r_k\}$, it will sense the channel inactive and hence commit to a transmit. This will result in a collision between the two nodes. This duration of the collision window is represented by $RTSI_k$ in Figure 6-4. The same argument is applicable to the original transmitting node k; while making a decision about the activity on the channel, it cannot be certain that the other node hasn't committed to a transmit within the interval $\{t_0-r_m, t_0\}$. This is shown in Figure 6-4 as $RTSI_m$. Thus the two competing nodes can unintentionally collide with each other within the collision window (W) resulting in an unintentional DOS for the transmitting node.

From Figure 6-4 we can calculate the size of collision window in presence of RTSI as shown below

$$W = \begin{cases} r_k + r_m + \varepsilon; & r_m \le t_0 \le (b - r_k) \\ t_0 + r_k + \varepsilon; & t_0 < r_m \\ b - t_0 + r_m + \varepsilon; & t_0 > (b - r_k) \end{cases} \quad \textbf{6-1}$$

where t_0 represents the time instant when a node decides to transmit data packet and ε represents the propagation delay. As the value of RTSI is in order of tens of milliseconds as compared to few microseconds associated with propagation delays, we will ignore the impact of propagation delay (ε) on collision window size.

In addition to decrease in network throughput, an increase in the probability of collision between contending nodes will result in a decrease in packet throughput observed by individual node. In order to highlight the performance impact observed by individual nodes and its dependency on RTSI delay profile, we first derive an expression for the conditional probabilities of collision observed by individual nodes. Consider a heterogeneous DDR network similar to the one considered in the previous paragraph, but comprising of N nodes with two different RTSI delay profiles ($\tilde{r}_k$, $\tilde{r}_m$). Let K nodes have a RTSI distribution given by $\tilde{r}_k \in \mathrm{N}(\mu_k,\sigma_k^2)$ and M nodes have a RTSI distribution given by $\tilde{r}_m \in \mathrm{N}(\mu_m,\sigma_m^2)$ (where $N=K+M$). Let the random variable t_i represent the time instant when a node decides to transmit a packet and be uniformly distributed over the contention interval $(0,b)$. For our analysis we will assume a memory less channel access i.e. the each node will attempt to access the channel irrespective of the outcome of the previous attempt (constant backoff window). Also

assume saturated load conditions i.e. every node in the network always has packets to transmit. Note that the RTSI delays do not affect the probability of a node to get channel access but rather the probability of a collision free transmission given that it has won the channel contention.

The conditional probability of collision for a node k with RTSI delays represented by $\tilde{r}_k$, at a time instant t_k, is given by

$$P(C/t_k = x) = 1 - \{\Pr(no\ nodes \quad collide)\} \qquad \textbf{6-2}$$
$$= 1 - \{(1 - (F(y < x + r_k) - F(y < x - r_k))^{(K-1)} *$$
$$(1 - (F(y < x + r_k) - F(y < x - r_m))^{M}\}$$
$$= 1 - \{(1 + F_u(v + r_k < 0) - F_w(v - r_k < 0))^{(K-1)}$$
$$* (1 + F_u(v + r_k < 0) - F_w(v - r_m < 0))^{M}\}$$

where $y,x \in U(0,b)$, $v=x-y$, $u=v+r_i$ and $w=v-r_i$. Similarly, the conditional probability of collision for a node m with RTSI delays represented by $\tilde{r}_m$ is given by

$$P(C/t_m = x) = 1 - \{\Pr(no\ nodes \quad collide)\} \qquad \textbf{6-3}$$
$$= 1 - \{(1 - (F(y < x + r_m) - F(y < x - r_k))^{K} *$$
$$(1 - (F(y < x + r_m) - F(y < x - r_m))^{(M-1)}\}$$
$$= 1 - \{(1 + F_u(v + r_m < 0) - F_w(v - r_k < 0))^{K}$$
$$* (1 + F_u(v + r_m < 0) - F_w(v - r_m < 0))^{(M-1)}\}$$

In order to obtain a closed form solution for probabilities of collision we need to obtain expressions for probability distribution functions (pdf) $f_u(u)$, $f_w(w)$ and $f_v(v)$. From 6-2 and 6-3 we observe that the random variable $\tilde{v}$ is obtained by subtracting two uniform random variables and hence would have a triangular distribution (Δ) given by

$$F_v(v) = \begin{cases} (v+b)^2/2; & -b < v < 0 \\ 1 - (v-b)^2/2; & 0 < v < b \end{cases} \qquad \textbf{6-4}$$
$$f_v(v) = \begin{cases} v + 1; & -b < v < 0 \\ 1 - v; & 0 < v < b \end{cases}$$

The random variables $\tilde{u}$ and $\tilde{w}$ are obtained by adding a random variable $\tilde{v} \in \Delta(b,b)$ and $\tilde{r}_i \in N(\mu_i,\sigma_i^2)$. The pdfs $f_u(u)$ and $f_w(w)$ are given by a Triangular-Gaussian convolution function, $P_{GT}(g)$ [22], [26]. For $\Delta(a,b)$ and $N(\mu_i,\sigma_i^2)$ this convolution takes the form as shown below:

$$P_{GT}(g) = (^{-Sg+c}/_{2})\left\{erf(\frac{g-\mu_i-b}{\sqrt{2}\sigma_i}) - erf(\frac{g-\mu_i-a}{\sqrt{2}\sigma_i})\right\} - \quad \textbf{6-5}$$

$$^{S\sigma}/_{\sqrt{2\pi}}\left\{\exp(-\frac{(g-\mu_i-b)^2}{2\sigma_i^2}) - \exp(-\frac{(g-\mu_i-a)^2}{2\sigma_i^2})\right\}$$

where S represents the slope of the right angled triangular function and c represents the intercept point. Using 6-2, 6-3, 6-4 and 6-5 we can calculate the probability of collisions observed by individual node depending upon the RTSI delay profile.

Equations 6-2 and 6-3 can be extended further to include a generic N-node heterogeneous LMR network which consists of $p_1, p_2 \ldots p_n$ n-types of nodes with RTSI delays of $r_1, r_2 \ldots r_n$ and a population of $s_1, s_2 \ldots s_n$ respectively ($s_1+s_2+..+s_n=N$). The conditional probability of collision for a node p_i in such a network can be computed as shown below:

$$P(^{C}/_{t_k} = x) = 1 - \{\Pr(no\ nodes \quad collide)\} \quad \textbf{6-6}$$

$$= 1 - \{(1 + F_u(v + r_i < 0) - F_w(v - r_i < 0))^{(s_i - 1)}$$

$$* \prod_{\substack{j=1 \\ j \neq i}}^{n-1} (1 + F_u(v + r_i < 0) - F_w(v - r_j < 0))^{s_j}\}$$

Using 6-1, 6-2 and 6-3 we can approximate the average values of collision window for k and m nodes as shown below:

$$W_{Mavg} = E[W_m] \approx {}^{[K(r_k + r_m) + (M-1)(2r_m)]}/_{N} \quad \textbf{6-7}$$

$$W_{Kavg} = E[W_k] \approx {}^{[(K-1)(2r_k) + M(r_k + r_m)]}/_{N}$$

The above equation assumes that each node always has data to transmit. Figure 6-5 shows the normalized collision window (W_{Mavg} / W_{Kavg}) size for a node m and k for various heterogeneous network configurations as a function of different RTSI delays. We can see that the average value of collision window (W_{Mavg}) for the node type m which has a higher RTSI value, r_m is higher than that for the node (W_{Kavg}) type k which has a lower RTSI value, r_k. In addition to the relation between the two RTSI values, the normalized collision window size also depends upon the number of k type nodes in the N node network. As the number of k type nodes increases, the ratio of W_{Mavg}/W_{Kavg} also increases. Furthermore, the rate of increase in this ratio is also dependent upon the difference between the values of RTSI delays. From 6-2, 6-3 and 6-7, it can also be concluded that greater the size of collision window, higher is the risk of unintentional denial of service due to collisions with other nodes. Thus nodes with larger RTSI delays (m-type in this case) will incur a higher probability

of collision as compared to that of nodes with lower RTSI delays (*n*-type in this case). Alternatively, nodes with lower RTSI delays will have a greater probability of successful transmissions. This leads to an asymmetry in the number of DOS seen by individual nodes in the same network and consequentially in the throughput observed by individual radios. In next section we present the results of theoretical analysis and simulations.

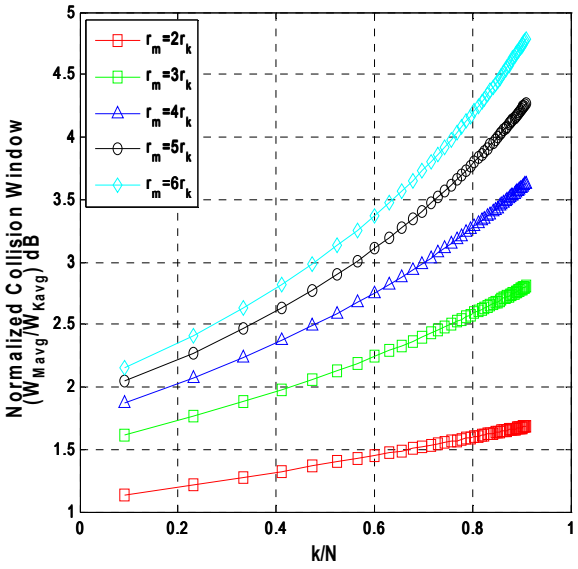

Figure 6-5: Difference in collision window sizes for *m* and *k* node

6.5. Results

Equation 6-2, 6-3, 6-4 and 6-5 give a closed form expression for computing the conditional probability of collision for an individual node in a *N*-node heterogeneous network in terms of the cumulative distribution functions (cdf) F_u and F_w. Form the objective of highlighting the effects of RTSI delays, two types of nodes (*k, m*) with different RTSI profiles will be considered for analysis and simulations. In order to compute the conditional probabilities in 6-2 and 6-3, let the RTSI profiles associated with two node types be represented by $N(\mu_k=0.08,\sigma_k^2=2.8e\text{-}6)$ and $N(\mu_m=0.11,\sigma_m^2=4.8e\text{-}6)$. Thus a *k* type node has a lower RTSI delay than a *m* type node ($\mu_k < \mu_m$). The contention interval (0,*b*) is assumed to be of length 32*max(μ_k, μ_m) which is the minimum value of contention window for the 802.11 standard [27].

Figure 6-6 and Figure 6-7 shows the difference in conditional probability of collision for a k type node and a m type node using the analytical model and simulations respectively. P_m represents the collision probability for a node with RTSI delay $\tilde{r}_m$ and P_k represents the collision probability for a node with RTSI delay $\tilde{r}_k$. From the plots in Figure 6-6 and Figure 6-7, we observe that the value of P_m is greater than P_k i.e the packets from m type nodes experience a greater number of collisions as compared to those from a k type node. The simulation results validate the analytical model developed for probability of collisions. From the figures it can be further inferred that the difference in conditional probabilities is a function of both the number of faster nodes in the network (K/N) and also the size of the total network (N). For the constant ratio between faster nodes to slower nodes, the difference in collision probabilities depends upon the total number of nodes. Greater the total number of nodes, we need a higher ratio between faster nodes and slower nodes to get the maximum asymmetry between DOS observed by nodes.

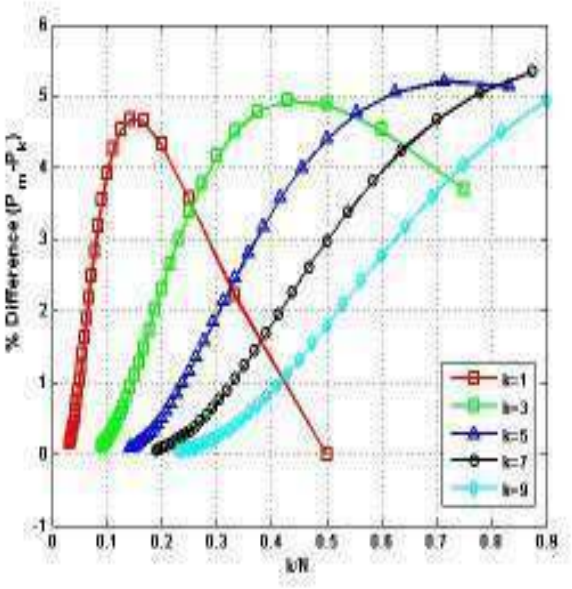

Figure 6-6: Theoretical differences in probability of collision between *m* nodes and *k* nodes

Figure 6-8 show the difference between the throughputs obtained for k type nodes (T_k) and m type nodes (T_m). The throughputs are normalized to the total network throughput obtained in simulations. From the figure it can be seen that there exists an asymmetry in the throughput observed by individual nodes depending upon their PTT delay profile. A faster node has an advantage over the

slower node in terms of the throughput ($T_k > T_m$) due to the lesser probability of collisions ($P_k < P_m$). This advantage increases as the distribution of faster nodes in the network increases. This means that if few faster nodes are introduced in a network of slower nodes, the throughput observed by the slower nodes will be lower than that observed if the new nodes introduced had similar PTT delay profile.

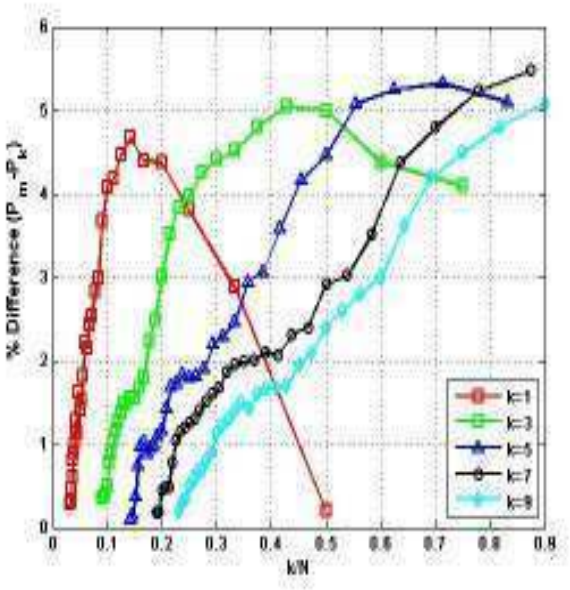

Figure 6-7: Simulated differences in probability of collision between *m* nodes and *k* nodes

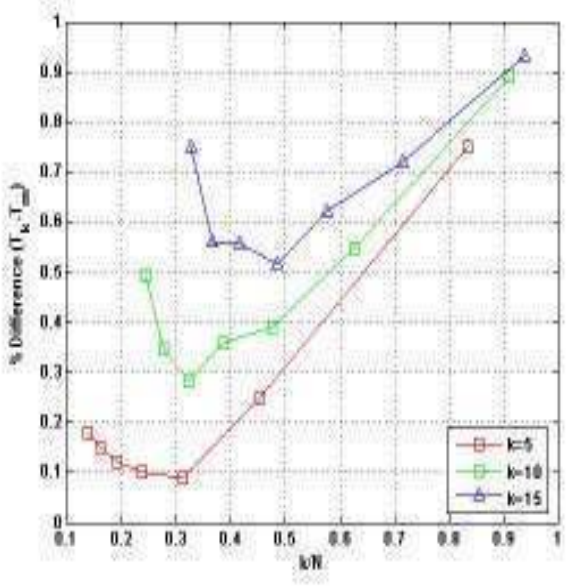

Figure 6-8: Difference between throughputs observed between *m* and *k* nodes

Also note that as the number of faster nodes in the network increases ($K/N \approx 1$) the throughput observed by the faster nodes almost equals that of the network, as expected. At lower densities ($K/N << 1$) too, the *k* type nodes have higher throughput than the *m* type node as seen in Figure 6-7. This observation has implications in capacity planning for heterogeneous LMR network designed to support data traffic as both the capacity and performance of the network, will not scale linearly as the number of nodes are increased.

6.6. Impact of RTSI delays on performance of DDR systems

From discussions in Sections 6.3 and 6.4 we can conclude that the throughput performance of DDR radios will be affected by PTT delays. In Section 6.2 we observed the snapshot at the output of FM transmitter, interfaced with a DDR modem. From the figure we can conclude that any baseband data which was sent to the FM transmitter in the RTSI interval (KEY_DELAY) would be lost as the FM carrier is never transmitted on the channel. This means that transfer of baseband data from DDR modem to FM transmitter should be delayed by the amount represented by RTSI delay. Furthermore, in order to minimize the number of collisions, the contention interval should be increased. Increasing the contention interval will decrease the probability that two or more nodes select transmit instants within the collision window. However, if the contention interval is too large, it is possible that the overall throughput of the system decreases due to a large backoff delay. This can be observed in Figure 6-9 and Figure 6-10. For simulations, the contention interval is varied in multiples of the maximum RTSI delay in the network and the number of nodes is varied from 10 to 30. The network is also assumed to be comprising of an equal number of radios with delay profiles $\tilde{r}_k \in \mathrm{N}(0.08, 2.8e\text{-}6)$ and $\tilde{r}_m \in \mathrm{N}(0.11, 4.6e\text{-}6)$. Figure 6-9 shows the relationship between collision rate and size of contention interval. We observe that for small values of contention interval, the collision rate is high. This is because smaller the contention window, higher is the probability that two or more nodes select transmit instants within the collision window as described in Section 6.4. Furthermore, we also observe that the collision rate also increases as the number of nodes in the network increase. For example, at the contention interval of $32*\max(\mu_k, \mu_m)$, for a network of 10 nodes, the collision rate observed is 35 %.

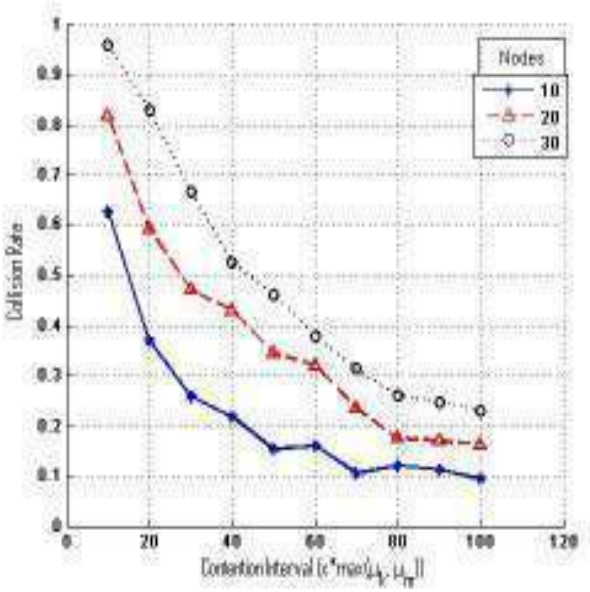

Figure 6-9: Collision rate for different contention intervals and number of nodes.

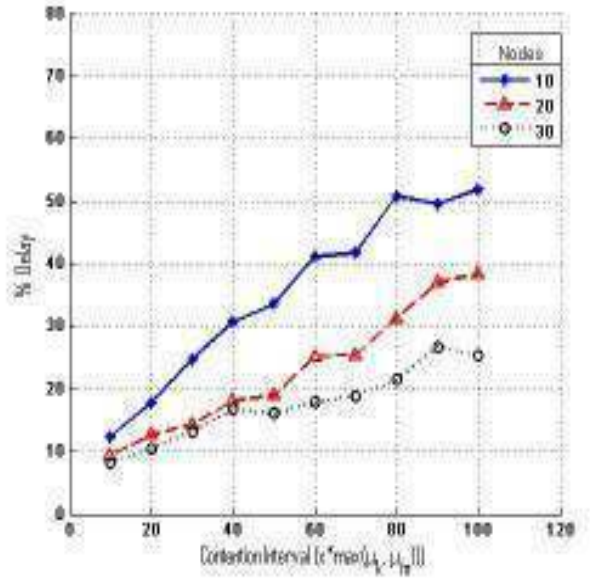

Figure 6-10: Delays observed for different number of contention interval and number of nodes

Figure 6-10 shows the relationship between average backoff delay as a function of different contention interval sizes. The delays are normalized with respect to maximum frame duration (PPDU) for a DDR modem. From the figure we observe that larger the size of contention interval, greater is the overhead encountered due to backoff delays. For example, in the case of a network comprising of

10 nodes and contention interval of 32*max(μ_k, μ_m), the backoff delay introduces a 25 % overhead. We also observe that as the number of nodes in the network increases, the average backoff delay observed by the network decreases. Thus we can conclude that an optimum size of contention interval depends upon number of factors like the number of nodes in the network and RTSI delays of individual radios.

6.7. Chapter Summary

In this chapter, we developed an analytical model to highlight the asymmetric throughput problem due to Push-To-Talk (PTT) in CSMA/CA based Land Mobile Radio (LMR) networks. A similar analysis can be extended to other variations of MAC layer protocol. The PTT delays discussed in this chapter can be separated into two parts RTSI and TRSI. TRSI introduces delays in the network while RTSI, in addition to delays, increase the collision window size. This increases the number of DOS events as the individual nodes in the network collide with each other more frequently. In addition to decreasing the total network throughput, this also results in an asymmetric performance amongst different radios depending upon their individual RTSI profile. The radios with lower RTSI delays will observe a lower DOS and hence an increased probability in successful transmissions as compared to radios with higher RTSI delays. These observations can prove useful during capacity planning for LMR networks since the probability of collision observed by nodes may change depending upon the PTT delay profile of the radios. We also observe that in case of DDR networks, the performance also depends upon the size of contention interval which in turn depends upon the number of radios in the network and the RTSI delays of those radios.

References

[1] A. Navalekar and W. Michalson, "A New Approach to Improve BER Performance of a High Peak-to-Average Ratio (PAR) OFDM signal over FM based LMRs", IEEE WTS, Pomona, 2008.

[2] A. Navalekar and W. Michalson, "A Linear Scaling Technique (LST) for improving BER performance of high PAR OFDM signal over FM-based LMR", *resubmitted*, IEEE Trans. on Broad., 2009.

[3] _____ , "Including VOIP over WLAN in a seamless Next- Generation Wireless Enviornment", Texas Insturments, White Paper.

[4] K. Pahlavan and A. Levesque, " Wireless Information Networks", 2nd Edition, Wiley Publications 2005.

[5] R. Desourdis *et al.* , "Emerging Public Safety wireless communication systems", Artech House 2002.

[6] _____ , " TETRA for Public Safety" , Exir Telecom, White Paper, 08.

[7] _____ , " APCOs P 25 Radio System", Daniel Electronics, TG 001-200, Jan 2007.

[8] L.Kleinrock and F.Tobagi, "Packet switching in radio channels: Part I- carrier Sense Multiple Access modes and their throughput-delay characteristics", IEEE Trans. On Comm. Vol.COM-23, no.12, 1975.

[9] F.Cali, M.Conti and E. Gregori, "IEEE 802.11 protocol: Design and performance evaluation of an adaptive backoff mechanism, " IEE J.Sel. Areas Comm. Vol 18 ,Sep, 2000.

[10] X.Yang and N. Vaidya, "Explicit and implicit pipelining for wireless medium access control," in Proc. IEEE Veh. Technoogy Conf. Oct. 2003.

[11] J. Kim and J. Lee, "Capture effects of wireless CSMA/CA protocols in Rayleigh and shasdow fading channel," IEEE Trans. Veh. Tech., Oct 2003.

[12] Li-Chun Wang, A. Chen and Shi-Yen Huang, "A Cross-Layer Investigation for the Throughput Performance of CSMA/CA-Based WLANs with Directional Antennas and Capture Effect", IEEE Transactions on Vehicular Technology, September 2007.

[13] A Lyakhov and V Vishnevsky, "Unfair access problem in Wi-Fi hot spots", IEEE PIMRC 2007.

[14] Dazhi Chen, Jing Deng and P Varshney, "Protecting wirless networks against a denial of service attack based on virtual jamming", ACM MobiCom, San Diego, 2003.

[15] A.C. Navalekar, W.R. Michalson, J. Kolanjery and J. Matthews , "Effects of Push-To-Talk delays on CSMA based capacity limited LMR networks", IEEE ISWPC, Santorini, Greece 2008.

[16] A.C. Navalekar, W.R. Michalson , J.S. Kolanjery and J.W. Matthews, " Effects of PTT delays on Throughput of CSMA/CA based Distributed Digital Radios for LMR networks", IEEE ICPP, Portland, OR, 2008.

[17] A.C. Navalekar and W.R. Michalson, " Effects of Unintentional Denial of Service (DOS) due to PTT delays on performance of CSMA/CA based adhoc LMR networks", ICST Adhocnets, Nigara Falls, CN, 2009.

[18] A.C. Navalekar and W.R. Michalson, " Assymetric throughput problem due to PTT delays in CSMA/CA based heterogenous LMR networks", IEEE Milcom, Boston, MA, 2009.

[19] Kai Chang, " RF Microwave wireless systems", Wiley, 2000.

[20] Motorola, "Astro XTS 5000 Specification Sheet," 2004.

[21] ICOM, "IC-T7H Instruction Manual," 1998.

[22] A. Leon-Garcia, "Probability and random processes for electrical engineering", Prentice Hall 2nd Edition, 1993.

[23] Colvin, "CSMA with Collision Avoidance," Computer Communications, vol.6, no.5, 1983.

[24] P.Karn, "MACA- anew channel access method for packet radio," ARRL/CRRL Comp. Network Conf. 1990.

[25] C.Fullmer and J.Gracia-Luna-Aceves, "FAMA in single channel wireless networks", Mobile networks and App., Kulwer Academic Pub. 1999..

[26] D Williamson *et al.*, "Partial volume tissue sgmentation using grey-level gradient", MIUA 2002.

[27] G. Bianchi, "Performance analysis of the IEEE 802.11 Distributed Coordination Function", IEEE Journal on Selected areas in Comm. MARCH 2000.

7. Conclusion

7.1. Research Achievements

A Land Mobile Radio (LMR) network forms a backbone of mobile communications for emergency response and disaster recovery applications like Law Enforcement and Emergency Medical Services (EMS). The DDR II technology, developed in this dissertation, provides a low-cost IP-based connectivity using conventional analog LMRs. The use of this technology also provides a novel way of integrating legacy networks like LMR with next generation wireless networks like Wi-Fi, WiMAX and LTE using the internet backbone. A typical implementation of next generation heterogeneous LMR network, using DDR II modems, capable of communicating critical data like physiological status of first responders, location information and environment data in addition to voice is shown in Figure 7-1.

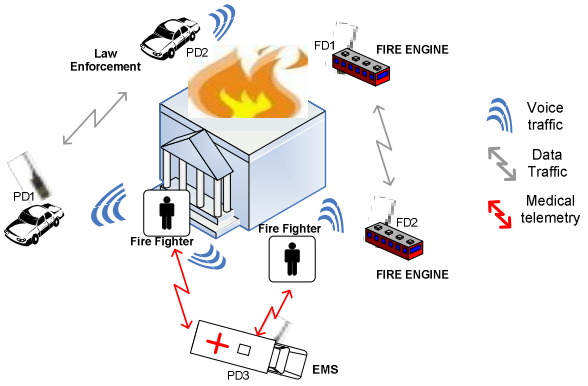

Figure 7-1: Next generation LMR network for public safety applications

The main objective of this dissertation was development of the second generation of DDR technology. A DDR II modem has an integrated service platform for voice and data, higher data rate and better throughput performance as compared to its predecessor DDR I. The achievements of this dissertation are as follows:

- In order to extend the ability of DDR I modem to service voice traffic in addition to data, a number of changes were made to the modem hardware. The firmware of DDR I modems was also upgraded to support the changes made in the hardware.

- In order to improve the PHY layer performance of DDR II modems, an analytical framework was developed to model the performance of an OFDM/FM system. The relationship between non-linear distortions of an OFDM baseband signal in a FM transmitter to the SNR at the output of a FM discriminator was derived.
- The impact of high PAR of OFDM signals on performance of OFDM/FM system was highlighted. Expressions for the theoretical bounds on PAPR and CF values for an OFDM baseband signal generated by the DDR modem were derived.
- A new PAPR reduction technique called LST was proposed. LST is based on optimizing the SNDR for an OFDM/FM system and results in no additional computations and has a minimum throughput overhead. By using LST it is possible to improve the data rate and the BER performance of the DDR II modems. An experimental test-bed was setup to compare the results obtained using simulations, theoretical model and real world performance.
- The impact of PTT delays on performance of LMR networks was highlighted. Typical values and distribution for commonly used handheld LMR radios were presented.
- A theoretical model to highlight the increase in probability of collisions in LMR networks due to RTSI delays was developed. This model underlined the influence of RTSI delays in achieving the desired throughput and latency for the network.
- The Asymmetric Throughput Problem in case of heterogeneous LMR networks was highlighted. The results obtained using simulations and theoretical models were compared and changes were made in the MAC layer implementation of DDR II modems to improve the throughput performance of networks using DDRs.

7.2. Future work

There are number of topics for research, based on this dissertation that can be pursued in future, as discussed below:

- A Cooperative Access Distributed Radio Enhancement (CADRE) modem based on the Distributed Digital Radio (DDR). Currently, a DDR modem supports digital/voice communication on a single LMR channel. A CADRE modem extends this DDR functionality over multiple channels, thus increasing the effective data rate. It uses a cooperative access mechanism to realize a truly self configurable adhoc network. The aggregate bandwidth of

CADRE modem is a function of number of radios and number of channel available for transmission.

- The framework developed for SNR calculations at FM discriminator modeled the clipper circuit in FM transmitter as a Soft Limiter (SL). A SL only accounts for AM/AM distortions introduced by a non-linear device. A more accurate analysis which includes AM/PM distortion is recommended.
- The SNDR model which was used to compute the BER at the FM discriminator accounted only for the additive noise effects of distortion. A more comprehensive model can be developed which takes into account the ICI and in-band distortion resulting from clipping of OFDM signal. This model can be used to obtain a better approximation of BER improvement possible and the optimum backoff ratio (χ) for a given IFFT size and modulation scheme.
- An analytical expression relating the contention interval to throughput performance and collision rate can be derived. This will aid in obtaining the optimum contention interval which will maximize the throughput of LMR networks.
- The deterioration in throughput performance of heterogeneous LMR networks due to radios with different PTT delay profile should be investigated further. This analysis will be of immense importance due to the long shelf life of LMR radios. Introduction of faster radios in the network can lead to asymmetry in throughput. This means that the network will not scale linearly every time more nodes are added to the network. This observation can significantly compromise the capacity of the LMR network and hence warrants further investigation.

Appendix A

The bandwidth of a FM signal *z(t),* is not determined simply by the spectrum of modulating signal *u(t)*. This is because a FM modulated signal is a non-linear function of the modulating signal. For modulating signals which are pure sinusoids, the FM signal bandwidth can be approximated by Carlson's Rule given in Section 3.2. In this section we calculate the bandwidth for an OFDM modulated FM signal. Consider a bandpass equivalent representation for modulated FM signal given in 1.

$$z(t) = A\,\mathrm{Re}\{v(t)e^{j(2\pi f_c t+\Theta)}\} \quad \textbf{1}$$

where *v(t)* represents the a complex base-band signal given by $e^{ju(t)}$. For a pure FM signal, $u(t) = \frac{\omega_d}{k_m}\int_0^t m(\xi)d\xi$, where *m(t)* represents the OFDM baseband signal. For this derivation, it is assumed that the modulating OFDM signal represents a zero-mean, wide sense stationary (WSS) Gaussian process. For a WSS process, autocorrelation for *z(t)* will be given by

$$R_z(\tau) = A\,\mathrm{Re}\{e^{j2\pi f_c\tau}R_v(\tau)\} \quad \textbf{2}$$

where $R_v(\tau)$ is given by

$$R_v(\tau) = E[e^{ju_{t+\tau}-u_t}] = E[e^{jQ(\tau)}] \quad \textbf{3}$$

Since *m(t)* is a zero mean Gaussian random variable, it can be shown that *u(t)* and *Q(t)= u(t+τ)-u(t)* are also Gaussian variables with zero mean (μ=0) and variances σ^2_u and σ^2_Q respectively. Under these assumptions, it is possible to calculate $R_v(\tau)$ and $R_z(\tau)$ using the characteristic function $\Phi(\omega)$ for Gaussian variables as shown below

$$R_v(\tau) = E[e^{jQ(\tau)}] = e^{j\mu-\frac{1}{2}\sigma_Q^2(\tau)} \quad \textbf{4}$$
$$= e^{-\frac{1}{2}\sigma_Q^2(\tau)}$$
$$R_z(\tau) = A^2/2\cos(2\pi f_c\tau)e^{-\frac{1}{2}\sigma_Q^2(\tau)}$$

Let $S_z(f)$ and $V(f)$ represent the psd of modulated FM signal, $Z(t)$ and the complex baseband $V(t)$, respectively. Both $S_z(f)$ and $V(f)$ can be obtained by computing the Fourier transform of their respective autocorrelation functions and are related to each other as shown in 5 and 6 below

$$S_z(f) = \int_{-\infty}^{\infty} R_z(\tau) e^{j\omega\tau} d\tau \qquad \textbf{5}$$

$$V(f) = \int_{-\infty}^{\infty} R_v(\tau) e^{j\omega\tau} d\tau$$

$$S_z(f) = \frac{A^2}{4}[V(f+f_0) + V(f-f_0)] \qquad \textbf{6}$$

From Equation 6 it can be seen that $S_z(f)$ consist of a scaled version of $V(f)$ centered about $\pm f_0$. Thus the bandwidth characteristics of $S_z(f)$ about $\pm f_0$ will be same as those for $V(f)$ about $f=0$. In order to calculate $V(f)$, the knowledge of second order statistics of $u(t)$ is necessary. For a WSS process, the variance σ^2_Q is a function of time difference τ alone and can be calculated as shown:

$$\sigma_Q^2(\tau) = E[(u_{t+\tau} - u_t)^2] = E\left[\left\{\frac{w_d}{k_m}\int_t^{t+\tau} m(\zeta)d\zeta\right\}^2\right] = \omega_d^2 \Big/ k_m^2 \; E\left[\int_0^{\tau} d\zeta_1 \int_0^{\tau} m(\zeta_1)m(\zeta_2)d\zeta_2\right] \qquad \textbf{7}$$

$$= \omega_d^2 \Big/ k_m^2 \int_0^{\tau} d\zeta_1 \int_0^{\tau} R_x(\zeta_1 - \zeta_2)d\zeta_2$$

Let $\overline{R}_v(\tau)$ and $\overline{V}(f)$ represent normalized autocorrelation and psd functions defined as shown:

$$\overline{R}_v(\tau) = R_v(\tau) \Big/ \varepsilon \quad ; \quad \overline{V}(f) = V(f) \Big/ \varepsilon \qquad \textbf{8}$$

where ε represents the mean-square power of $V(t)$ given by $\varepsilon = R_v(0) = \int_{-\infty}^{\infty} V(f)df$. The normalized autocorrelation $\overline{R}_v(\tau)$ can be expressed in terms of normalized $\overline{V}(f)$ using the Fourier transform:

$$\overline{R}_v(\tau) = \int_{-\infty}^{\infty} \overline{V}(f) e^{j2\pi f\tau} df \qquad \textbf{9}$$

The normalized psd $\overline{V}(f)$ is a nonnegative even function of f with unit area. The mean-square bandwidth f^2_v can be calculated as shown:

$$f_v^2 = \int_{-\infty}^{\infty} f^2 \overline{V}(f) df \qquad \textbf{10}$$

This mean-square power can be represented in terms of $\overline{R}_v(\tau)$ by first differentiating Equation 9 with respect to τ and then substituting τ=0 as shown:

$$\overline{R}_v''(0) = -\int_{-\infty}^{\infty}(2\pi f)^2 \overline{V}(f)df \quad ; \quad f_v^2 = -\overline{R}_v''(0) \Big/ (2\pi)^2 \tag{11}$$

Using Equations 4, 11 and 8, $\overline{R}_v''(0)$ can be expressed as:

$$\overline{R}_v''(0) = R_v''(0)/\varepsilon = \frac{1}{\varepsilon}\frac{d^2[e^{-\sigma^2(\tau)/2}]}{d\tau^2}\bigg|_{\tau=0} = \frac{1}{\varepsilon}\left\{-\frac{1}{2}[\frac{d^2}{d\tau^2}\sigma^2(\tau)] + \frac{1}{2}[\frac{d}{d\tau}\sigma^2(\tau)]^2\right\}e^{-\sigma^2(\tau)/2}\bigg|_{\tau=0} \tag{12}$$

Substituting the expression for $\sigma^2(\tau)$ from 7 into 12, and using Leibnitz's Rule for differentiation of an integral it can be shown:

$$\frac{k_m^2}{\omega_d^2}[\frac{d}{d\tau}\sigma^2(\tau)]\bigg|_{\tau=0} = 0 \quad ; \quad \frac{k_m^2}{\omega_d^2}[\frac{d^2}{d\tau^2}\sigma^2(\tau)]\bigg|_{\tau=0} = 2R_x(0); \quad \varepsilon = R_v(0) = 1 \tag{13}$$

$$\overline{R}_v''(0) = R_v''(0)/\varepsilon = \frac{1}{\varepsilon}\frac{d^2[e^{-\sigma^2(\tau)/2}]}{d\tau^2}\bigg|_{\tau=0} = \left\{-\frac{\omega_d^2}{k_m^2}R_x(0)\right\}$$

Using Equations 13 and 11 the expression for mean-square bandwidth reduces to:

$$f_v^2 = -\overline{R}_v''(0) \Big/ (2\pi)^2 = (f_d^2 \Big/ k_m^2)R_x(0) \tag{14}$$

Thus the rms value of the bandwidth can be expressed as:

$$\sqrt{f_v^2} = (f_d \Big/ k_m)R_x(0) = f_d\sigma_m \tag{15}$$

where σ_m represents the normalized rms value of modulating signal given by $\sigma_m = R_x^{1/2}(0) \Big/ k_m = \sigma_x \Big/ k_m$. From 15, we observe that in case of a FM carrier modulated by an OFDM signal, the rms bandwidth f_v depends upon the maximum frequency deviation f_d, proportionality constant k_m and rms value of the modulating baseband signal σ_x.

Appendix B

The output of the FM discriminator, as discussed in Section 3.4, is the baseband modulating signal. For modulating signals consisting of single sinusoids it is trivial to prove that the FM modulation/demodulation is a lossless process. In this section the proof will be extended to a modulating signal comprising of multiple sinusoids like OFDM. We start with a baseband signal *m(t)* comprising of two sinusoids as given below

$$m(t) = A_1 \cos(\omega_1 t) + A_2 \cos(\omega_2 t) \quad (1)$$

As seen in 1, the modulating signal *m(t)*consists of two sinusoids of frequencies ω_1 and ω_2. Without the loss of generality assume that A_1 and A_2 are unity, in that case the FM signal can be expanded using standard trigonometric identities as shown below

$$\begin{aligned} z(t) &= A_c \cos(\omega_c t + {\omega_d}/{\omega_1} \sin(\omega_1 t) + {\omega_d}/{\omega_2} \sin(\omega_2 t)) = A_c \cos(\omega_c t + \beta_1 \sin(\omega_1 t) + \beta_2 \sin(\omega_2 t)) \\ &= A_c[\cos(\omega_c t)\cos(\beta_1 \sin(\omega_1 t))\cos(\beta_2 \sin(\omega_2 t)) - \cos(\omega_c t)\sin(\beta_1 \sin(\omega_1 t))\sin(\beta_2 \sin(\omega_2 t)) \\ &\quad - \sin(\omega_c t)\sin(\beta_1 \sin(\omega_1 t))\cos(\beta_2 \sin(\omega_2 t)) - \sin(\omega_c t)\cos(\beta_1 \sin(\omega_1 t))\sin(\beta_2 \sin(\omega_2 t))] \end{aligned} \quad (2)$$

where $\beta_1 = \omega_d/\omega_1$ and $\beta_2 = \omega_d/\omega_2$ represents the respective modulation indices. Equation 2 can be reduced by using the Bessel expansion identities given below

$$\begin{aligned} \cos(\beta \sin(\omega_m t)) &= J_0(\beta) + 2J_2(\beta)\cos(2\omega_m t) + ... \\ \sin(\beta \sin(\omega_m t)) &= 2J_1(\beta)\sin(\omega_m t) + 2J_3(\beta)\sin(3\omega_m t) + ... \end{aligned} \quad (3)$$

Thus the FM signal, *z(t)* in 1 can be rewritten as

$$\begin{aligned} z(t) = A_c[&-\cos(\omega_c t)\{J_0(\beta_1)J_0(\beta_2) + 2J_0(\beta_1)J_2(\beta_2)\cos(2\omega_2 t) + 2J_2(\beta_1)J_0(\beta_2)\cos(2\omega_1 t) \\ &+ 4J_2(\beta_1)J_2(\beta_2)\cos(2\omega_1 t)\cos(2\omega_2 t) + 4J_1(\beta_1)J_1(\beta_2)\sin(\omega_1 t)\sin(\omega_2 t) + ...\} \\ &- \sin(\omega_c t)\{2J_1(\beta_1)J_0(\beta_2)\sin(\omega_1 t) + 4J_1(\beta_1)J_2(\beta_2)\sin(\omega_1 t)\cos(2\omega_2 t) \\ &+ 2J_0(\beta_1)J_1(\beta_2)\sin(\omega_2 t) + 4J_2(\beta_1)J_1(\beta_2)\cos(\omega_1 t)\sin(2\omega_2 t) + ...\}] \end{aligned} \quad (4)$$

In case of OFDM signals, the sub-carriers are orthogonal to each other and the spacing between adjacent sub-carriers is *1/T*. Let $1/T = \Delta\omega$ and $\omega_1 = \Delta\omega$, $\omega_2 = 2\Delta\omega$. As seen in Chapter 3, a FM signal consists of infinite number of sidebands. For sinusoid modulation, 99% of the power is contained in Bessel functions of order *n=0,1,*2. For the purposes of this derivation we will consider sidebands upto the 2nd order Bessel functions of modulation index as shown below

$$\begin{aligned} z(t) = J_0(\beta_1)J_0(\beta_2)\cos(\omega_c t) + &[(-J_1(\beta_1)J_1(\beta_2) + J_1(\beta_1)J_0(\beta_2))\cos(\omega_c + \Delta\omega) + \\ &(-J_1(\beta_1)J_1(\beta_2) - J_1(\beta_1)J_0(\beta_2))\cos(\omega_c - \Delta\omega)] + ... \end{aligned} \quad (5)$$

Equation 5 represents the time domain expression for the transmitted FM Signal. Similar to the derivation of the received signal at the FM discriminator in Chapter 3, we will assume no channel distortion and a large SNR value. The output of the limiter under these assumptions can be represented as

$$r_L(t) = A_L[J_0(\beta_1)J_0(\beta_2)\cos(\omega_c t) + [(-J_1(\beta_1)J_1(\beta_2) + J_1(\beta_1)J_0(\beta_2))\cos(\omega_c + \Delta\omega) + (-J_1(\beta_1)J_1(\beta_2) - J_1(\beta_1)J_0(\beta_2))\cos(\omega_c - \Delta\omega)] + ...] \quad \textbf{6}$$

Operation of an FM discriminator can be approximated by a differentiator (FM-AM conversion) followed by an envelope detector (AM -detection). We follow the same steps as with single modulation signal shown in Chapter 3.

$$\begin{aligned} f_1(t) = \frac{dv_L(t)}{dt} = A_L\{&\cos(\omega_c t)[2\Delta\omega J_1(\beta_1)J_1(\beta_2)\sin(\Delta\omega t) - 6\Delta\omega J_1(\beta_1)J_1(\beta_2)\sin(3\Delta\omega t) \\ &- 2\omega_c J_1(\beta_1)J_0(\beta_2)\sin(\Delta\omega t) - 2\omega_c J_0(\beta_1)J_1(\beta_2)\sin(2\Delta\omega t) + ...] \\ &+ \sin(\omega_c t)[-\omega_c J_0(\beta_1)J_0(\beta_2) + 2\omega_c J_1(\beta_1)J_1(\beta_2)\cos(\Delta\omega t) \\ &- 2\omega_c J_1(\beta_1)J_1(\beta_2)\cos(3\Delta\omega t) - 2\Delta\omega J_1(\beta_1)J_0(\beta_2)\cos(\Delta\omega t) + ...]\} \end{aligned} \quad \textbf{7}$$

Simplifying 7 using trigonometric identities we have

$$\begin{aligned} f_1(t) = A_L\{&-\omega_c \sin(\omega_c t)[J_0(\beta_1)J_0(\beta_2) - 2J_1(\beta_1)J_1(\beta_2)\cos(\Delta\omega t) + ...] \\ &+ \cos(\omega_c t)[2\Delta\omega J_1(\beta_1)J_1(\beta_2)\sin(\Delta\omega t) + ...] - \omega_c \cos(\omega_c t)[2\omega_c J_1(\beta_1)J_0(\beta_2)\sin(\Delta\omega t) + ...] \\ &- \sin(\omega_c t)[2\Delta\omega J_1(\beta_1)J_0(\beta_2)\cos(\Delta\omega t) + ...]\} \end{aligned} \quad \textbf{8}$$

Substituting Bessel expansion identities given in 3 and 9 into 8 we get 10

$$\begin{aligned} \beta\cos(\omega_m t)\cos(\beta\sin(\omega_m t)) &= 2J_1(\beta)\cos(\omega_m t) + 6J_3(\beta)\cos(3\omega_m t) + ... \\ \beta\cos(\omega_m t)\sin(\beta\sin(\omega_m t)) &= 4J_2(\beta)\sin(2\omega_m t) + 8J_4(\beta)\sin(8\omega_m t) + ... \end{aligned} \quad \textbf{9}$$

$$\begin{aligned} f_1(t) = -A_L\{&\omega_c[\sin(\omega_c t)\{\cos(\beta_1\sin(\Delta\omega t))\cos(\beta_2\sin(2\Delta\omega t)) - \sin(\beta_1\sin(\Delta\omega t))\sin(\beta_2\sin(2\Delta\omega t))\} \\ &+ \cos(\omega_c t)\{\sin(\beta_1\sin(\Delta\omega t))\cos(\beta_2\sin(2\Delta\omega t)) - \cos(\beta_1\sin(\Delta\omega t))\sin(\beta_2\sin(2\Delta\omega t))\}] \\ &+ (\beta_1\Delta\omega\cos(\Delta\omega t) + \beta_2 2\Delta\omega\cos(2\Delta\omega t))[\sin(\omega_c t)\{\cos(\beta_1\sin(\Delta\omega t))\cos(\beta_2\sin(2\Delta\omega t)) \\ &- \sin(\beta_1\sin(\Delta\omega t))\sin(\beta_2\sin(2\Delta\omega t))\} + \cos(\omega_c t)\{\sin(\beta_1\sin(\Delta\omega t))\cos(\beta_2\sin(2\Delta\omega t)) - \\ &\cos(\beta_1\sin(\Delta\omega t))\sin(\beta_2\sin(2\Delta\omega t))\}] \\ = -A_L(&\omega_c + \beta_1\Delta\omega\cos(\Delta\omega t) + \beta_2 2\Delta\omega\cos(2\Delta\omega t))[\sin(\omega_c t)\{\cos(\beta_1\sin(\Delta\omega t))\cos(\beta_2\sin(2\Delta\omega t)) \\ &- \sin(\beta_1\sin(\Delta\omega t))\sin(\beta_2\sin(2\Delta\omega t))\} + \cos(\omega_c t)\{\sin(\beta_1\sin(\Delta\omega t))\cos(\beta_2\sin(2\Delta\omega t)) - \\ &\cos(\beta_1\sin(\Delta\omega t))\sin(\beta_2\sin(2\Delta\omega t))\}] \\ = -A_L(&\omega_c + \beta_1\Delta\omega\cos(\Delta\omega t) + \beta_2 2\Delta\omega\cos(2\Delta\omega t))[\sin(\omega_c t + \beta_1\sin(\Delta\omega t) + \beta_2\sin(2\Delta\omega t))] \end{aligned} \quad \textbf{10}$$

The output of the envelope detector, s_o can be calculated as

$$s_o(t) = -\sigma A_L(\omega_c + \beta_1 \Delta\omega \cos(\Delta\omega t) + \beta_2 2\Delta\omega \cos(2\Delta\omega t)) \quad \textbf{11}$$

$$For: \quad \beta_1 = \frac{\omega_d}{\Delta\omega}; \quad \beta_2 = \frac{\omega_d}{2\Delta\omega}$$

$$= -\sigma A_L(\omega_c + \omega_d \cos(\Delta\omega t) + \omega_d \cos(2\Delta\omega t))$$

$$= \cos(\Delta\omega t) + \cos(2\Delta\omega t) = \cos(\omega_1 t) + \cos(\omega_2 t); \quad for \qquad \sigma = \frac{-1}{A_L \omega_d}$$

Thus from 1 and 11 we conclude that the output of the FM discriminator is the baseband signal comprising of two sinusoids. This analysis can be extended to a baseband signal consisting of N orthogonal sinusoids. The output of the envelope detector for an OFDM signal consisting of N sub-carriers is shown below

$$s_o(t) = -\sigma A_L(\omega_c + \beta_1 \Delta\omega \cos(\Delta\omega t) + \ldots + \beta_N N\Delta\omega \cos(N\Delta\omega t)) \quad \textbf{12}$$

$$For: \quad \beta_1 = \frac{\omega_d}{\Delta\omega}; \quad \ldots; \beta_N = \frac{\omega_d}{N\Delta\omega}$$

$$= -\sigma A_L(\omega_c + \omega_d \cos(\Delta\omega t) + \ldots + \omega_d \cos(N\Delta\omega t))$$

$$= \cos(\Delta\omega t) + \ldots + \cos(N\Delta\omega t) = \cos(\omega_1 t) + \ldots + \cos(\omega_n t); \quad for \qquad \sigma = \frac{-1}{A_L \omega_d}$$